NOAA Technical Report NESDIS 67

THE RELATIONSHIP BETWEEN WATER VAPOR PLUMES AND EXTREME RAINFALL EVENTS DURING THE SUMMER SEASON

Washington, D.C.
May 1993

U.S. DEPARTMENT OF COMMERCE
National Oceanic and Atmospheric Administration
National Environmental Satellite, Data, and Information Service

NOAA TECHNICAL REPORTS

National Environmental Satellite, Data, and Information Service

The National Environmental Satellite, Data, and Information Service (NESDIS) manages the Nation's civil Earth-observing satellite systems, as well as global national data bases for meteorology, oceanography, geophysics, and solar-terrestrial sciences. From these sources, it develops and disseminates environmental data and information products critical to the protection of life and property, national defence, the national economy, energy development and distribution, global food supplies, and the development of natural resources.

Publication in the NOAA Technical Report series does not preclude later publication in scientific journals in expanded or modified form. The NESDIS series of NOAA Technical Reports is a continuation of the former NESS and EDIS series of NOAA Technical Reports and the NESC and EDS series of Environmental Science Services Administration (ESSA) Technical Reports.

A limited number of copies are available by contacting Nancy Everson, NOAA/NESDIS, E/RA22, 5200 Auth Road, Washington D.C., 20233. Copies can also be ordered from the National Technical Information Service (NTIS), U.S. Department of Commerce, Sills Bldg., 5285 Port Royal Road, Springfield, VA. 22161, (703) 487-4650 (prices on request for paper copies or microfiche, please refer to PB number when ordering). A partial listing of more recent reports appear below:

NESDIS 12 Utilization of the Polar Platform of NASA's Space Station Program for Operational Earth Observations. John H. McElroy and Stanley R. Schneider, September 1984. (PB85 1525027/AS)

NESDIS 13 Summary and Analyses of the NOAA N-ROSS/ERS-1 Environmental Data Development Activity. John W. Sherman III, February 1985. (PB85 222743/A3)

NESDIS 14 NOAA N-ROSS/ERS-1 Environmental Data Development (NNEEDD) Activity. John W. Sherman III, February 1985. (PB86 139284/AS)

NESDIS 15 NOAA N-ROSS/ERS-1 Environmental Data Development (NNEEDD) Products and Services. Franklin E. Kniskern, February 1985. (PB86 213527/AS)

NESDIS 16 Temporal and Spatial Analyses of Civil Marine Satellite Requirements. Nancy J. Hooper and John W. Sherman III, February 1985 (PB86 212123/AS)

NESDIS 18 Earth Observations and the Polar Platform. John H. McElroy and Stanley R. Schneider, January 1985. (PB85 177624/AS)

NESDIS 19 The Space Station Polar Platform: Intergrating Research and Operational Missions. John H. McElroy and Stanley R. Schneider, January 1985. (PB85 195279/AS)

NESDIS 20 An Atlas of High Altitude Aircraft Measured Radiance of White Sands, New Mexico, in the 450-1050 nm Band. Gilbert R. Smith, Robert H. Levin and John S. Knoll, April 1985. (PB85 204501/AS)

NESDIS 21 High Altitude Measured Radiance of White Sands, New Mexico, in the 400-2000nm Band Using a Filter Wedge Spectrometer. Gilbert R. Smith and Robert H. Levin, April 1985. (PB85 206084/AS)

NESDIS 22 The Space Station Polar Platform: NOAA Systems Considerations and Requirements. John H. McElroy and Stanley R. Schneider, June 1985. (PB86 6109246/AS)

NESDIS 23 The Use of TOMS Data in Evaluating and Improving the Total Ozone from TOVS Measurements. James H. Lienesch and Prabhat K. K. Pandey, July 1985. (PB86 108412/AS)

NESDIS 24 Satellite-Derived Moisture Profiles. Andrew Timchalk, April 1986. (PB86 232923/AS)

NESDIS 26 Monthly and Seasonal Mean Outgoing Longwave Radiation and Anomalies. Aronold Gruber, Marylin Varnadore, Phillip A. Arkin and Jay S. Winston, October 1987. (PB87 160545/AS)

NESDIS 27 Estimation of Broadband Planetary Albedo from Opertional Narrowband Satellite Measurements. James Wydick, April 1987. (PB88 107644/AS)

NESDIS 28 The AVHRR/HIRS Operational Method for Satellite Based Sea Surface Temperature Determination. Charles Walton, March 1987. (PB88 107594/AS)

NESDIS 29 The Complementary Roles of Microwave and Infrared Instruments in Atmospheric Soundings. Larry McMillin, February 1987. (PB87 184917/AS)

NESDIS 30 Planning for Future Generational Sensors and Other Priorities. James C. Fischer, June 1987. (PB87 220802/AS)

NOAA Technical Report NESDIS 67

THE RELATIONSHIP BETWEEN WATER VAPOR PLUMES AND EXTREME RAINFALL EVENTS DURING THE SUMMER SEASON

Wassila Thiao, Roderick A. Scofield, and Jacob Robinson
Office of Research and Applications
Satellite Applications Laboratory
Physical Science Branch

Washington, D.C.
May 1993

U.S. DEPARTMENT OF COMMERCE
Ronald H. Brown, Secretary

National Oceanic and Atmospheric Administration
Diana H. Josephson, Acting Under Secretary

National Environmental Satellite, Data, and Information Service
Gregory W. Withee, Acting Assistant Administrator

Contents

The Relationship Between Water Vapor Plumes and Extreme Rainfall Events During The Summer Season

Wassila Thiao*, Roderick A. Scofield, and Jacob Robinson
NOAA/NESDIS/SAL/Physical Science Branch
Washington, DC 20233

*This work was done while the author held a USA National Research Council Postdoctoral Associateship at NOAA, NESDIS, and SAL

ABSTRACT

GOES 6.7 μm Water Vapor (WV) images were used to study the relationships between the WV plumes and the upper and lower level circulation patterns related to extreme heavy rainfall (125 mm or more in a 24 hour period) over the United States.

The study covers three summer periods (May through October, 1989-1991). One hundred and twenty nine cases were selected; 87% were associated with a well defined WV plume. These WV plumes originated essentially in tropical ocean areas, such as the Pacific Ocean, Gulf of Mexico or the Caribbean Sea. As the plumes move northeastward into the United States, they are often aligned with low-level equivalent potential temperature ridge axes and upper-level forcing mechanisms i.e. jet streams, short waves, and vortices. Occasionally these plumes from the tropics interact with WV plumes originating from the polar regions or from the subtropics. These interactions often result in MCSs that produce flash floods.

WV plumes associated with extreme heavy rainfall, were classified into four categories. The categories were a function of the plume and jet stream structures. Extreme heavy rainfall can also occur in situations that are not directly associated with plumes. Conceptual models of several types of heavy precipitation situations, as observed in the WV imagery, are briefly discussed. In addition, 12-24 hour forecast technique for heavy rainfall is presented.

The present study shows that the WV plume appears to be one connecting link between the global (climate) scale and the mesoscale/storm scale.

I. Introduction

GOES (Geostationary Operational Environmental Satellite) 6.7 μm Water Vapor (WV) imagery is an excellent tool for locating large scale features responsible for Mesoscale Convective Systems (MCSs) that produce extreme heavy rainfall (EHR) over the United States (U.S.) (Scofield and Robinson, 1990, 1992). A discussion of Mesoscale Convective Complexes (MCCs) and other satellite convective cloud categories associated with heavy rainfall is presented by Maddox (1980) and Scofield (1985), respectively.

WV Plumes (WVPs) are observed in the animated WV imagery as northward surges of well

defined boundaries of moisture from the Intertropical Convergence Zone (ITCZ). Northward moving plumes often become aligned with equivalent potential temperature (theta-e) ridge axes at low and mid-levels. These plumes and theta-e ridge axes have been shown to be a precursor for flash flood producing thunderstorms (Scofield and Robinson, 1990). The authors developed a conceptual model that locates the flash flood and severe weather producing MCSs within the proximity of the WVP and the theta-e pattern at low and mid-levels. In addition to the WVP, other preferred WV patterns for flash flood producing thunderstorms have been observed and illustrated as Conceptual Models.

Another key factor for generation and maintenance of conditions favorable for intense convective storms is the diffluent configuration induced by the presence of a polar and subtropical jet streams ahead of an advancing trough (Whitney, 1976). Upper level divergence associated with the exit region of the southern jet and the entrance region of the northern jet creates a configuration of indirect and direct transverse vertical circulations in the exit and entrance region, respectively, of the two jets. This enhanced upper level divergence between the two jets results in intense vertical motions that favor the development of convective clouds and precipitation (Uccellini and Johnson, 1979). In addition, the role of upper tropospheric jet streaks and low-level jet maxima in destabilizing the atmosphere and contributing to low-level heat and moisture transports has been widely documented (Uccellini and Johnson, 1979; Kocin et al., 1986); these jet phenomena generate and maintain conditions favorable for intense convective storms. The advection of cool, dry air within the middle troposphere and the rapid northward transport of heat and moisture by the lower-level jet create a differential transport that increases low-level theta-e and the resulting convective instability.

The purpose of this study is: to document the location of MCSs that produce EHR relative to the position of the: (1) WVP; (2) 300 mb jet streaks; and (3) low-level theta-e ridge axes; and to test the conceptual model developed by Scofield and Robinson (1990, 1992) that heavy rainfall producing thunderstorms develop in the proximity of the tropical WVP and the low to mid-level (850 to 700 mb) theta-e ridge axis. There is also a section that briefly describes EHR events in the WV imagery that are not directly associated with tropical WVPs. Conceptual models of EHR situations and a 12-24 hour prediction technique for heavy rainfall are also presented.

This study is part of a project to understand how each meteorological scale interacts and prepares the environment for convection that leads to flash floods. The scales involved range from the global to synoptic scale down to the mesoscale to storm scale and of course the feedback from the smaller scales to the larger scales.

In this paper, the 6.7 μm WV imagery, the 300 mb analyses and the theta-e analyses at 850 to 700 mb have been used to describe the global and synoptic scale features associated with the EHR events for three summer periods.

II. Selection of Extreme Heavy Rainfall Events

The River Forecast Centers' daily 24 hour rainfall charts for the period 1989 through 1991 were examined to identify and select the EHR events. These 24 hour rainfall charts are valid at 1200 GMT and contain data from the regular National Weather Service's rain gauge network as well as other data from cooperative observers.

An EHR event is defined as 125 mm (about 5 inches) of rainfall or more reported in a given state during a 24 hour period. The maximum 24 hour rainfall amount reported during that 3-year period was 390 mm (15.6 inches) over northwestern Florida on June 9, 1989. This EHR event resulted from heavy rain producing MCSs that developed over eastern Texas and moved slowly eastward resulting in flash floods over Mississippi, Alabama, and Florida between June 8, and 9.

Most of the EHR events occurred between May and October. A mean monthly distribution of occurrence, displayed in Figure 1, shows that the EHR events are more frequent in May-June with a maximum of 11.7 occurrences in June. Thus, for the purpose of this paper, the study will focus on EHR events that took place between May and October, of 1989-1991.

A total of 181 events were selected (remember that at least 125 mm of rain had to occur to be considered as an event). The geographical distribution of the events in this study (Figure 2) shows that the EHR events develop more frequently in the southern U.S.. Most of the events (39%) occurred in Texas, Louisiana and Mississippi while no event was reported over the western U.S.. However, tropical WVP events are associated with the southwest monsoon and are a major cause of the flash floods in the western U.S. during the summer season. It should be emphasized that a typical flash flood event in the western region is less than 125 mm of rain. Due to the soil type and structure and the presence of steeply sloped terrain, generally only 25 to 50 mm is needed to produce a flash flood in the western region. Of course the lack of validating rain gauge observations in the western region is also a major problem and could account for some of the rather low observed rainfall amounts that accompany many of the flash floods.

Note that different MCSs may produce EHR in different states during a 24 hour period. In such cases, the EHR reported in those states is considered as an individual event and is referred to as an event day. Thus, in this study, a total of 129 event days will be considered.

III. Global and Synoptic Scale Aspects of the Extreme Heavy Rainfall

1) Water Vapor imagery characteristics

Characteristics of the Water Vapor (WV) imagery have been detailed by Weldon and Holmes (1991) and others, therefore, they will only be described briefly in this paper. The 6.7 μm WV channel measures and integrates the radiations emitted by WV between 700 and 200 mb, with a peak response in the middle to upper troposphere between 500 and 300 mb. The resultant image is representative of the middle level moisture and cloudiness (see Figures 3, 4, and 5). The common convention is that lighter (whiter) gray shades indicate lower energy measurements from areas of large amounts of moisture and give an indication that middle or high clouds are being detected or a deep layer of moist air is present above 500 mb. Very dark gray shades indicate dry areas i.e. no clouds and little WV are present in the middle and upper troposphere. Medium gray shades represent atmospheric moisture somewhere between 700 to 200 mb; the precise location cannot be determined from the WV image, itself.

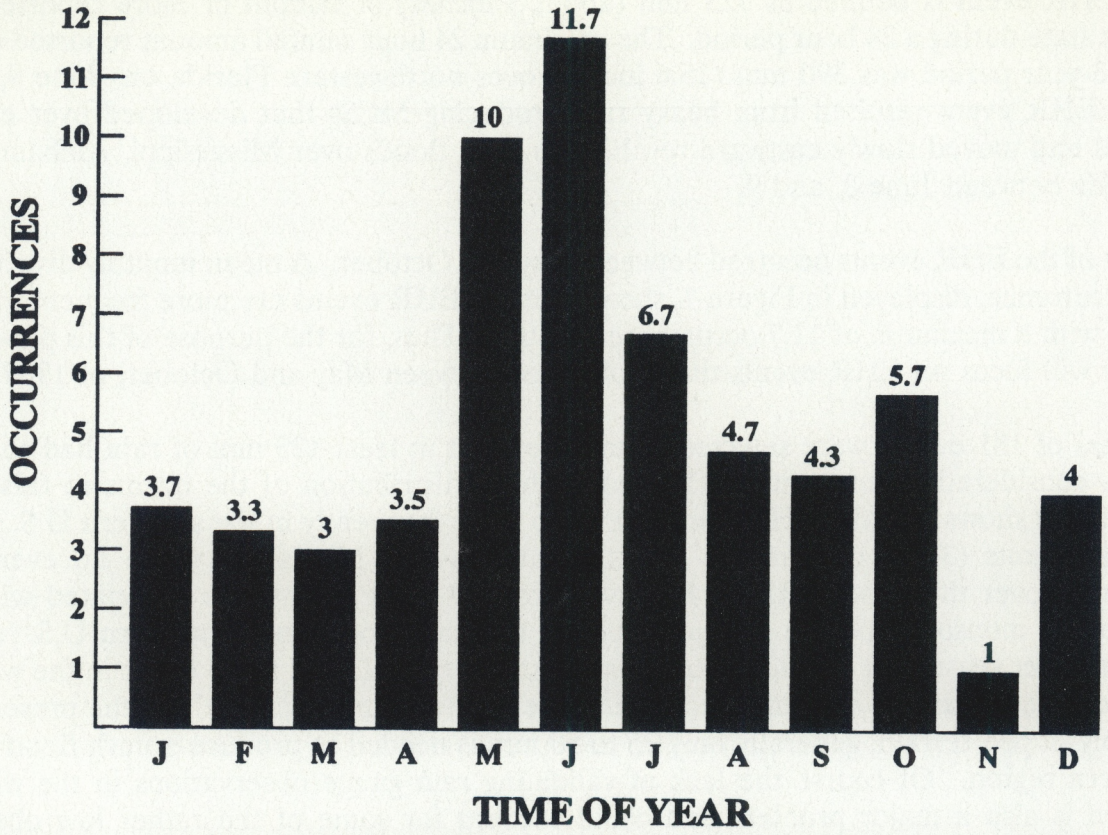

Figure 1. *Mean monthly distribution of extreme heavy rainfall event occurrences.*

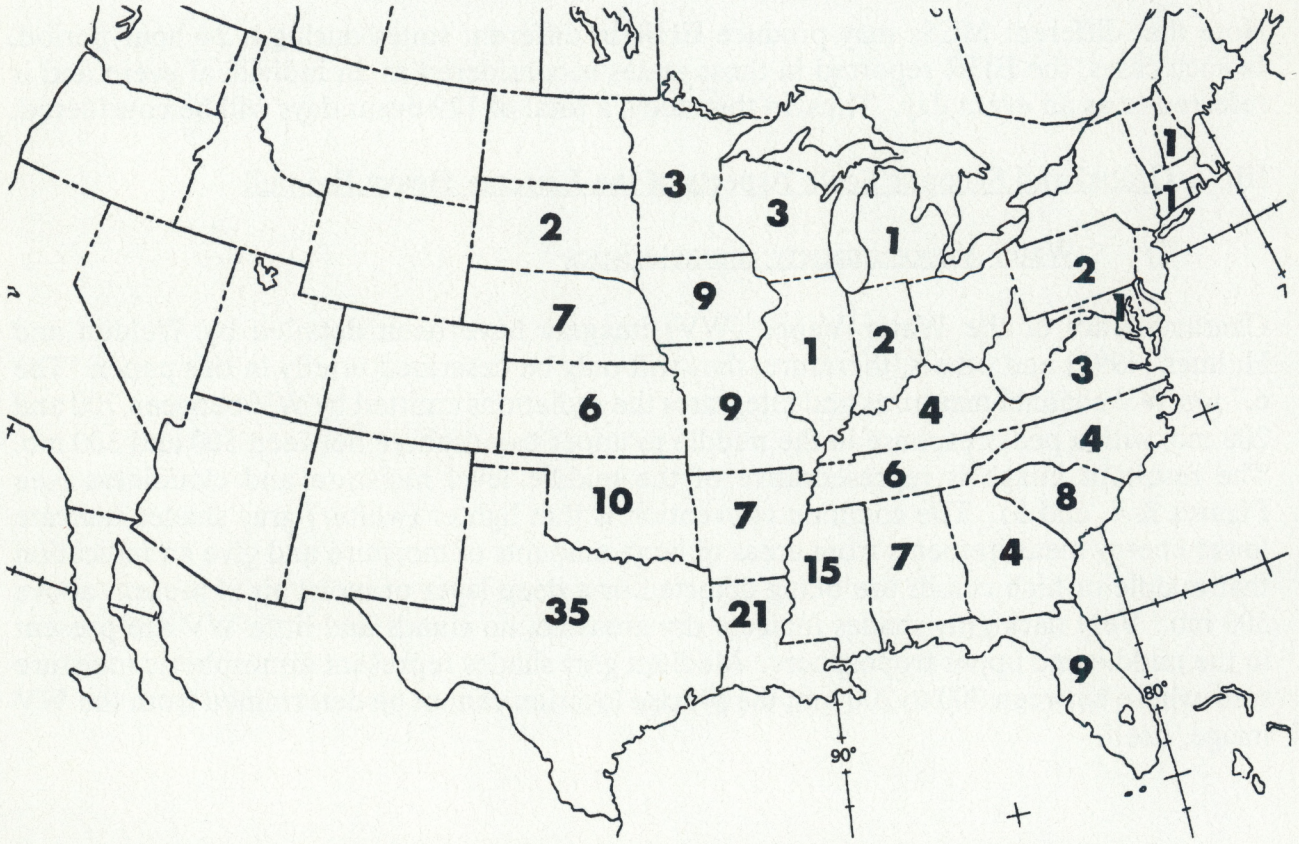

Figure 2. *Geographical distribution of extreme heavy rainfall events.*

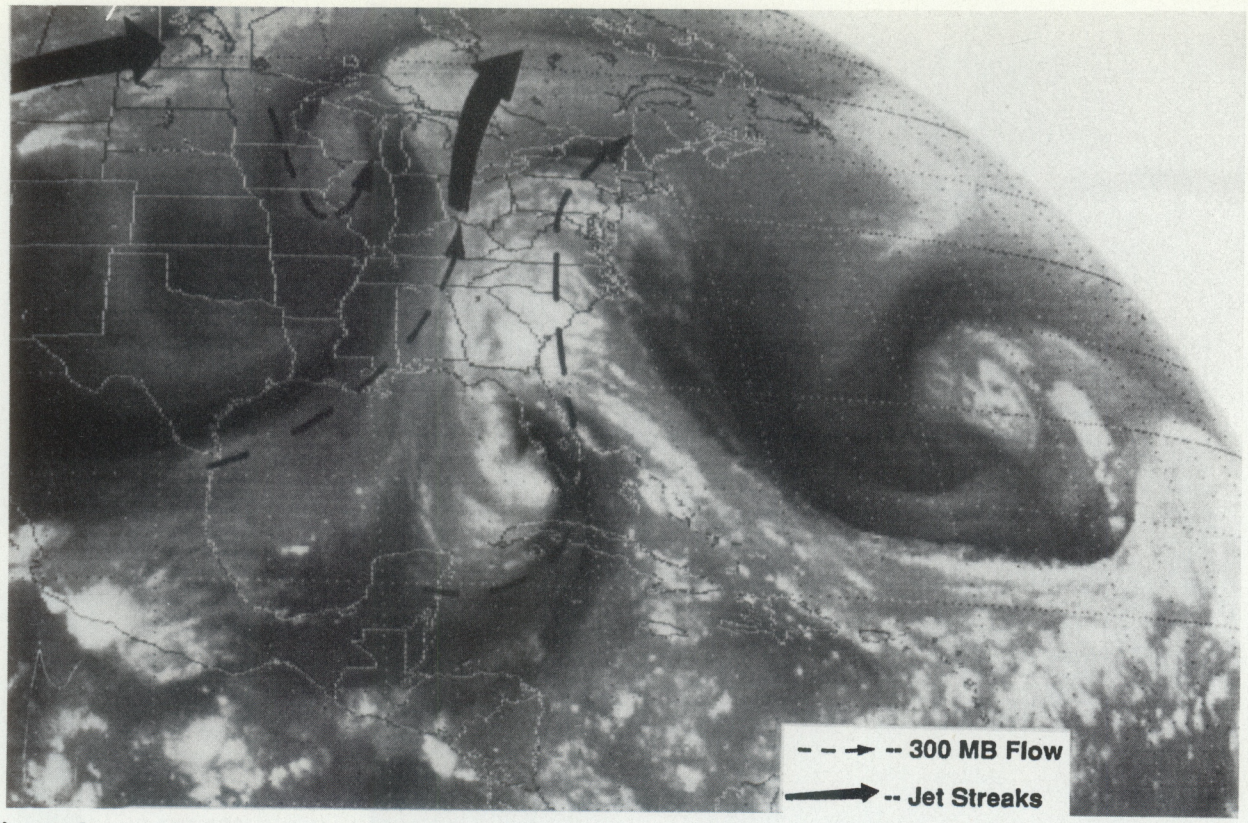

Figure 3. *Example of water vapor plumes in the Eastern and Southern Regions with 300 mb flow superimposed, October 10, 1990, 1701 GMT; flash flooding occurred over S. Carolina and Georgia.*

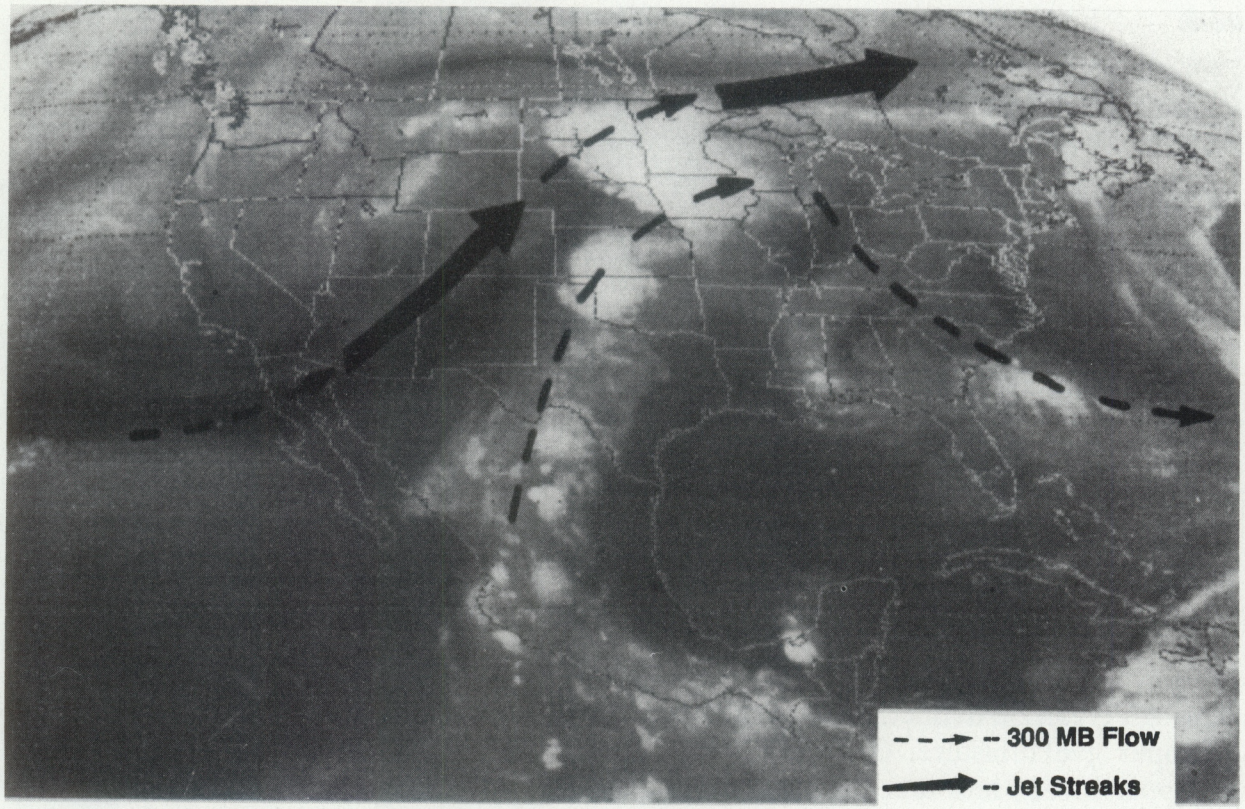

Figure 4. *Example of water vapor plume in the Central Region with 300 mb flow superimposed, June 16, 1990, 0601 GMT; flash flooding occurred over Minnesota, Iowa and the Dakotas.*

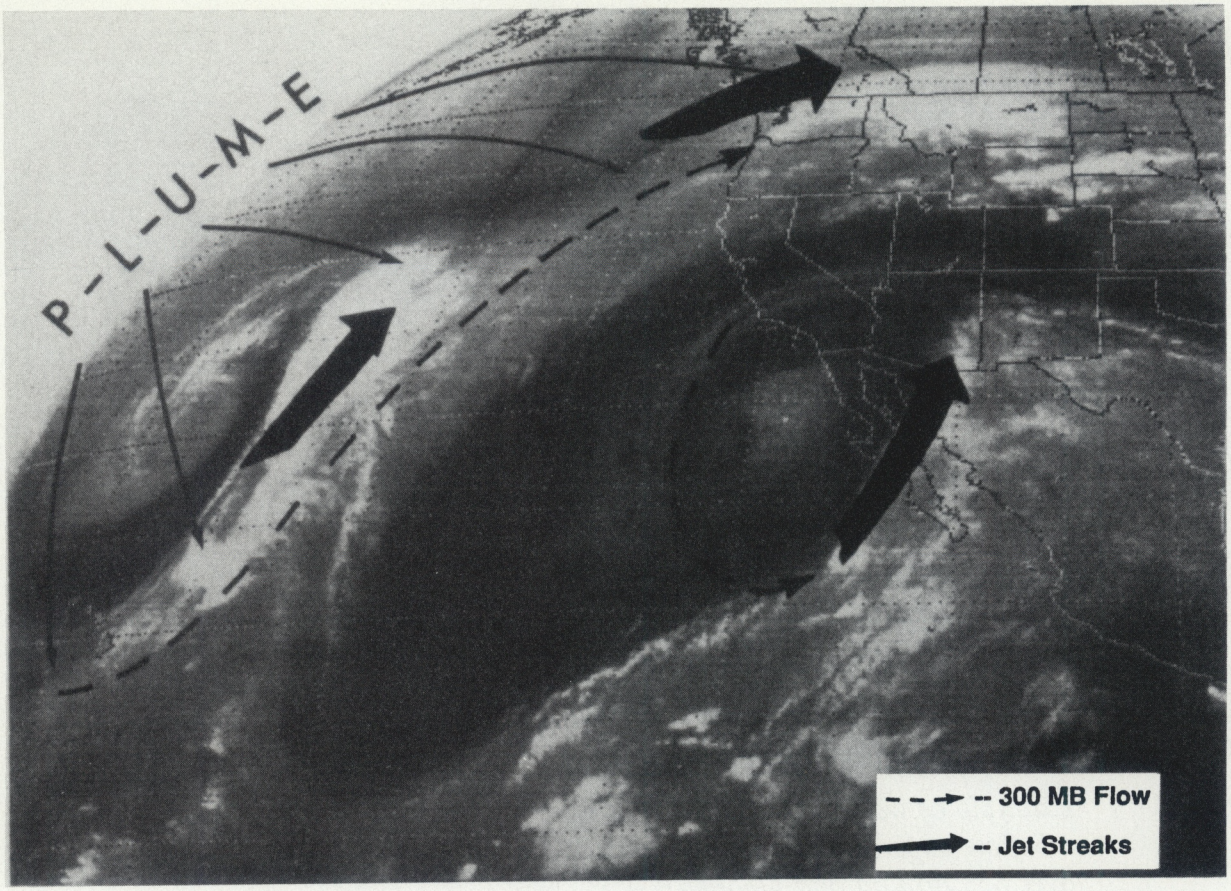

Figure 5. *Example of water vapor plume in the Western Region with 300 mb flow superimposed, November, 25, 1990, 0701 GMT; flash flooding occurred over Washington.*

When viewed in time lapse, WV imagery exhibits a spatial and temporal continuity of the vertical motion field associated with mid-level systems (Scofield and Funk, 1986 and Funk, 1990). However, use caution in making this interpretation because some of these WV patterns could be due to pure advection. Mid-level features that are associated with upward vertical motion can become coupled with low-level theta-e ridge axes and create favorable conditions for thunderstorm development.

2) Water Vapor Plumes

In this study, GOES 6.7 μm WV imagery described in the above section were used to characterize the WVPs related to the EHR events.

a) Definition

The WVP can be defined as movements or surges of well shaped global scale bands of mid to upper level moisture. Generally, WVPs are associated with large scale circulations at mid to upper levels, and take on a plume-like appearance in animated WV images (Scofield 1991, 1990b). WVPs can easily be distinguished from other general areas of moisture as they are often associated with deepening troughs and building ridges. Northward moving WVPs are often associated with southward moving digging jet streams and troughs in the westerlies.

As time sequential images have been used in this study, a WVP was considered present for any selected event day if a stream or surge of moisture from the tropics seemed to move towards the EHR areas almost in parallel with the 300 mb flow. The WVP usually originates from the Intertropical Convergence Zone (ITCZ) and extends northward to the U.S.. Examples of WVPs are shown in Figures 3, 4, and 5; 300 mb flow is also indicated on the imagery. These are referred to as tropical WVPs or simply tropical plumes. In Figure 3, flash floods occurred over South Carolina and Georgia, while in Figure 4, flash floods were reported in Iowa, Minnesota and the Dakotas and finally in Figure 5, floods took place in Washington.

Adang and Gall (1989) related the tropical plume to the onset of the southwest monsoon during the summer season, and the resulting flash flood producing thunderstorms over the southwestern U.S.. An example of a plume associated with the southwest monsoon is depicted in Figure 6 (at "S - W"). Another plume is observed in the eastern region (at "E - R"). Within the next 12 hours, flash floods occurred with these plumes over New Mexico and Arizona and from Georgia to Virginia. McGuirk and Ulsh (1990), have also investigated the evolution of tropical WVPs.

The WVP can also originate in the subtropics and middle latitudes in which case they are referred to as subtropical or polar plumes; these plumes are normally associated with the subtropical and polar jet streams, respectively. A schematic showing the configuration and relationship of a typical subtropical/polar plume and the tropical plume appears in Figure 7a. A polar (P- P') plume approaching a tropical (T-R) plume is shown in Figure 7b. In this case, flash floods occurred with the large MCS over Nebraska where deep layer moisture was present. Severe weather was noted with the MCSs over the Texas and Oklahoma Panhandles; however, no floods were reported. The occurrence of severe weather and lack of EHR was partially due to the close proximity of the dry air (dark area in Figure 7b) to the west of the MCSs.

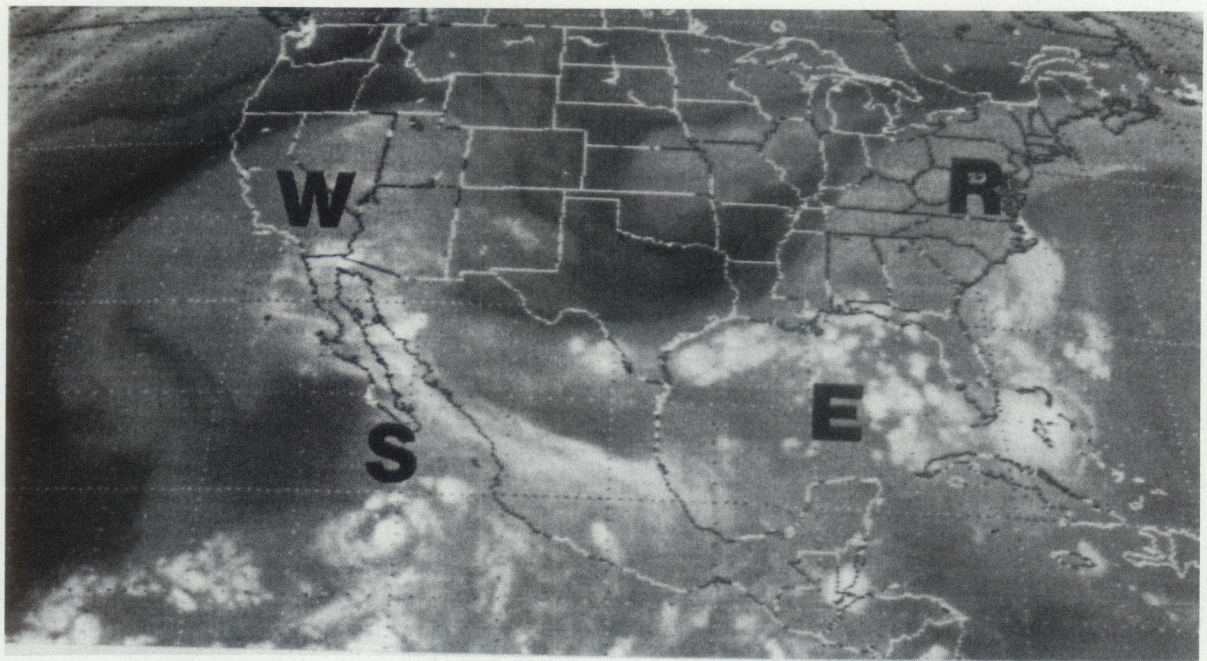

Figure 6. *Examples of 2 water vapor plumes: (1) associated with the Southwest Monsoon and (2) located in the Eastern Region, July 13, 1200 GMT, 1990.*

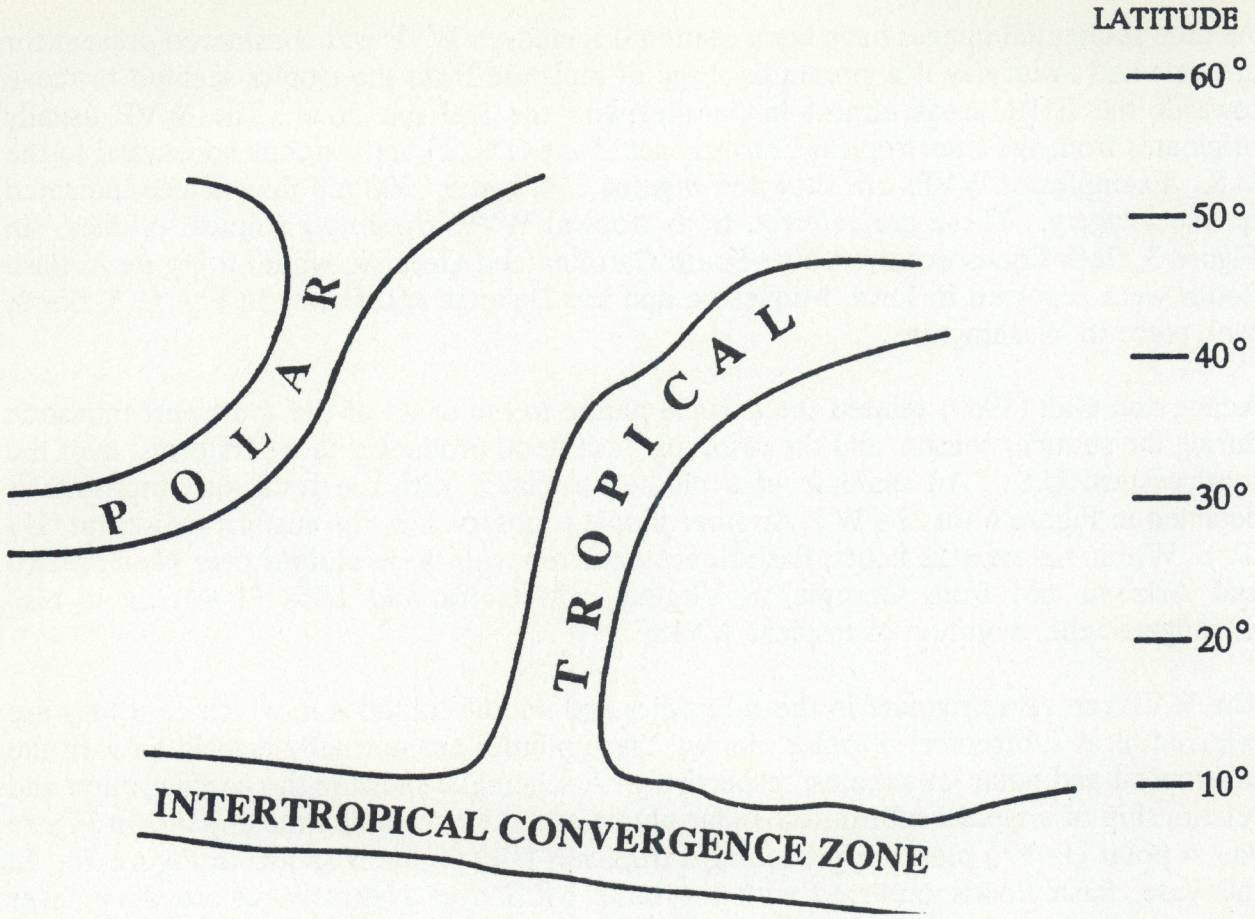

Figure 7a. A conceptual model of the polar and tropical water vapor plumes.

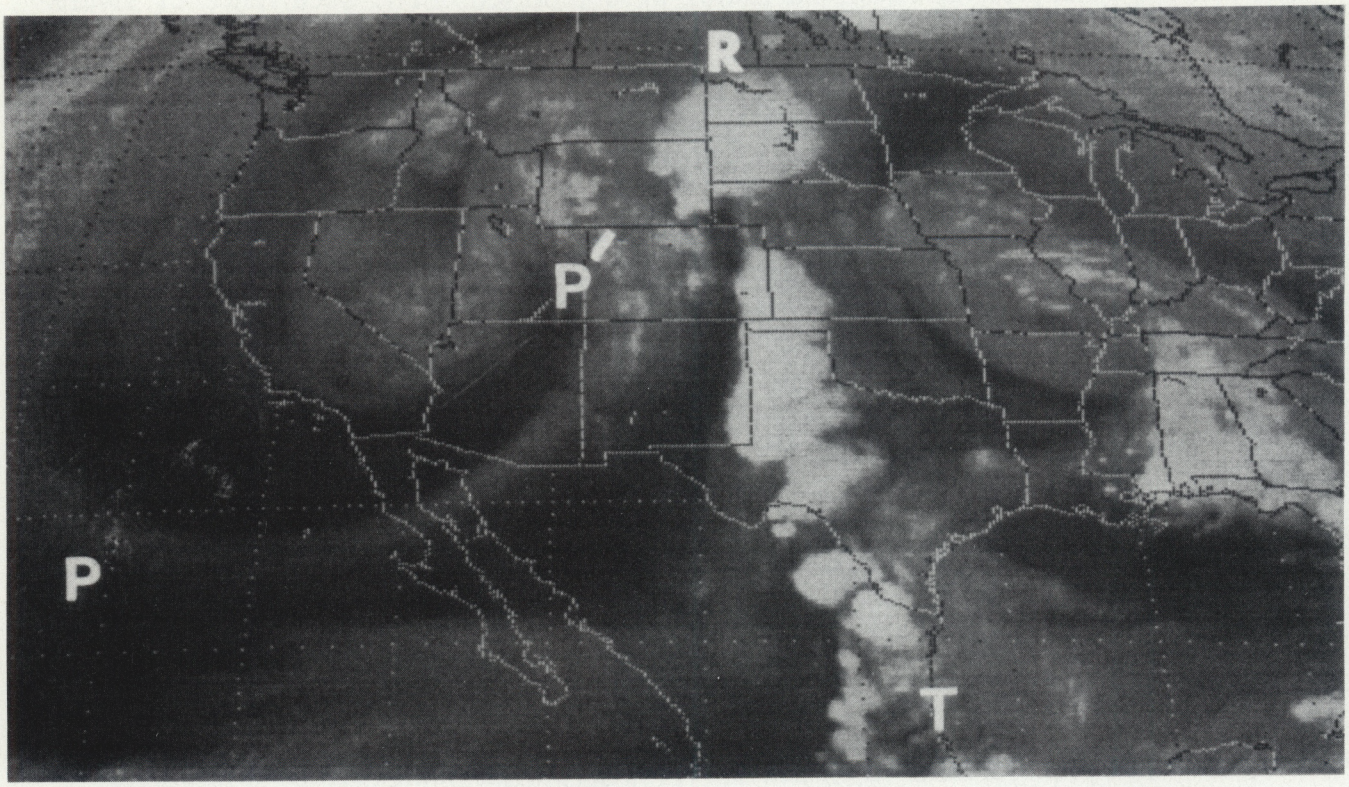

Figure 7b. An example of a double water vapor plume, May 11, 1991, 0101 GMT.

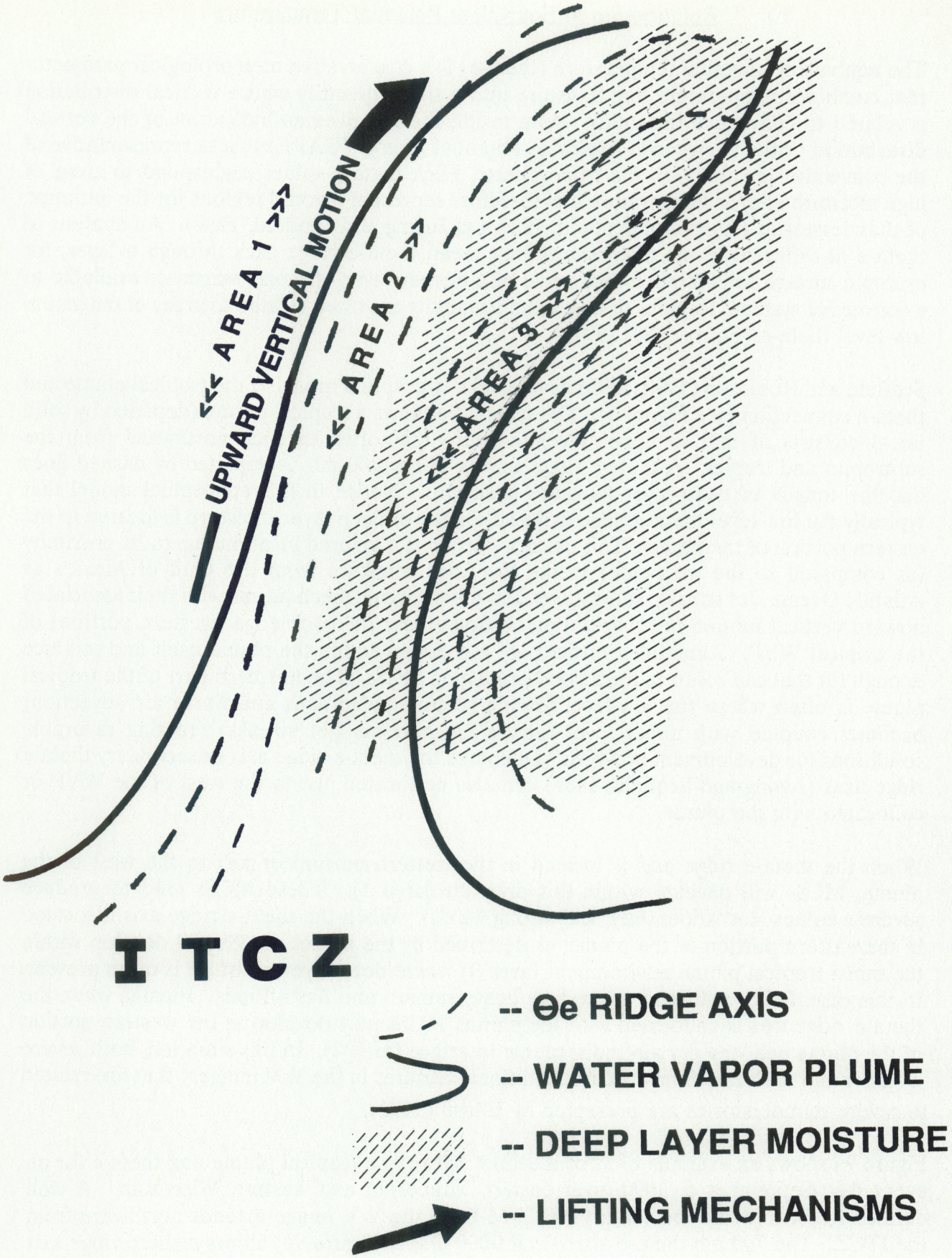

Figure 8 *A conceptual model of the tropical water vapor plume and theta-e connection.*

b) Relationship to Equivalent Potential Temperature

The equivalent potential temperature (theta-e) is a conservative meteorological parameter that combines temperature and moisture into a single quantity whose vertical distribution is related to convective instability. As a result, theta-e gives an indication of the vertical distribution of the Convective Available Potential Energy (CAPE) that is representative of the convective instability in the troposphere. High theta-e values correspond to areas of high moisture and/or temperature and therefore represent favored regions for the initiation of thunderstorms (Jiang and Scofield, 1987 and Juying and Scofield, 1989). An analysis of theta-e at different levels often shows that mean theta-e ridge axes through a layer, for example surface to 700 mb, is indicative of a deeper layer of moist, warm air available to a convective system. Regions of maximum instability are often related to areas of maximum low-level theta-e (Funk, 1989, 1991).

Scofield and Robinson (1990, 1992) developed a conceptual model of the tropical plume and theta-e connection (see Figure 8). The schematic shows a tropical plume (depicted by solid lines) consists of mid to upper level moisture that often extends northward from the subtropics and tropics. A theta-e ridge axis at 850 to 700 mb, is depicted by dashed lines and the tongue of deep layer moisture is shaded. Notice in this conceptual model that typically the low level theta-e ridge axis and tongue of deep layer moisture is located in the eastern portion of the plume. This eastern portion is a favored location due to its proximity (as compared to the west side) to the low level moisture from the Gulf of Mexico or Atlantic Ocean. Jet streaks, short waves and other forcing mechanisms with their associated upward vertical motion fields are often observed near the back edge (western portion) of the tropical WVP. Sometimes vortices are embedded within the plume itself and produce enough lift that can result in flash flood producing MCSs. The northern part of the tropical plume is often where the low-level forcing (theta-e ridge axes and warm air advection) becomes coupled with upper level forcing mechanisms (jet streaks) creating favorable conditions for development of MCSs. Of course the theta-e ridge axis or secondary theta-e ridge axes (Juying and Scofield, 1989) can also be located just to the west of the WVP or collocated with the plume.

When the theta-e ridge axis is located in the western portion or just to the west of the plume, MCSs will develop within this drier air (area 1). These MCSs tend to produce severe weather (tornadoes, hail, and strong winds). When the theta-e ridge axis is located in the eastern portion of the plume, as described by the model, MCSs will develop within the moist tropical plume environment (area 3) where deep layer moisture is often present. In this case, MCSs will tend to produce heavy rainfall and flash floods. Finally, when the theta-e ridge axis is collocated with the plume, MCSs may develop in the western portion of the plume near the dry air/moist plume interface (area 2). In this situation, both severe weather and flash floods can occur. Additional features in the WV imagery that are related to severe thunderstorms are presented by Ellrod (1992).

Figure 9a shows an example of a "connection" between a tropical plume and theta-e for an event day, September 6, 1990, over eastern Minnesota and western Wisconsin. A well defined tropical plume located at "P-L-U-M-E" in the WV image extends northward from the ITCZ. The 700 mb theta-e analysis at 0000 GMT (Figure 9b) shows a sharp ridge axis

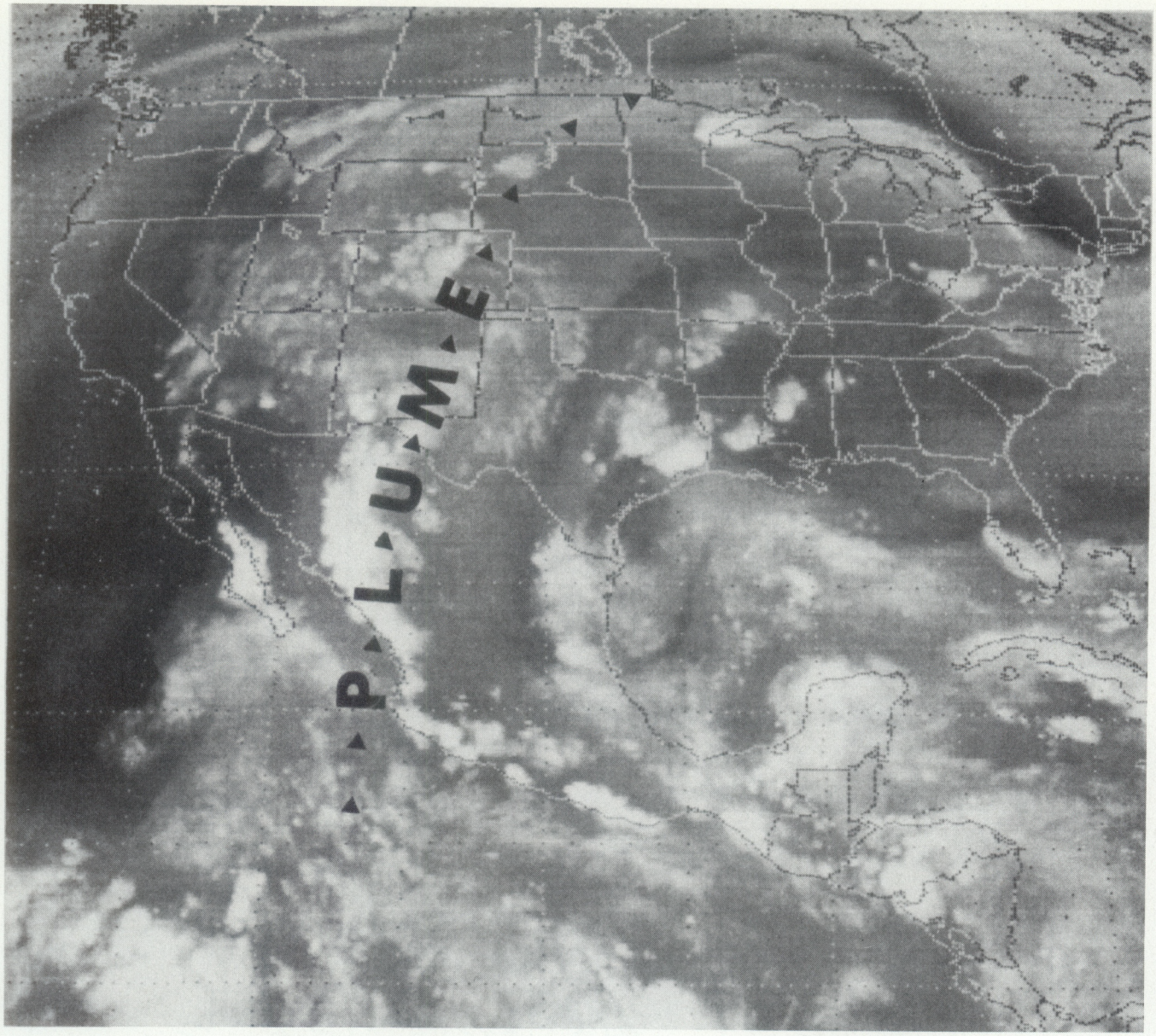

Figure 9a. 6.7 μm water vapor imagery for September 6, 1990, 0000 GMT.

(dashed line) oriented from northern Mexico into Nebraska and eastward into the Minnesota-Wisconsin area. This axis corresponds quite closely to the location of the tropical plume in the WV imagery (Figure 9a) and represents a region of high convective potential juxtaposed with an area of less favorable convective conditions across western Texas and Oklahoma where theta-e values were lower. Another relative theta-e maximum was located over east Texas, Louisiana, Arkansas and Missouri. A MCS developed within the moist air and theta-e ridge axis in the northern part of the plume over Minnesota; this MCS moved eastward to Wisconsin. In addition to the presence of the plume and theta-e ridge axis, the surface and upper air composite (Figure 9c), shows that a stationary front and relatively strong low level southwesterly winds are present over Minnesota; a jet streak is located just to the north. The location of the MCS (from Figure 9a) is depicted in Figure 9c. EHR and flash flooding were reported in this part of Minnesota.

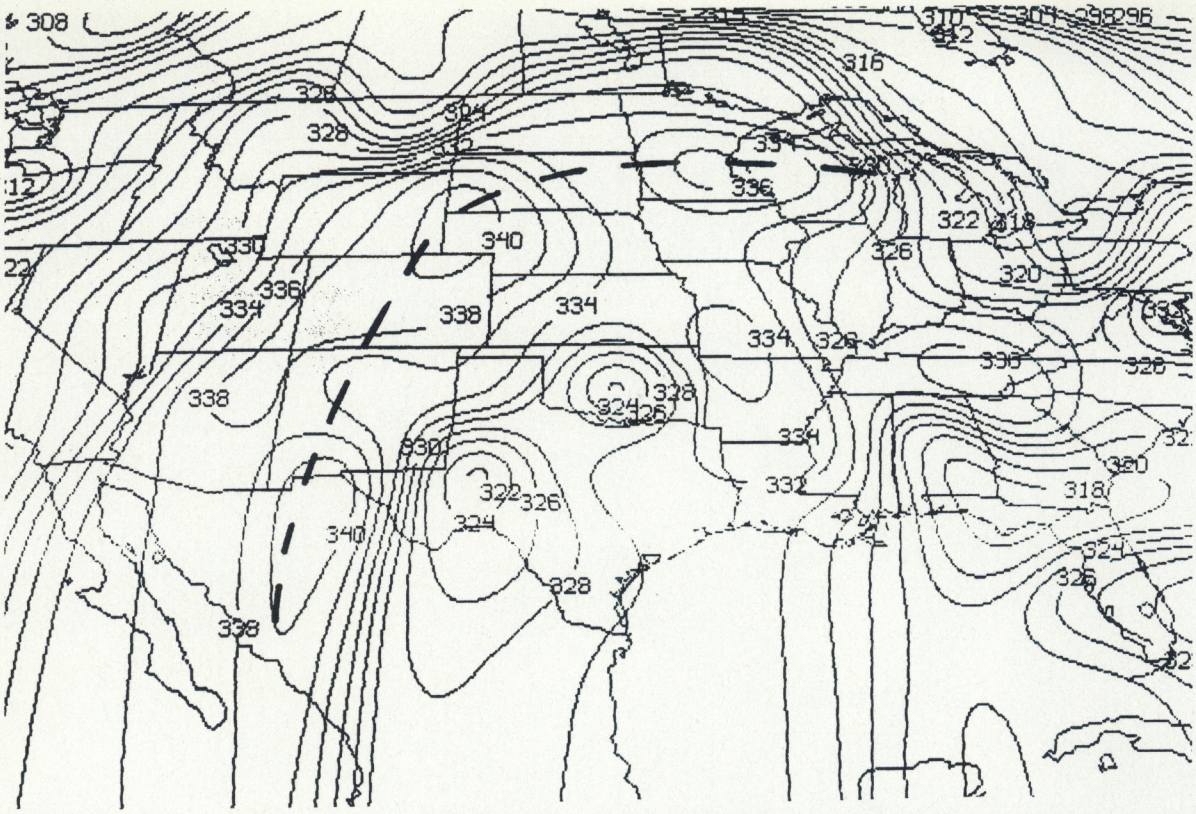

Figure 9b. 700 mb theta-e analysis (°K) for September 6, 1990, 0000 GMT.

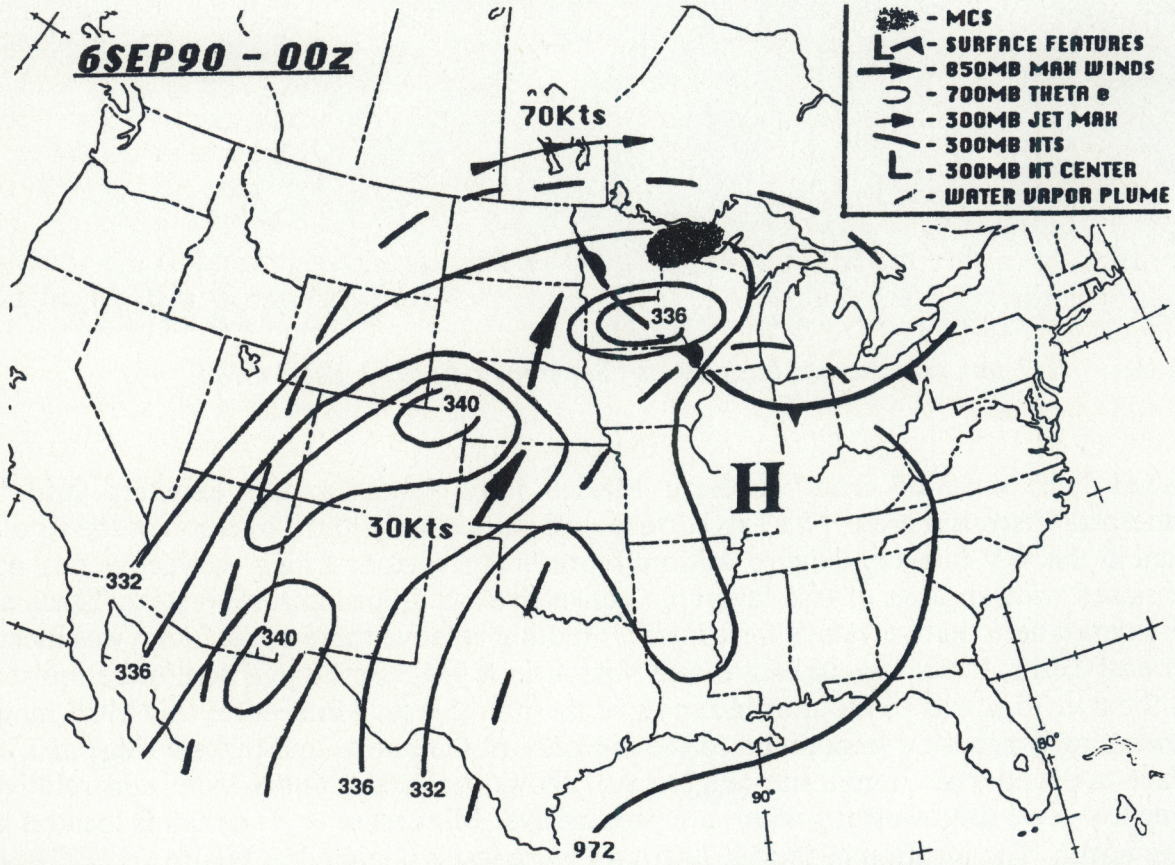

Figure 9c. Surface and upper composite of meteorological features associated with extreme heavy rainfall producing MCSs, for September 6, 1990, 0000 GMT.

3) 300 mb Wind Analyses

Every 12-hours, 300 mb wind analyses from the National Meteorological Center (NMC) were used to study the interactions between the positions of the upper level jet maxima and the WVP. The procedure consisted of examining closely the upper level features as shown on the WV imagery, and the 300 mb wind analyses. The jet streak positions were recorded on the WV imagery. This operation was repeated for the 129 event days and it was clear that for most of the cases, there was a WVP associated with a jet stream. The interactions between the WVP and the jet stream structure can be separated into two categories.

a) WV plume associated with a dual jet streak

An example of a WVP associated with a double jet streak structure took place on October 25, 1991. This was an event day for Oklahoma and Iowa. It is displayed in Figures 10a-10f. The 300 mb analysis (Figure 10b) shows a deep meridional trough located over the western U.S. with two jet streaks. One is located over the southwestern U.S. ("J - S" in Figure 10a) at the base of the trough with a maximum wind of 115 kts. Another jet streak (maximum wind 95 kts) is observed on the forward side of the trough extending from western Iowa towards eastern Canada.

The WV imagery on October 25, 1991, at 0000 GMT (Figure 10a) exhibits a tropical plume (T - P') originating from the ITCZ in the Pacific Ocean moving northeastward and nearly parallel to the subtropical jet stream axis, especially from the southwest U.S. into the southern and central Plains. This type of configuration where the jet stream axis and plume are quasi-parallel is often associated with slow moving and flash flood producing MCSs, especially when other conditions are favorable. Weldon and Holmes (1991) described this "parallel" configuration as well as those cases where the jet stream axis is more nearly normal to the plume. In these more normal configurations, MCSs tend to move faster. It has also been noted that slow moving plumes and MCSs are associated with mid-level isotherms that are quasi-parallel to the mid-level height contours. Faster moving plumes and MCSs are associated with mid-level isotherms that are nearly normal to the contours. In this case, the low-level theta-e ridge axes (dashed in Figure 10d) was also closely aligned to the eastern portion of the WVP.

A feature often observed with slow moving and back-building MCSs was thickness difluence (Jiang Shi and Scofield, 1987 and Juying and Scofield, 1989). Such was the case in this event, where the 850-300 mb thickness isopleths (Figure 10e) were diffluent over the southern and central plains and a back-building MCS was observed in Figure 10f at (B) over Oklahoma. Furthermore, the location of two jet streaks north and south of the EHR area respectively, created a transverse vertical circulation (Junker et al., 1990 and Corfidi, et al., 1990) in the exit and entrance regions of the two jet streaks. This supported intense vertical motions and the development of MCSs with EHR. Transverse vertical circulations helped to maintain the northward moisture transport from the ITCZ to the central U.S.. The relationship between EHR and the all important double jet streak structure was developed by NMC forecasters. This relationship is presented as a conceptual model in Figure 11.

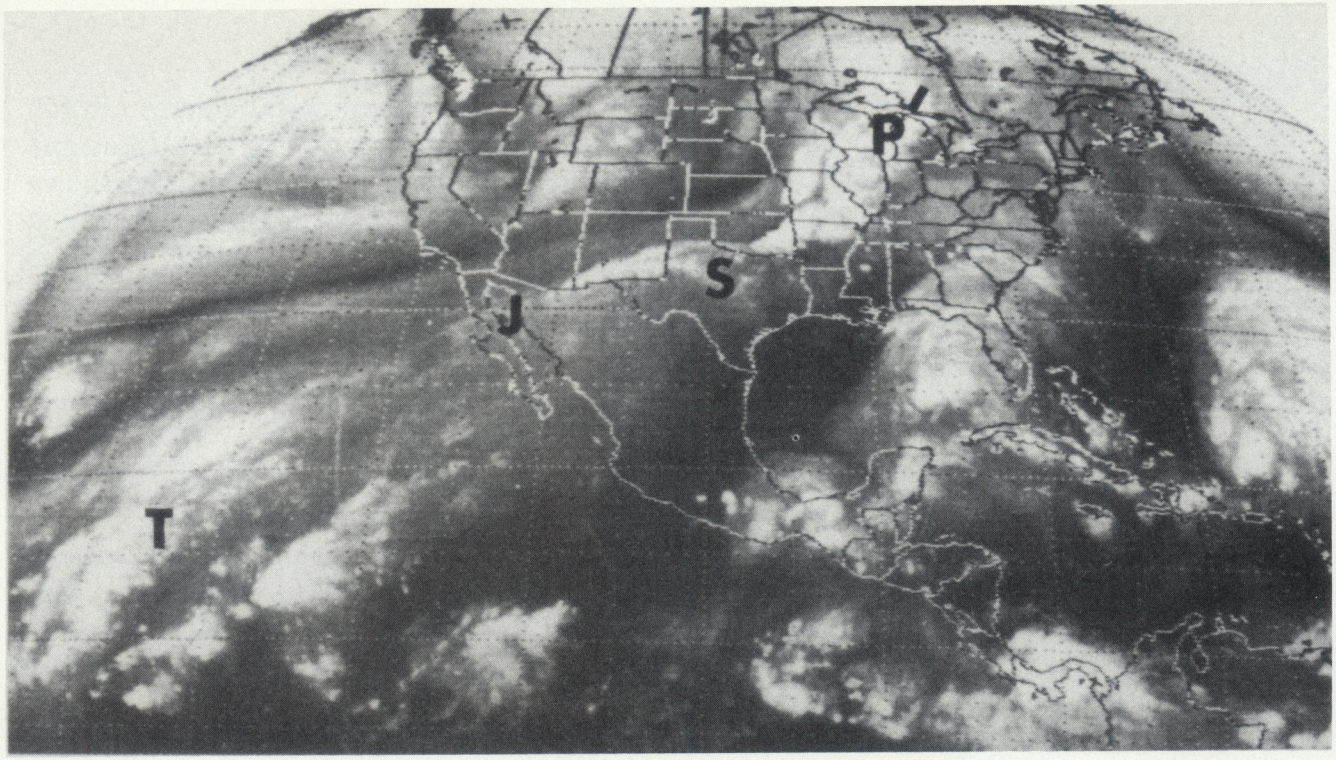

Figure 10a. 6.7 μm water vapor imagery for October 25, 1991, 0000 GMT.

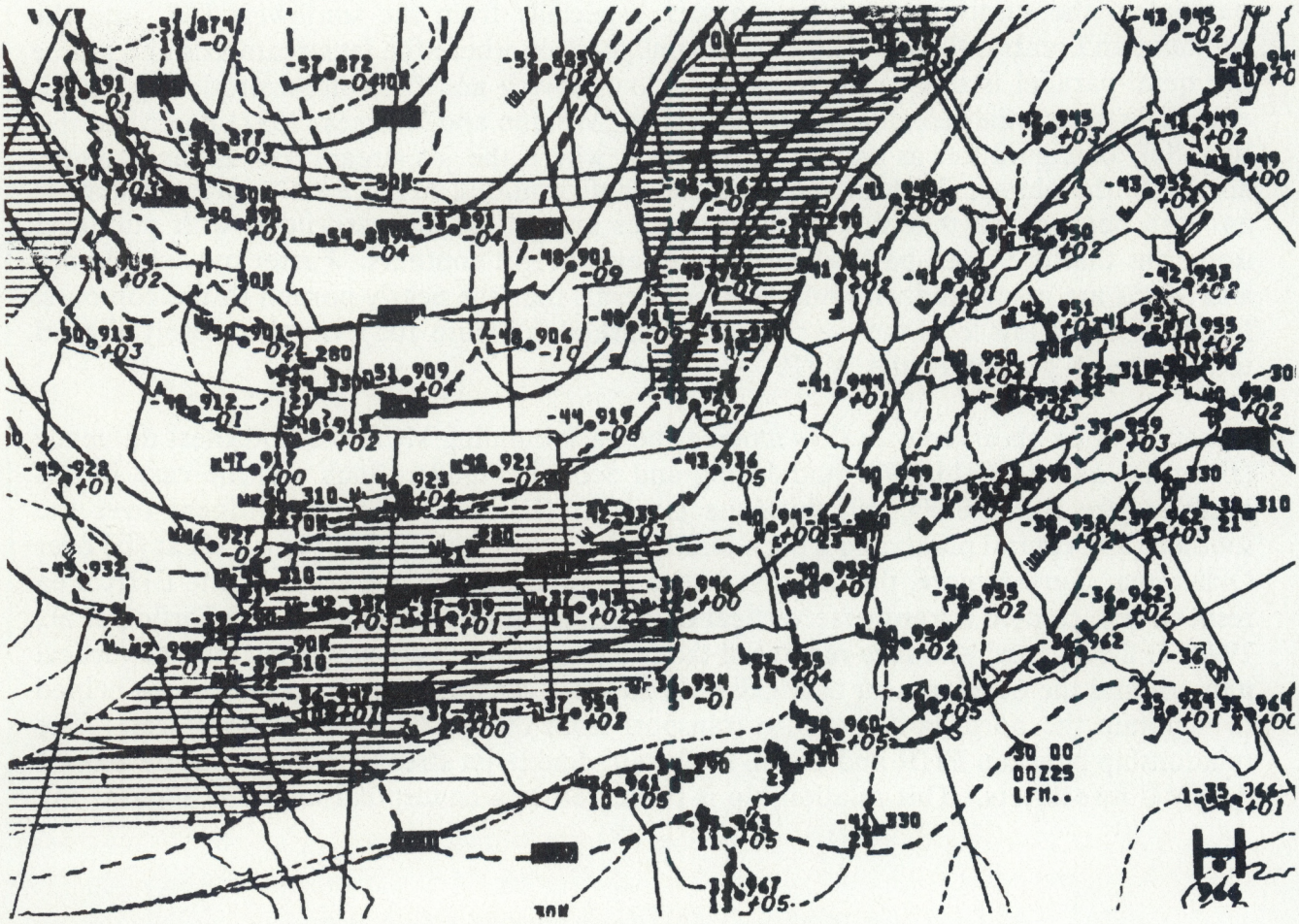

Figure 10b. 300 mb analysis for October 25, 1991, 0000 GMT.

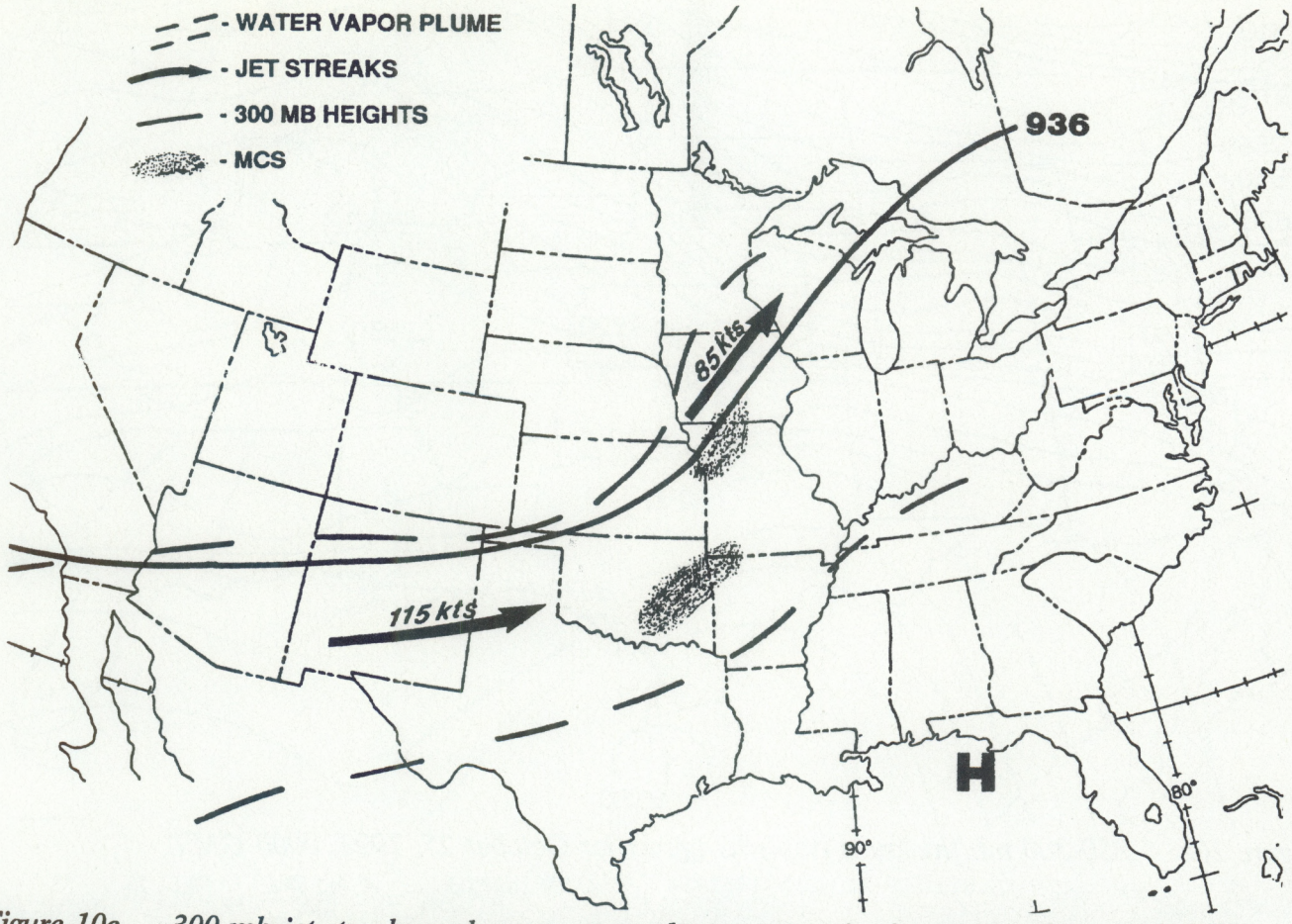

Figure 10c. 300 mb jet streaks and water vapor plume composite for extreme heavy rainfall events of October 25, 1991.

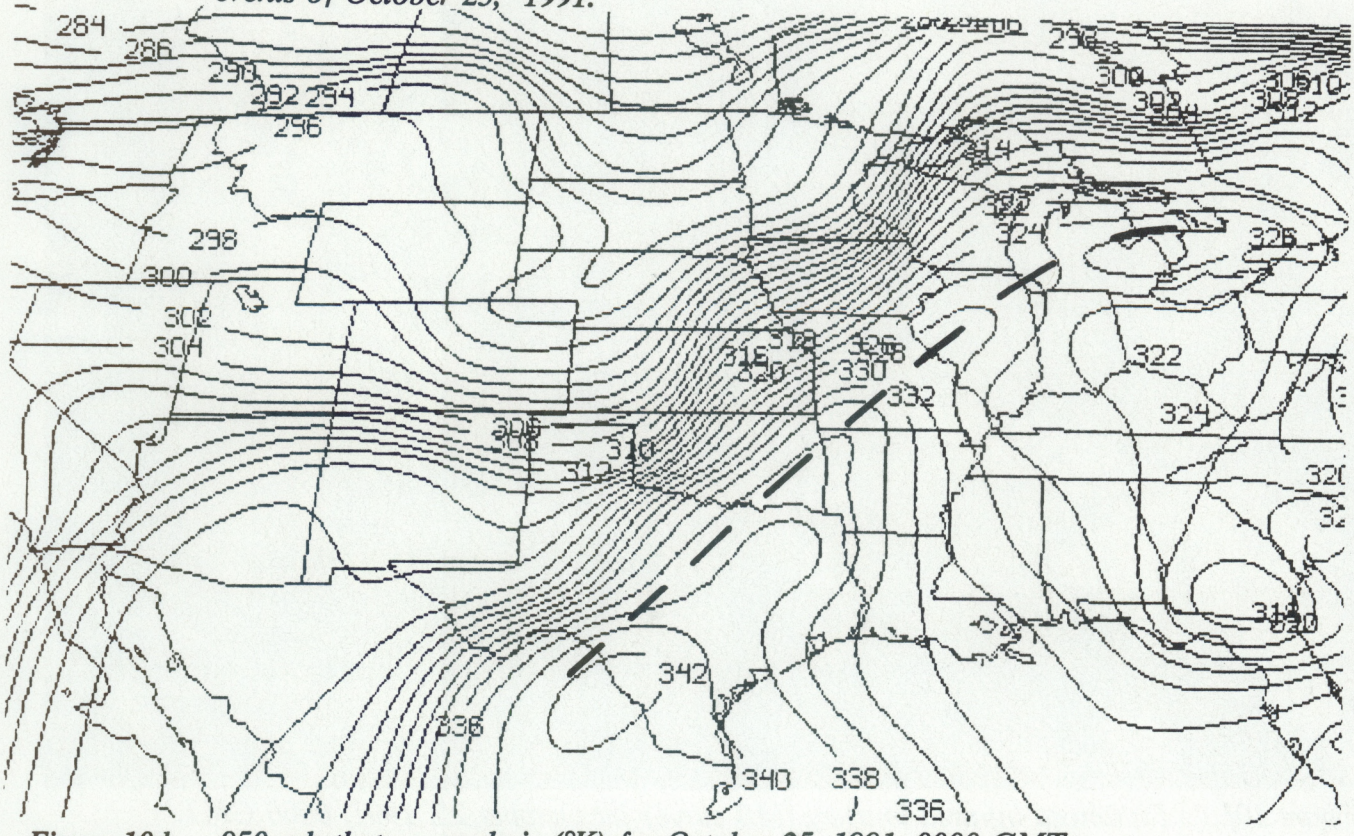

Figure 10d. 850 mb theta-e analysis (°K) for October 25, 1991, 0000 GMT.

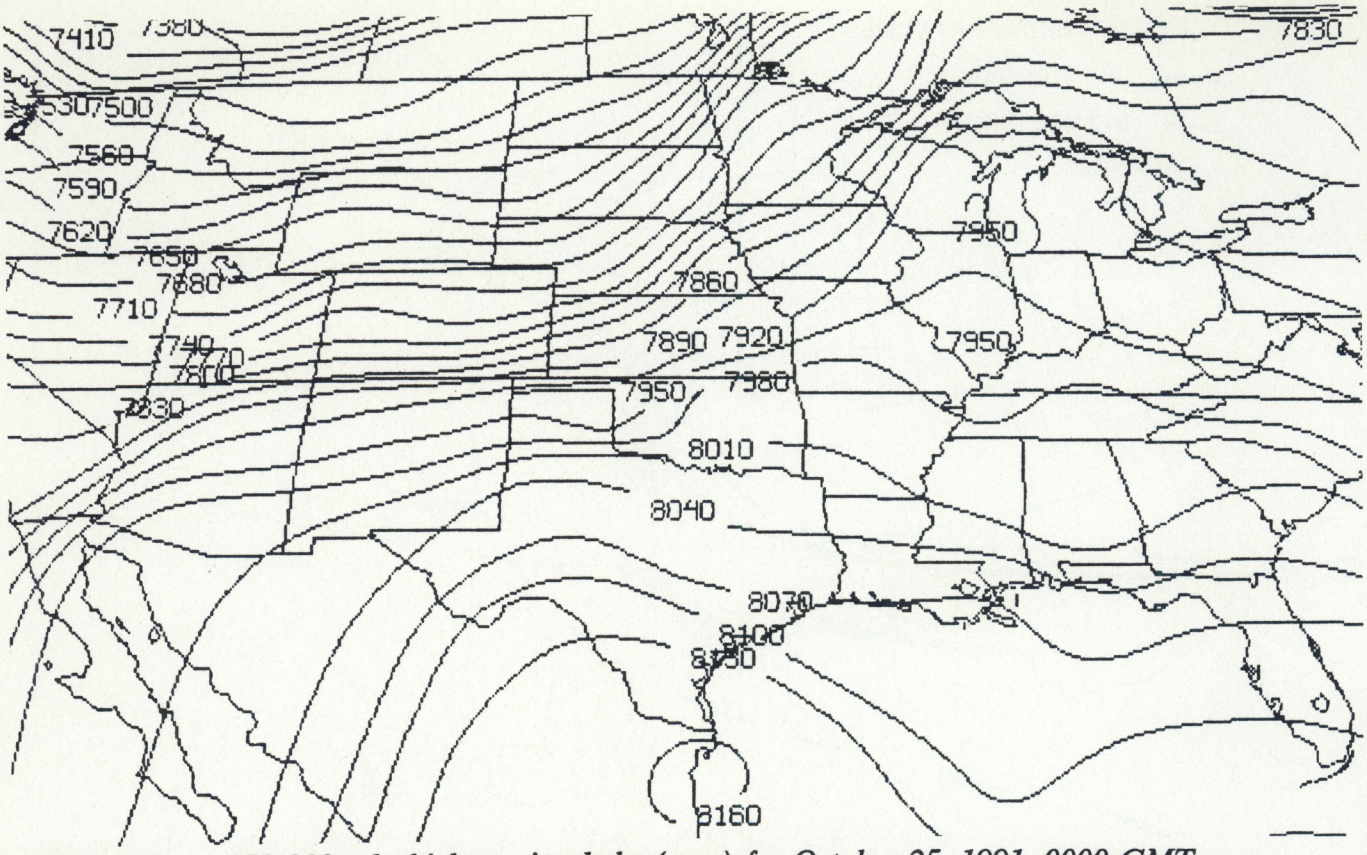

Figure 10e. 850-300 mb thickness isopleths (gpm) for October 25, 1991, 0000 GMT.

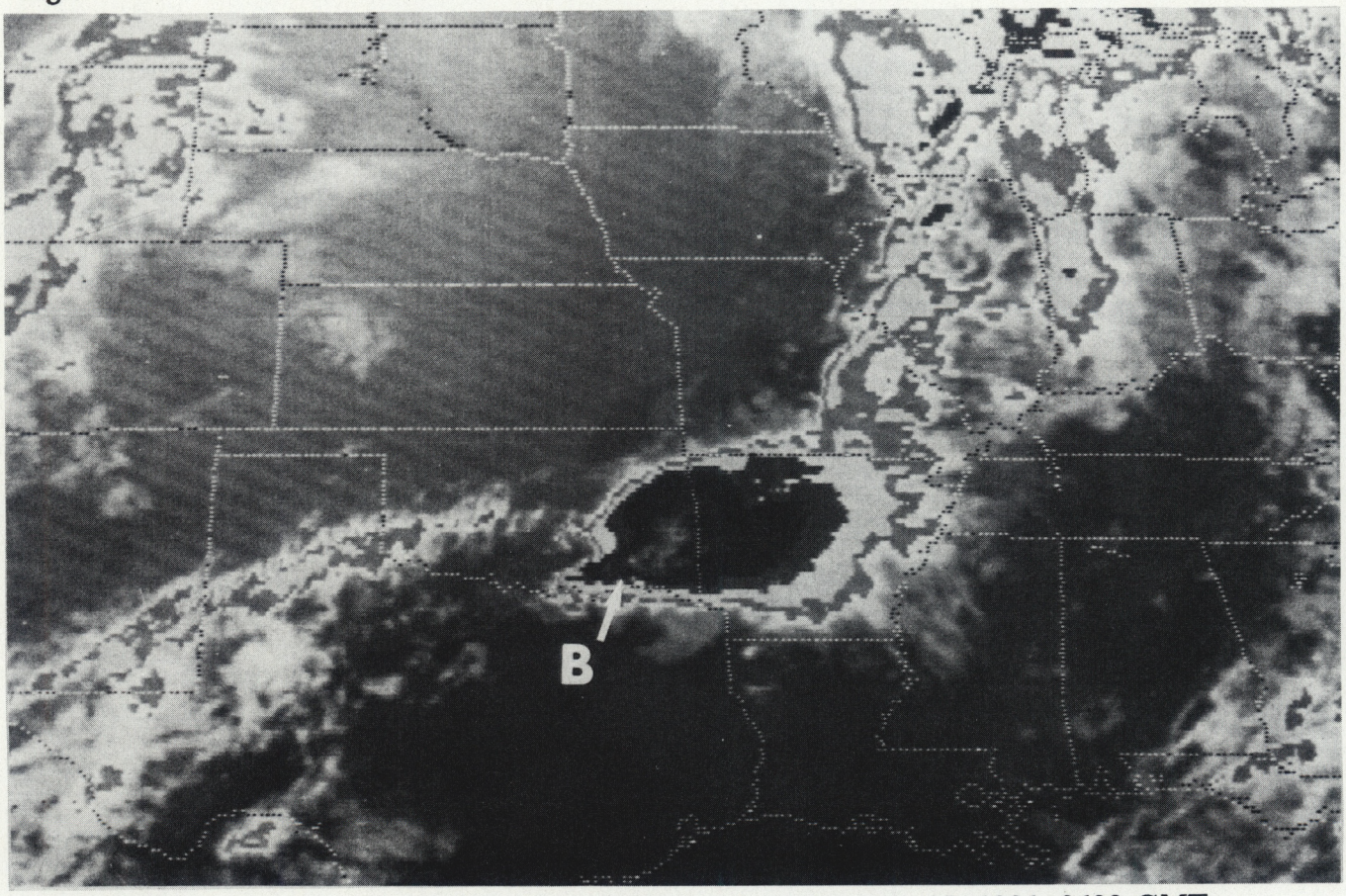

Figure 10f. Enhanced infrared imagery (MB curve) for October 25, 1991, 0600 GMT.

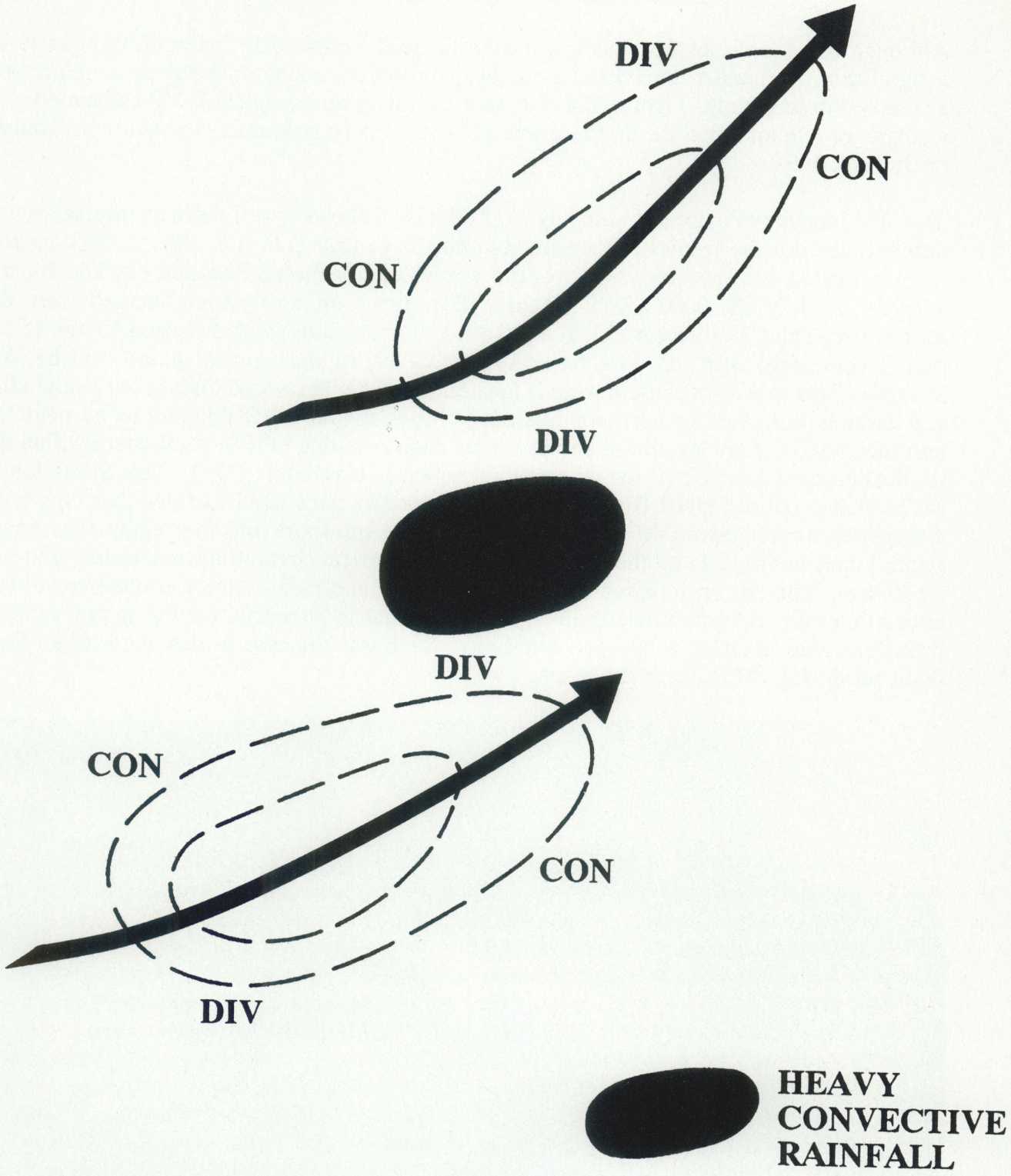

Figure 11. Conceptual model of a double jet streak structure.

b) WV plume associated with a single jet streak

Although the double jet streak configuration discussed previously has been thought to be a significant mechanism for initiating intense convection, a single jet streak structure was also noted in this study. Figures 12a, 12b, and 12c illustrate a tropical WVP associated with a single jet stream structure on the event day over Texas, Arkansas, and southern Kansas on July 28, 1991.

The WV imagery (Figure 12a) on July 27, 2100 GMT shows a well defined tropical plume originating from the tropics and extending into the central U.S. (T - P'); a dark narrow band is located on its western side over the Texas and Oklahoma Panhandles. The 300 mb analysis on July 28, 0000 GMT (Figure 12b) shows an anticyclone located over the southwestern and southeastern U. S. and an axis of maximum winds between 55 and 65 kts that is coincident with the dark back edge ("D - B") of the tropical plume on the WV imagery. This axis of maximum wind is located from the Texas and Oklahoma panhandles and extends northeast to northern Missouri. Much of the EHR appears to be near the entrance region of the jet streak. Intense convection resulting in EHR took place within the tropical plume just south of the jet entrance region in Oklahoma (12c). This formation of MCSs that produced EHR from a single jet streak structure demonstrates that high level divergence creates favorable conditions for moisture transport into the region. The heavy rainfall does not have to be the result of transverse vertical circulations associated with two jet streaks. The entrance region of a single jet streak and its associated transverse vertical circulation may induce sufficient divergence aloft that is favorable for lifting any capping inversions and releasing convective instability. Such was the case in this event when flash flood producing MCSs were the result.

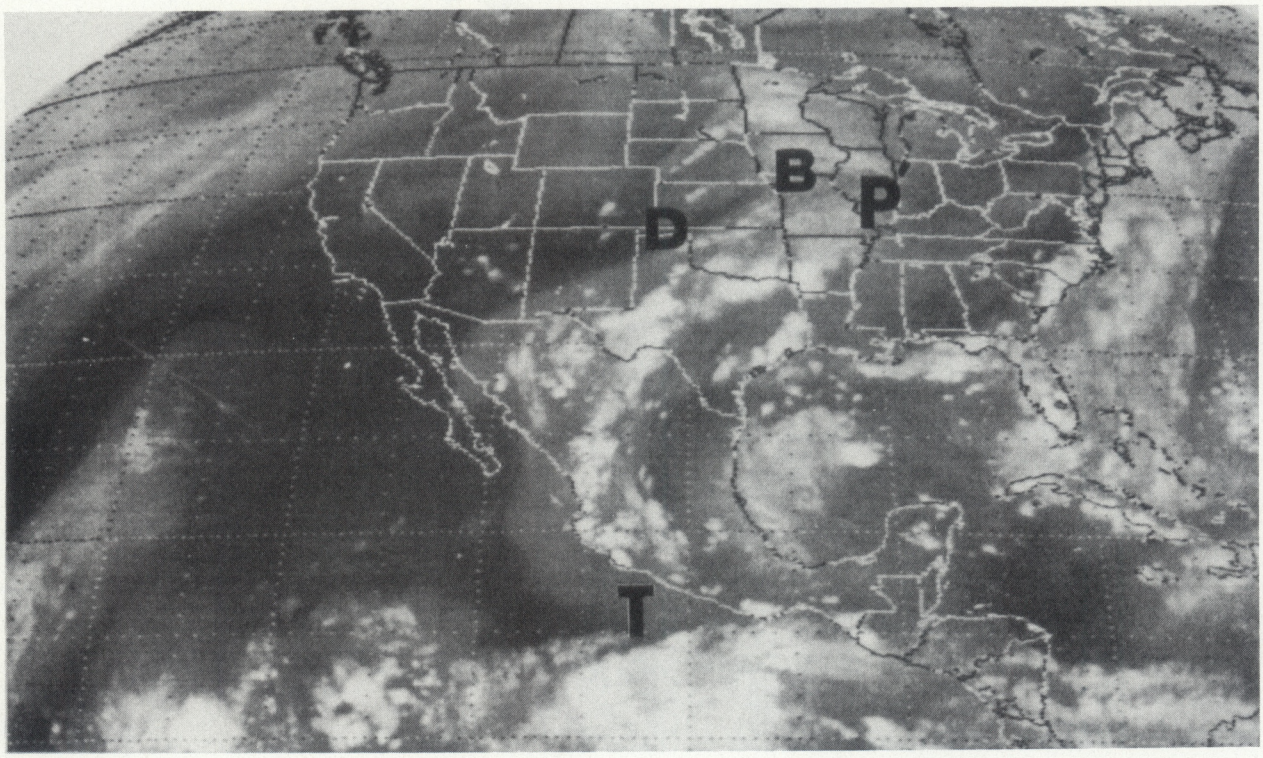

Figure 12a. 6.7 μm water vapor imagery for July 27, 1991, 2100 GMT, 1991.

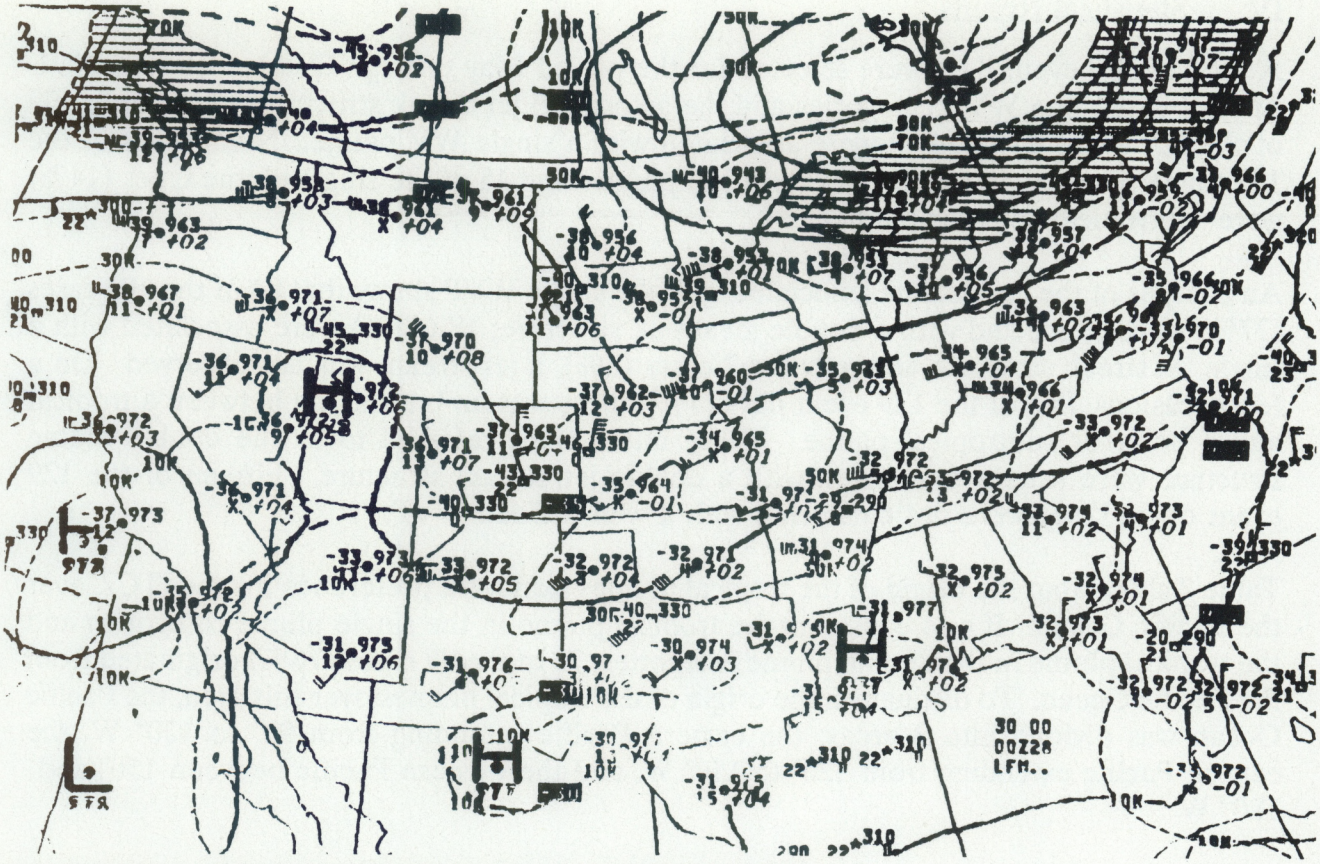

Figure 12b. 300 mb analysis for July 28, 1991, 0000 GMT.

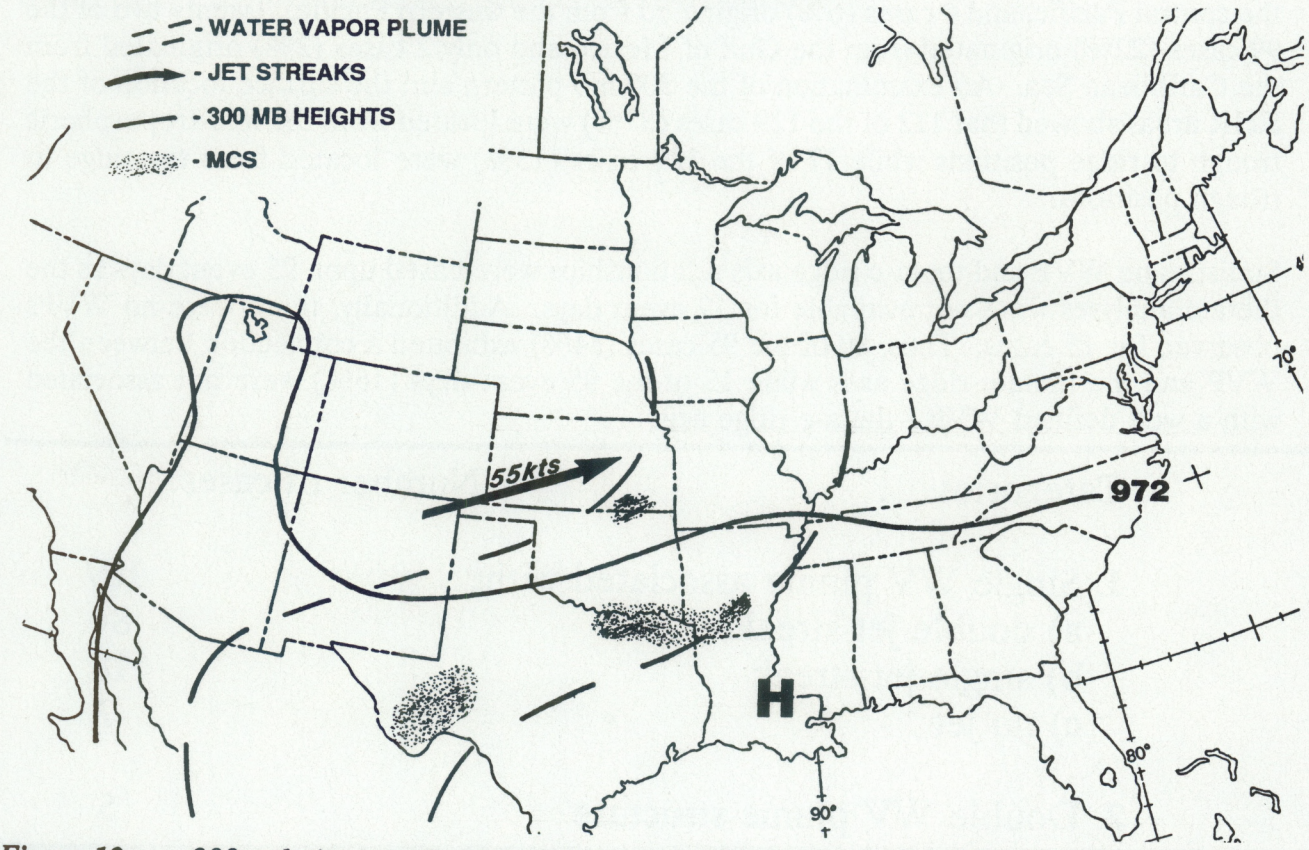

Figure 12c. 300 mb jet streak and water vapor plume composite for the extreme heavy rainfall event of July 28, 1991.

IV. Statistical Results

A total of 129 event days were selected for the period May through October of 1989-1991. Table 1 shows the WVP categories and the associated jet streak structures at 300 mb; 109 of the 129 event days (84%) were associated with a single WV plume. Ninety four of the 109 single plume types (86%) were tropical plumes and 15 of the single plume types (14%) were subtropical or polar plumes.

An analysis of the jet maxima associated with the single WVP shows that 84 of the 109 cases (77%) were connected with a double jet streak structure; 18 (17%) were associated with a single jet streak structure and only for 7 cases (6%), a jet stream was not observed. On a few occasions, five of the 129 event days (4%), there was an interaction between a tropical and a polar or subtropical plume. These interactions referred to as the double plume structure were usually associated with a double jet stream structure. Fifteen of the 129 event days (12%) were not connected with a well defined WVP.

Table 2 shows that the origin of the tropical plumes exhibits a preference for the ITCZ over the Pacific Ocean. If one considers the tropical plume in the single plume categories and the tropical plume in the double plume categories, 75 of the 99 cases (76%) originated from the Pacific Ocean. To distinguish the origin of the tropical plumes over this area, the Pacific Ocean was divided into 3 areas: the eastern Pacific extending from 90° to 120° W, the central Pacific extending from 120° to 150° W, and the western Pacific between 150° and 180° W.

Forty six cases (61%) originated from the eastern Pacific, 25 cases (33%) originated from the central Pacific, and 4 cases (6%) originated from the western Pacific. Twenty two of the 99 cases (22%) originated from the Gulf of Mexico and only 2 cases (2%) originated from the Caribbean Sea. An examination of the 300 mb pattern and the surface location of the EHR areas showed that 112 of the 129 cases (87%) were located from the mid-tropospheric trough to ridge positions while 17 of the 129 cases (13%) were located from the ridge to trough positions.

Statistics on WVP and theta-e ridge axis relationships were based upon 95 event days as the theta-e analyses were not available for 19 event days. Additionally, there were no WVPs observed for 15 cases. Thus, 80 of the 95 cases (84%) exhibited a connection between the WVP and the theta-e ridge axes while 15 of the 95 event days (16%) were not associated with a well defined WVP - theta-e ridge axis.

Categories	Number of cases
1. Single WV plume associated with:	109
a) double jet streaks	84
b) single jet streak	18
c) no jet	7
2. Double WV plume structure	5

Table 1. Water Vapor Plume Categories

Origins	Number of trop. plume
Pacific Ocean	75
Gulf of Mexico	22
Caribbean Sea	2

Table 2. Origin of the Tropical Plumes

V. Examples of Extreme Heavy Rainfall events

1) Event Day of June 16, 1989

EHR occurred over southern Alabama where two stations reported 9.0 inches (225 mm) and 7.3 inches (182.5 mm), respectively, and over Kentucky where one station reported 9.6 inches (240 mm). If the report is correct, the event over Kentucky could be the result of a stationary, orographic-induced, "warm infrared (IR) top" MCS (Scofield, et. al., 1980) located under the tropical WVP. Figure 13 shows the location of the EHR. Note that during the 24 hour period ending on June 16, 1989 at 1200 GMT, heavy rainfall occurred over Alabama, Georgia, Tennessee, and Kentucky. The following discussion will focus on the EHR that fell over Alabama. WV imagery for June 15, 0000 and 1200 GMT, displayed in Figures 14a and 14b, respectively, indicates a double plume structure was present. The double plume structure was depicted by: (1) a subtropical plume indicated by (S - P'), originating from the Pacific Ocean, that moved northeastward to the northwestern U.S. and then southward to northern Mexico; it then stretched east-northeastward and approached, (2) a tropical plume indicated by (T - P'), extending from the ITCZ north-northeastward to the Ohio Valley. During this 12 hour period (0000 to 1200 GMT), the subtropical and tropical plumes became connected. Several embedded MCSs developed within the tropical plume.

An observation of earlier IR images (not shown here) showed that MCSs developed over Texas, Louisiana and Mississippi on June 14, and 15, 1989, and produced EHR over these areas. As the MCSs moved slowly to the east, EHR was reported over southern Alabama. Enhanced IR imagery (at 1200 GMT) displayed in Figure 15a revealed well defined MCSs over the Gulf of Mexico (at "M") and southern Alabama (at "S"). A sequential view of the IR imagery showed that newly formed clusters developed over southern Alabama on June 15, 0900 GMT. During the next six hours, these clusters merged into a MCS that exhibited back building characteristics as the MCS over southern Alabama (at "S") built backwards and in turn merged with MCSs moving northward from the Gulf of Mexico. IR imagery at 1400 GMT (Figure 15b) showed that back building MCSs (at "S") tended to be quasi-stationary and produced EHR. These MCSs developed in the eastern side of the tropical plume and moved eastward to southwestern Georgia where 100 mm of rain were reported.

Composites of meteorological features are shown in figures 16a and 16b. On June 15, 0000 GMT, two surface fronts extended from Texas to a low located over northern Indiana and from Mississippi to another low located over Maryland. By 1200 GMT, both lows weakened and the western surface front disappeared while the eastern front advanced slowly to the east (Figure 16b). At 300 mb, a jet stream with associated jet streaks was located over the northwestern U.S. and the northern Ohio Valley. The jet stream was connected with a ridge over the Rocky Mountains and a rather deep meridional trough over the central U.S.. A time lapse view of WV imagery showed that the movements of the plumes were well related to the circulation field at 300 mb. The 300 mb jet stream axis nearly paralleled the tropical plume in the southeastern U.S.. As mentioned earlier in Section III-3-a, slow moving and flash flood producing MCSs often occurred with this "parallel" type of configuration between the jet stream axes and the plumes; this of course assumes that other conditions were favorable. Some of these other conditions are now discussed. The location of the 850 mb maximum winds and theta-e ridge axis in figure 16a and 16b showed that low-level warm and moist air advection (theta-e advection) were occurring over Alabama, Tennessee and Kentucky. A theta-e ridge axis at 850 mb was located from the Gulf of Mexico northward into Kentucky. The orientation of the potential energy axes (i.e. axes of the theta-e ridge and the low-level maximum wind) as described by Scofield and Robinson (1990, 1992) were closely aligned with the tropical plume. Thickness difluence (not shown) was also present over the southeastern U.S..

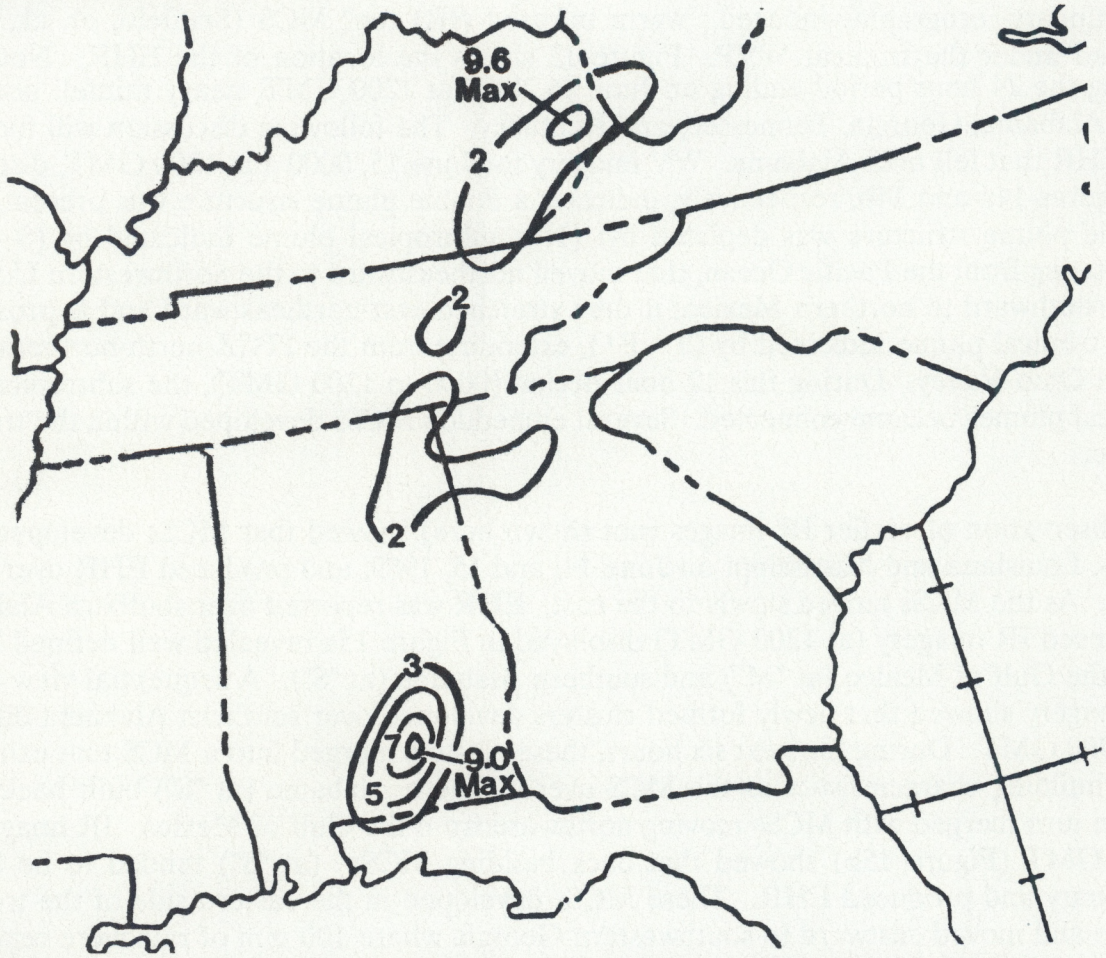

Figure 13. 24 hour rainfall analysis (inches) ending at June 16, 1989 1200 GMT.

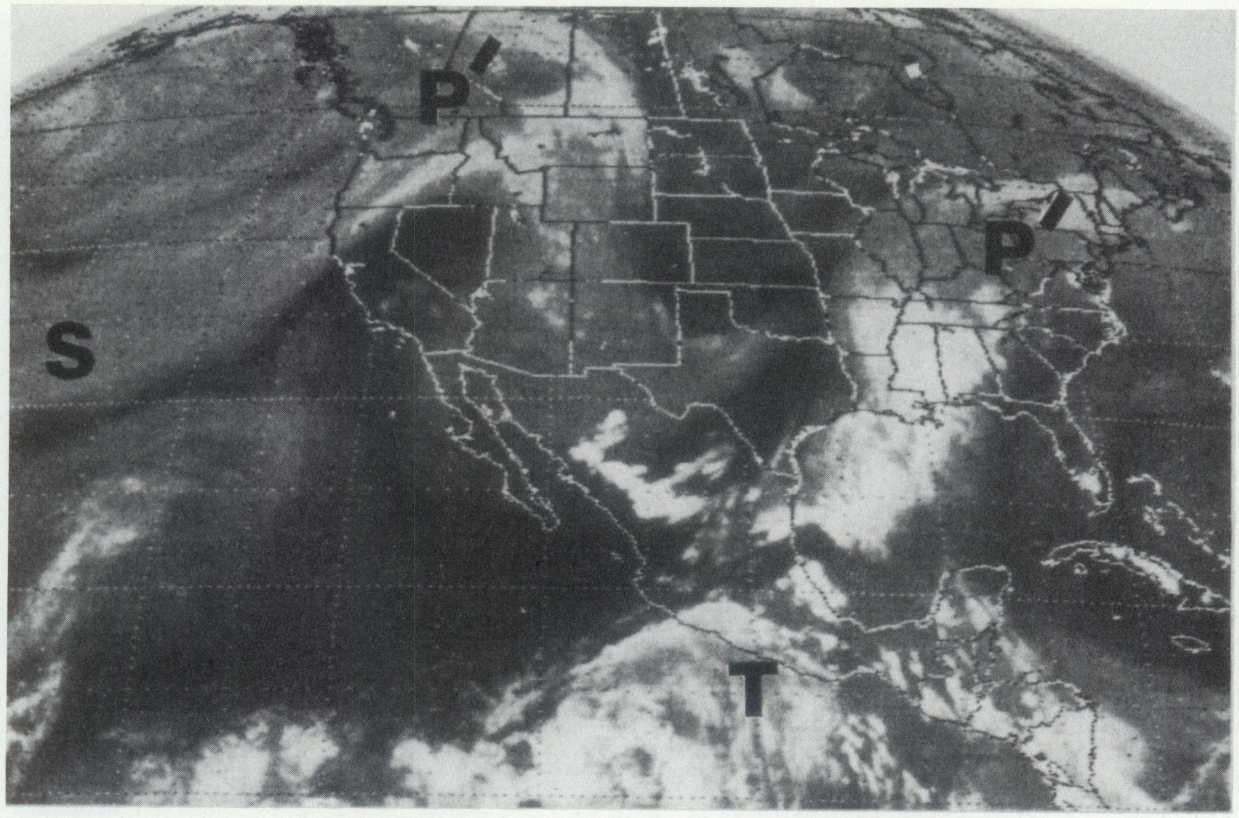

Figure 14a. 6.7 μm water vapor imagery for June 15, 1989, 0000 GMT.

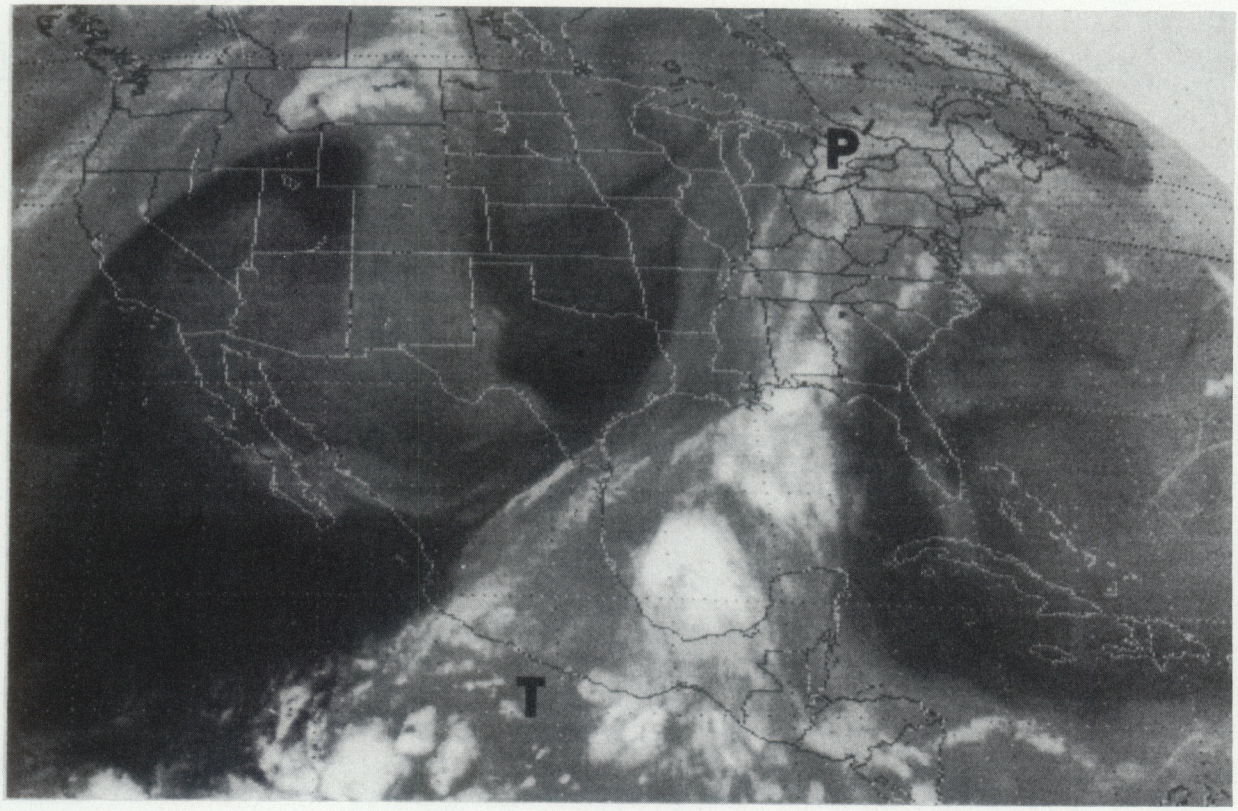

Figure 14b. 6.7 μm water vapor imagery for June 15, 1989, 1200 GMT.

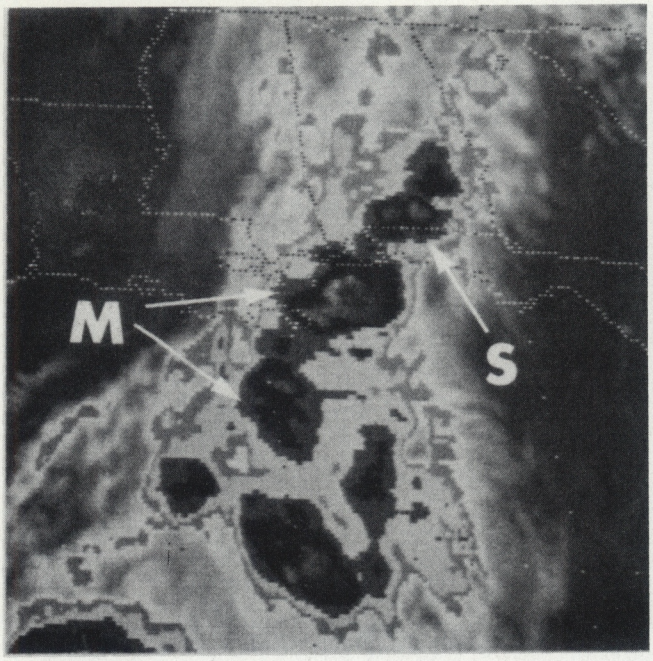

Figure 15a. Enhanced infrared imagery (MB Curve) for June 15, 1989, 1200 GMT.

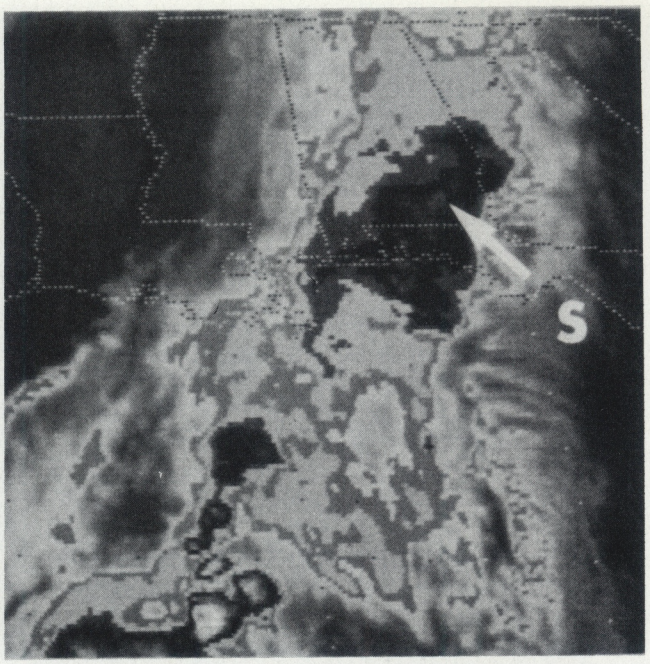

Figure 15b. Enhanced infrared imagery (MB Curve) for June 15, 1989, 1400 GMT.

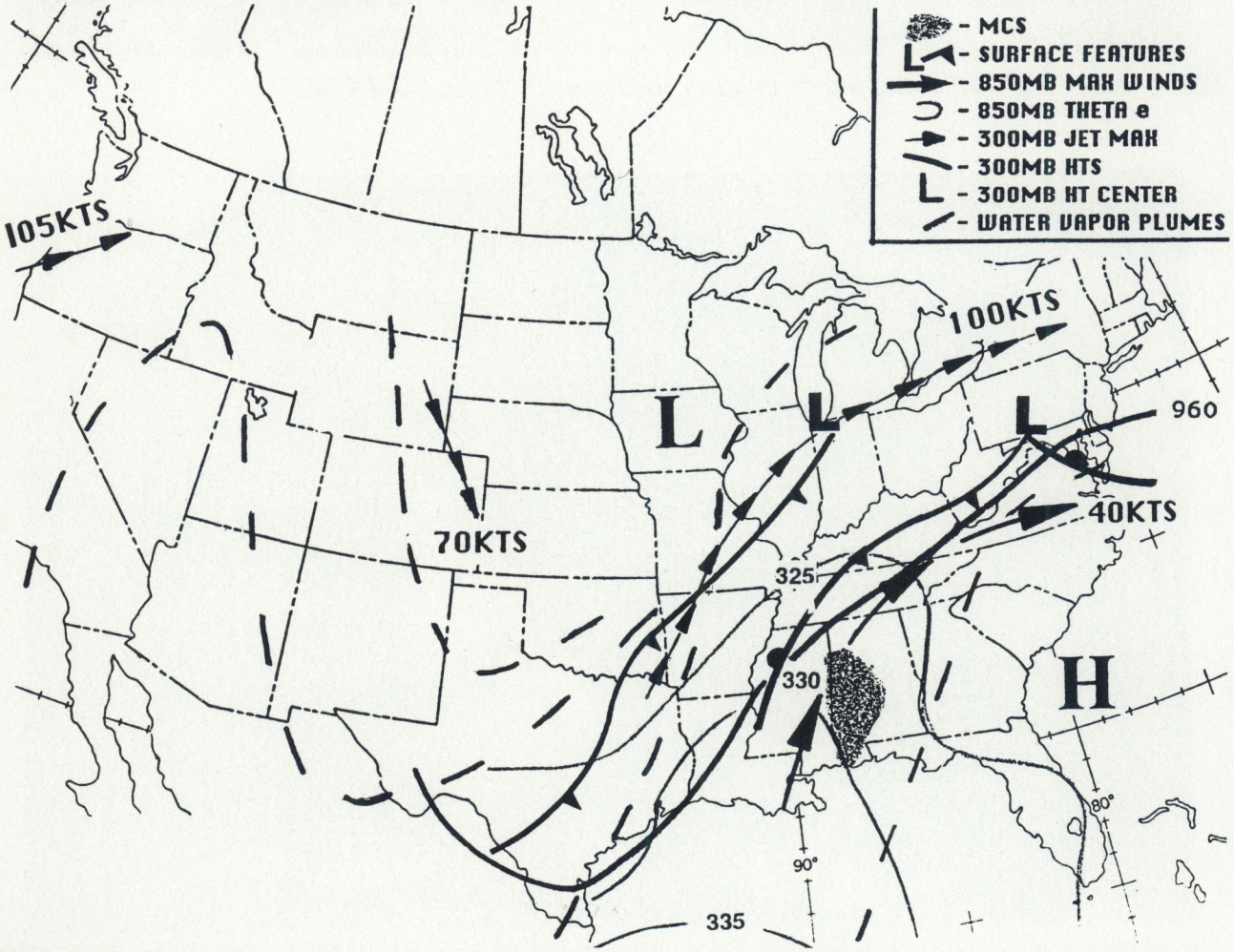

Figure 16a. Surface and upper air composite of meteorological features associated with extreme heavy rainfall MCSs for June 15, 1989, 0000 GMT.

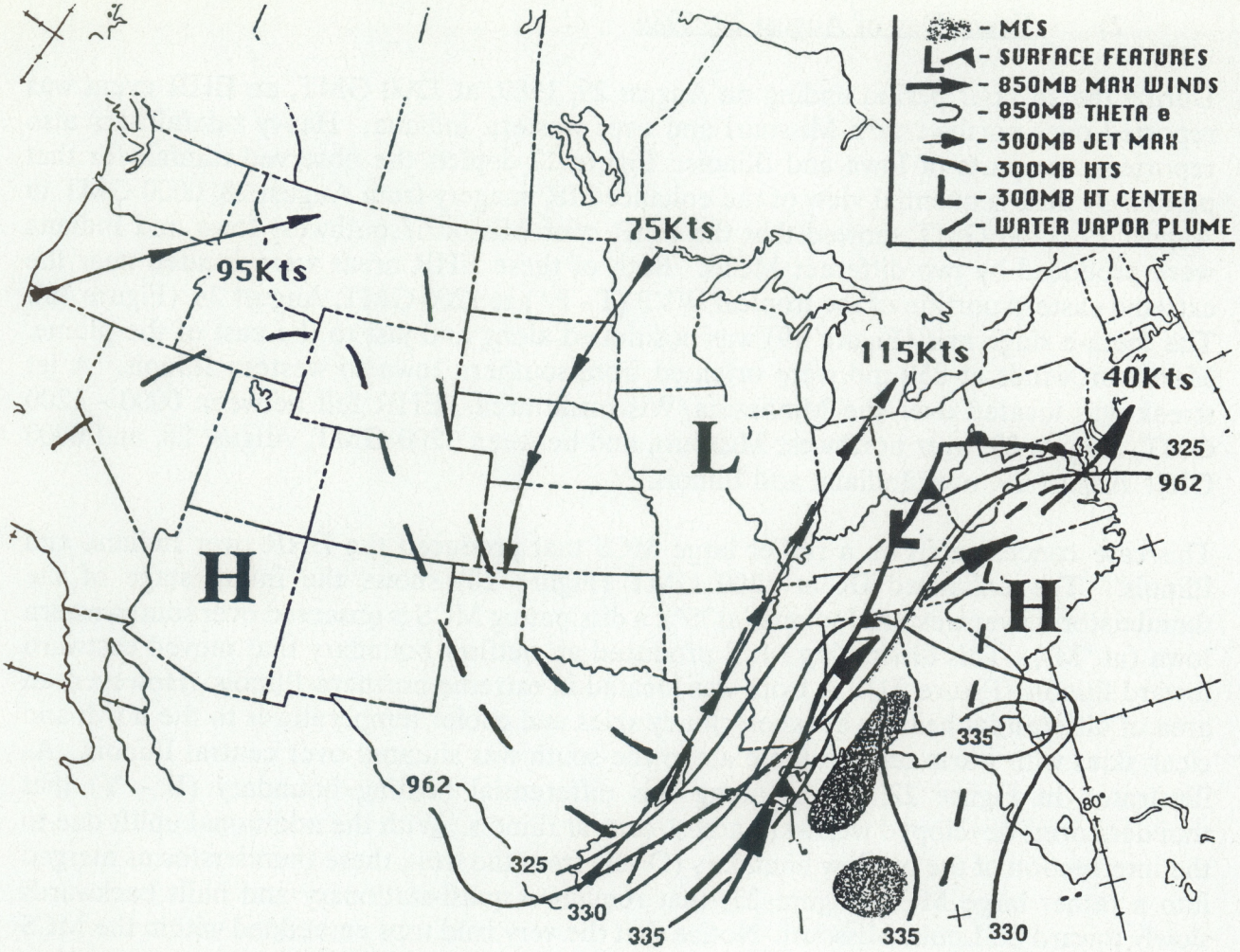

Figure 16b. Surface and upper air composite of meteorological features associated with extreme heavy rainfall MCSs for June 15, 1989, 1200 GMT.

In summary, the above features showed: (1) the presence of a tropical WVP; (2) a continuous replenishment of moist unstable air to the southeastern U.S.; and (3) the presence of upward vertical motion since the southeast was located in the front-entrance region of the jet streak positioned over the northern Ohio Valley. All of these features contributed to the development of slow moving (back building) MCSs that produced flash floods and ERH over the southeastern U.S..

2) Event Day of August 29, 1989

During the 24 hour period ending on August 29, 1989, at 1200 GMT, an EHR event was reported over northwestern Missouri and over western Indiana. Heavy rainfall was also reported over parts of Iowa and Illinois. Figure 17 depicts the observed rainfall for that period. A time sequential view of the enhanced IR imagery from August 28, 0000 GMT to August 29, 1200 GMT showed that the EHR over Missouri/southwest Iowa and Indiana were produced by two different MCSs. Both of these EHR areas were located near the extreme eastern portion of the tropical WVP (T - P') at 1200 GMT, August 28, (Figure 18). The theta-e ridge axis (Figure 19) was positioned along and just to the east of the plume. Maximum winds at 850 mb were oriented from southern Iowa to western Illinois. A jet streak was located over the Minnesota/Wisconsin area. EHR fell between 0000 - 1200 GMT, August 29, over northwest Missouri, and between 1200 GMT, August 28, and 0000 GMT August 29, over Indiana and Illinois.

This case concentrated on a rather large MCS that produced the EHR over Indiana and Illinois. The enhanced IR at 1200 GMT (Figure 20) shows the initial stage of the thunderstorm over western Indiana (at "S"); a dissipating MCS is observed over southwestern Iowa (at "M"). This dissipating MCS produced an outflow boundary that moved eastward toward Illinois (Figure 21). A front was located in extreme northern Illinois. However, an area of differential heating between cloudy skies and cooler temperatures to the north and clear skies with warm and unstable air to the south was situated over central Illinois. As illustrated in Figure 22, it was along this differential heating boundary (B - Y) that thunderstorms developed westward across central Illinois. With the additional uplift due to the intersection of the outflow boundary (O - B) from the west, these thunderstorms merged into a rather large MCS (Figure 23) that remained quasi-stationary and built backwards slowly toward St. Louis, Missouri. Notice that the very cold tops embedded within the MCS (at "H") were associated with extremely heavy rainfall. The surface and upper composites for August 29, 0000 GMT depicted that the MCS over the Illinois/Indiana area modified the environment with its rain cooled air and created a rather pronounced theta-e minimum over the same area (Figure 24). However, a key feature is revealed by the fact that high theta-e air was being replenished in western Illinois by relatively strong low-level winds. This instability advection along with thickness difluence (not shown) helped to produce the back building MCS observed over western Illinois. A jet streak continued to be present over the Minnesota/Wisconsin area.

The WV imagery ending on August 29, 0000 GMT (Figure 25) showed that the tropical plume was nearly stationary during this 12 hour period (1200 GMT, Figure 18 to 0000 GMT, Figure 25). Notice how the MCSs developed in the eastern portion of the plume from west Texas north-northeastward to Illinois and Indiana. As mentioned before, the theta-e ridge axis was also located in the eastern portion of this plume. In fact, a time sequential view of the WV imagery showed that the tropical plume was indeed quasi-stationary and that the inside boundary on its western edge was becoming more distinct. Formation of this inside boundary is usually associated with deformation and upper air anticyclogenesis (Weldon and Holmes, 1991). As a result, the location of upper air features, such as the tropical plume, will be slow to change. Thus a synoptic scale pattern that favors heavy rainfall and flash floods should persist.

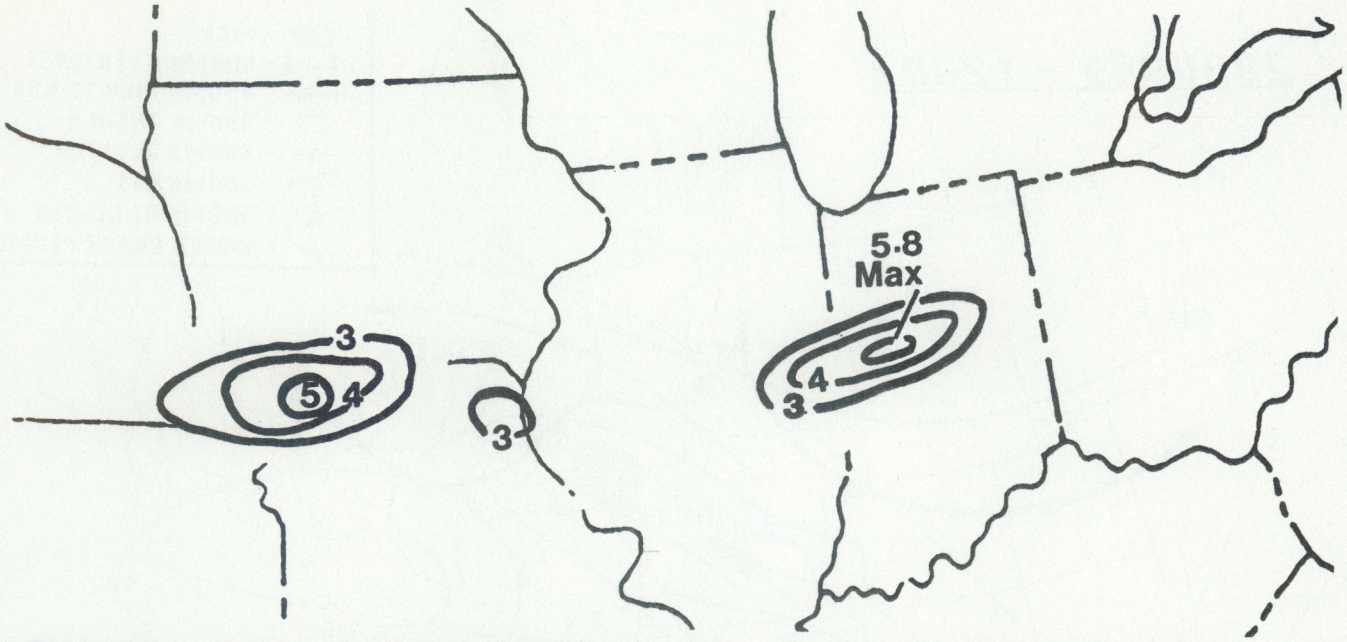

Figure 17. 24 hour rainfall analysis (inches) ending at August 29, 1989, 1200 GMT.

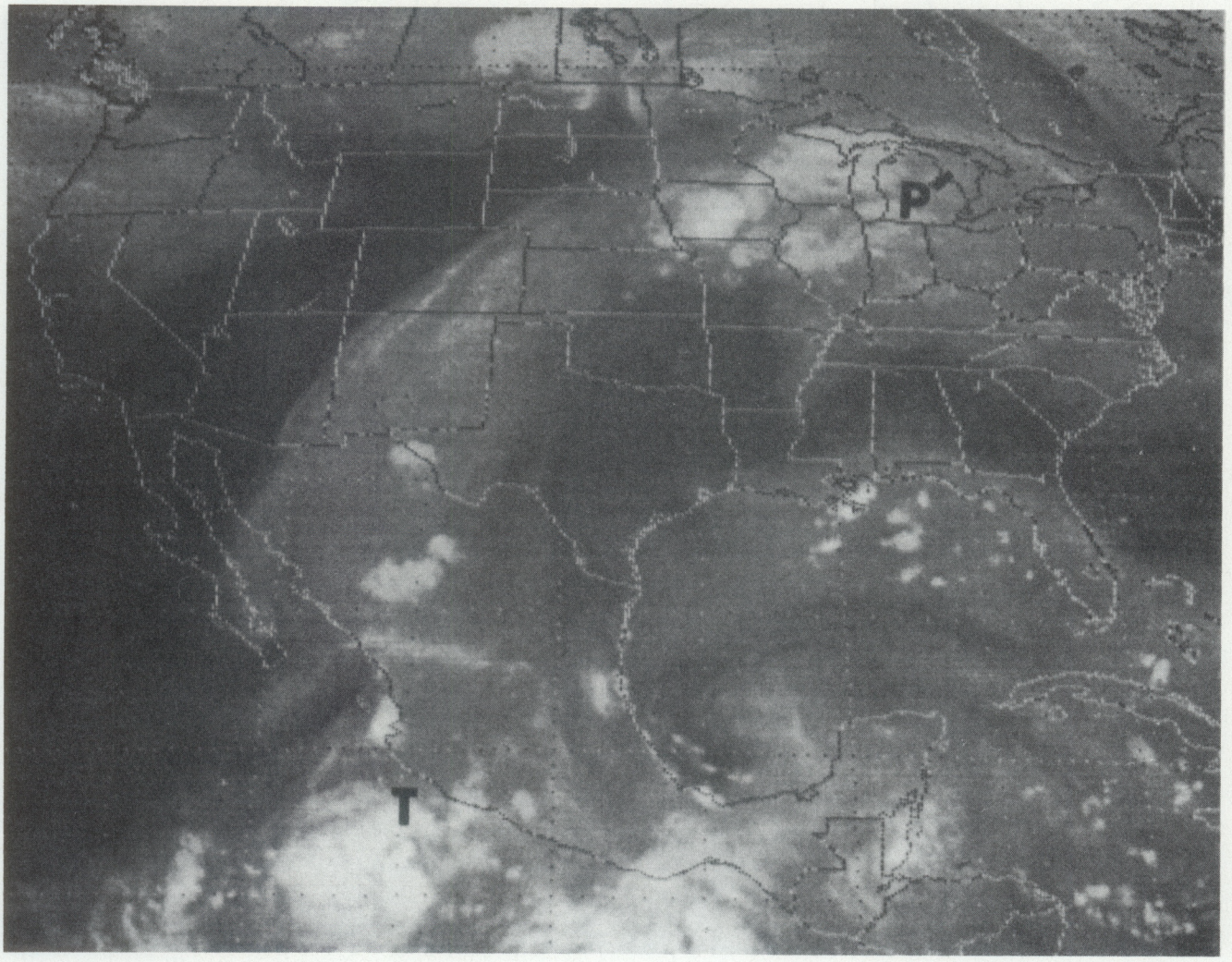

Figure 18. 6.7 μm water vapor imagery for August 28, 1989, 1200 GMT.

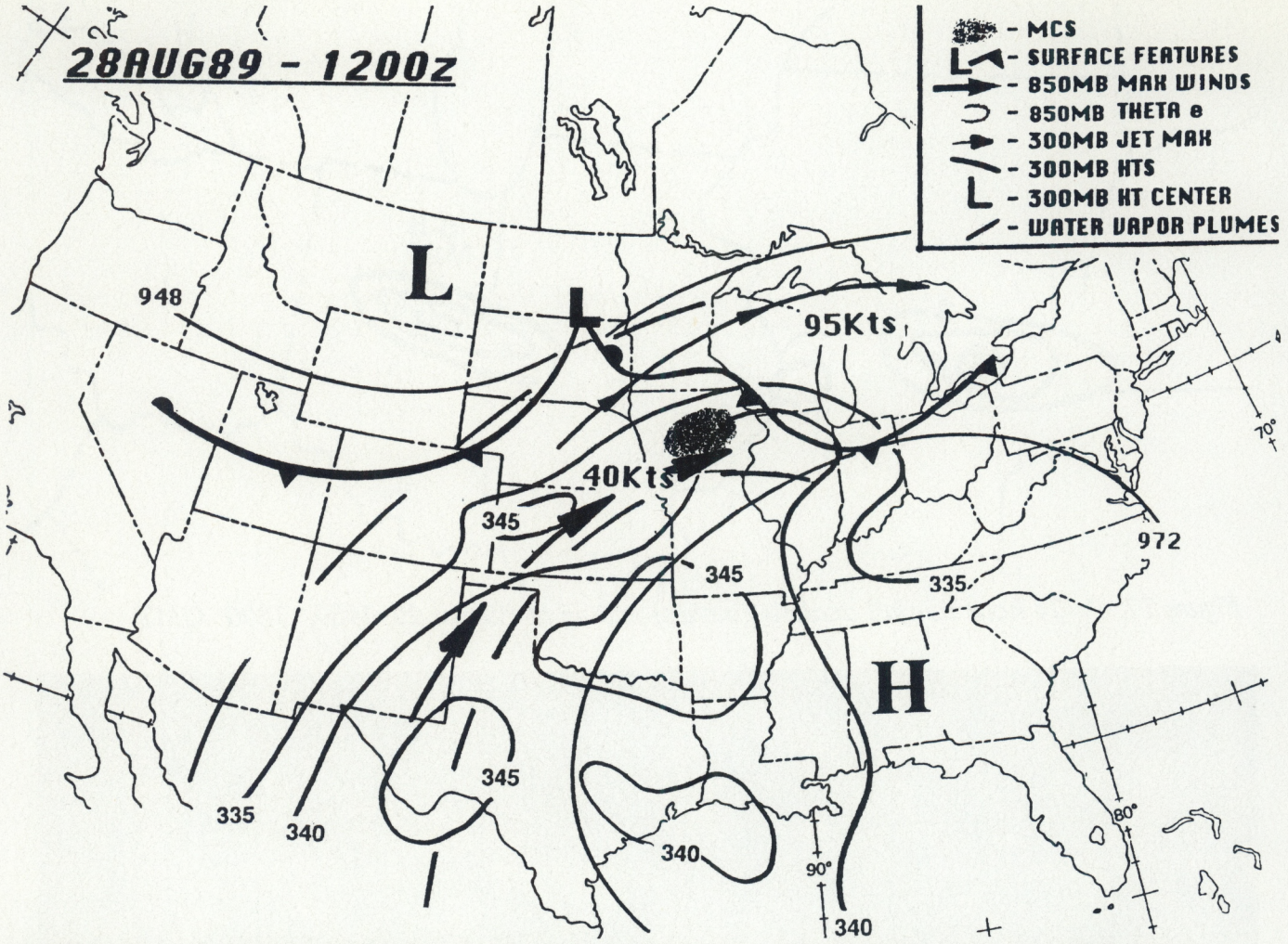

Figure 19. Surface and upper air composite of meteorological features associated with extreme heavy rainfall MCSs for August 28, 1989, 1200 GMT.

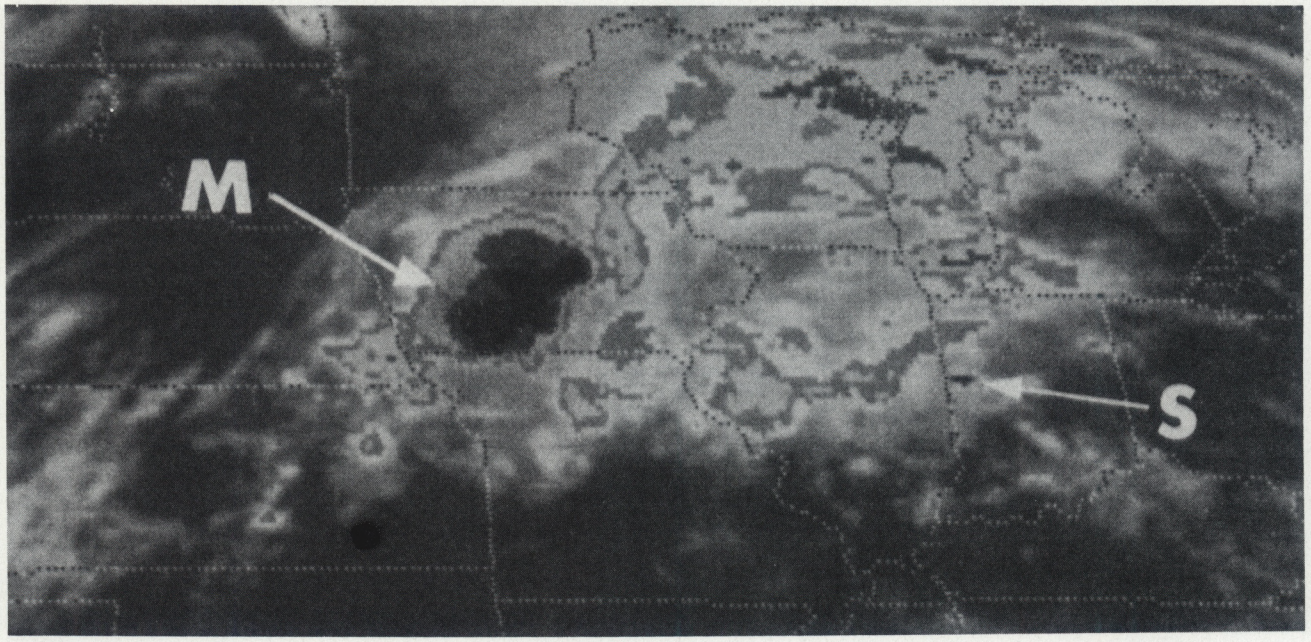

Figure 20. Enhanced infrared imagery (MB Curve) for August 28, 1989, 1200 GMT.

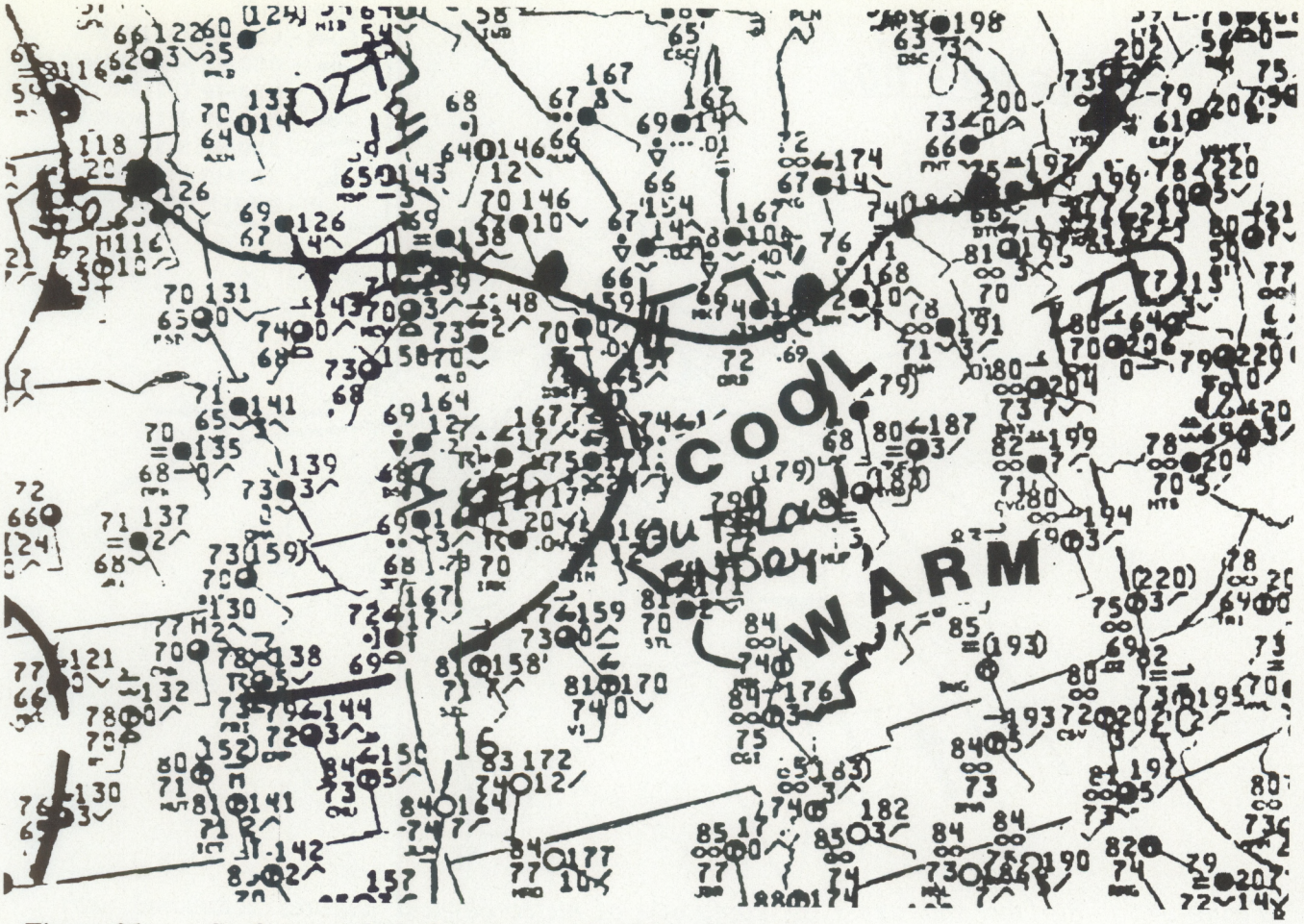

Figure 21. Surface analysis for August 28, 1989, 1500 GMT.

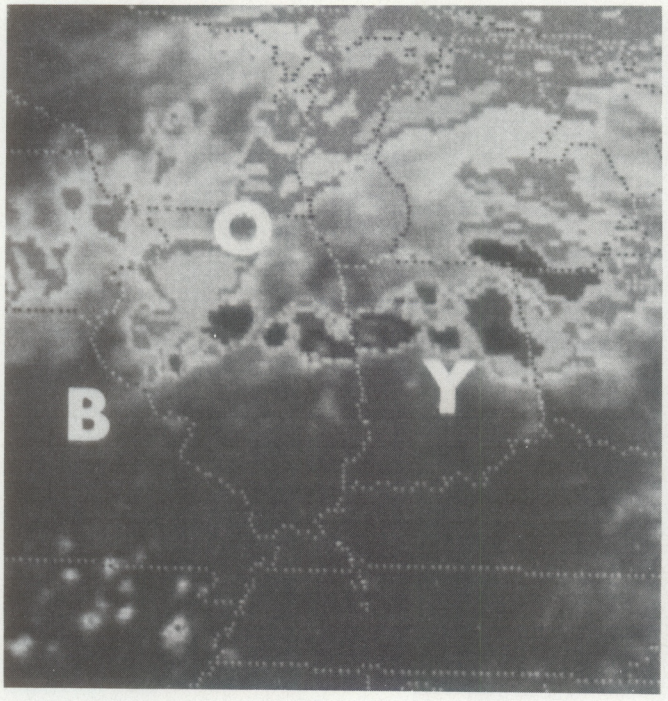

Figure 22. Enhanced infrared imagery (MB Curve) for August 28, 1989, 1800 GMT.

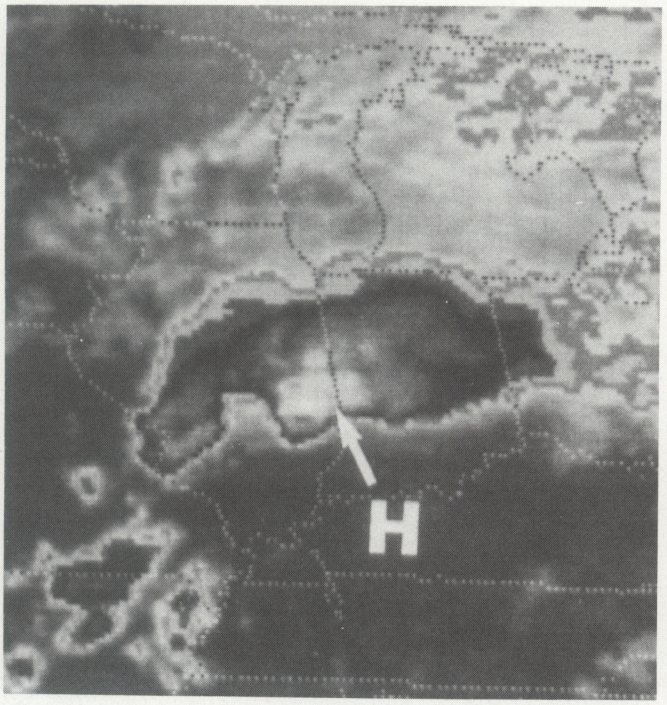

Figure 23. Enhanced infrared imagery (MB Curve) for August 28, 1989, 2100 GMT.

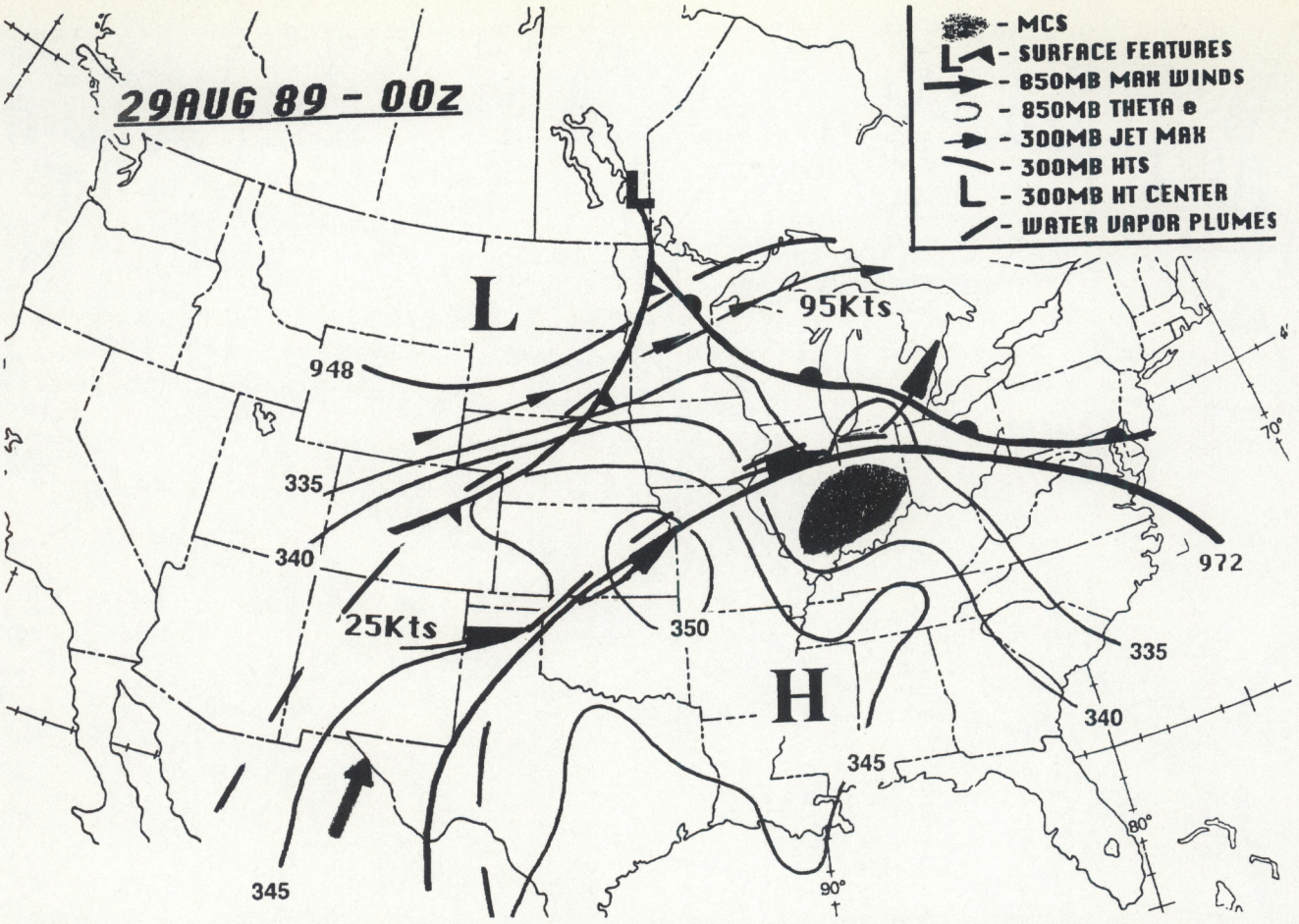

Figure 24. Surface and upper air composite of meteorological features associated with extreme heavy rainfall MCSs for August 29, 1989, 0000 GMT.

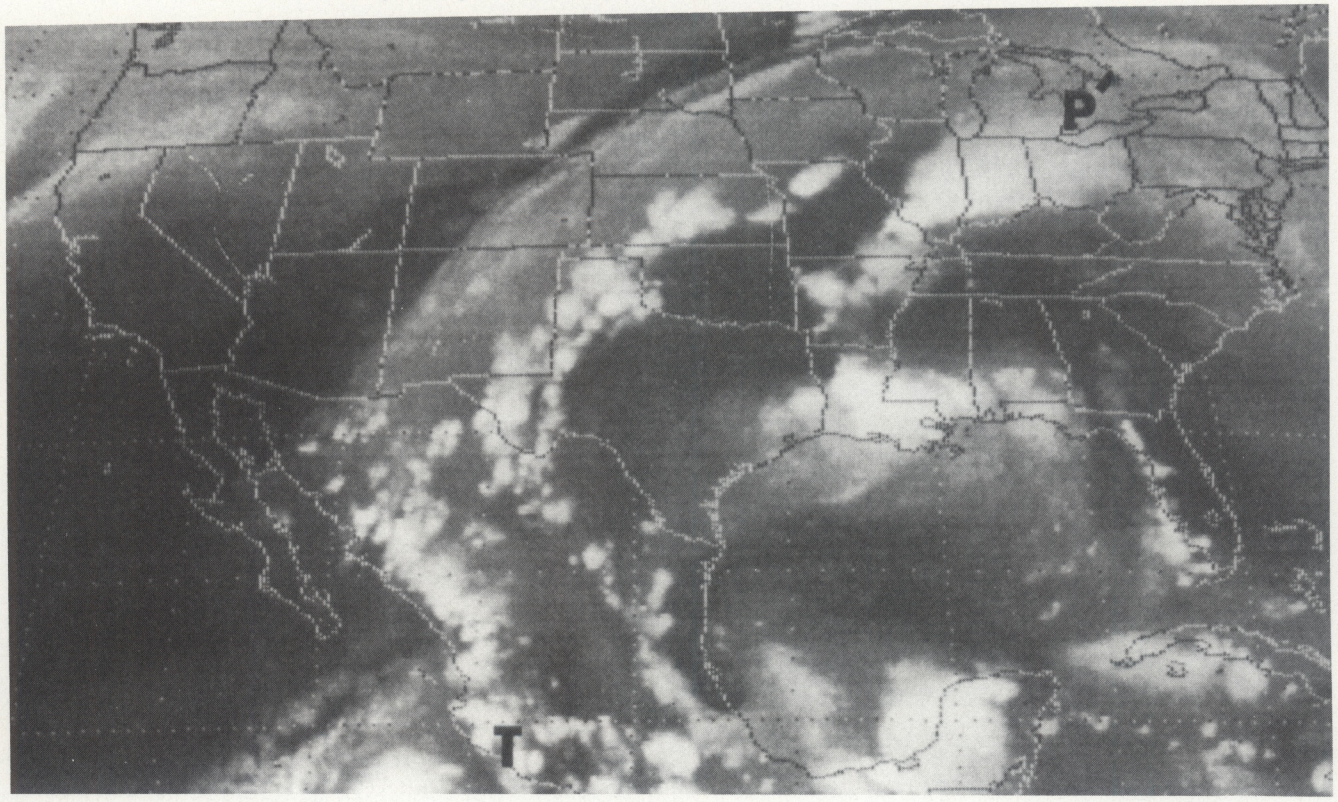

Figure 25. 6.7 μm water vapor imagery for August 29, 1989, 0000 GMT.

VI. Conceptual Models Of Heavy Precipitation In The Water Vapor Imagery

Flash floods can occur without the presence of tropical plumes. After studying the WV imagery for the past several years, six conceptual models of heavy precipitation have been developed. These conceptual models can be used for diagnosing global and synoptic scale features favorable for producing heavy precipitation and flash floods.

The conceptual models are now briefly discussed:

(1) Direct Plume (Figure 8)

This model was the focus of this paper and it has the following characteristics:

- o a low-level theta-e ridge axis, deep layer moisture and an upper level disturbance (s);
- o low level maximum winds are present and are replenishing moist, unstable air;
- o often associated with a double jet streak structure;
- o sometimes associated with a double plume structure (polar and tropical plumes).

As discussed in Section III-2-b, depending on where the low-level theta-e ridge axis is located with respect to the plume, flash floods and/or severe weather can occur.

(2) Indirect Plume (Figure 26)

The Indirect Plume is an extension of the "Direct Plume" model to the backside of a ridge. The backside of a ridge can be favorable for flash floods if:

- o deep layer moisture is present;
- o warm air advection and upper-level disturbance(s) are present.

Depending on the intensity of the upper level disturbance and the magnitude of destabilization, severe weather can also occur on the back side of a ridge.

(3) Area Of Moisture Under An Upper-Level Ridge (Figure 26)

An Area Of Moisture Under A Ridge can be favorable for flash floods if the moisture is deep and there is sufficient upward vertical motion to remove any capping inversion. Additional favorable characteristics for flash floods under the ridge are:

- o the presence of a low-level theta-e ridge axis;

- a surge of moisture from the tropics;

- heating due to solar insolation --- this is the dominant mechanism that results in a convective maximum during the afternoon followed by dissipation after sunset.

Examples of MCSs occurring within an area of moisture under a ridge are shown in Figure 9a (over Texas, Louisiana, and Mississippi) and in Figure 25 over Louisiana.

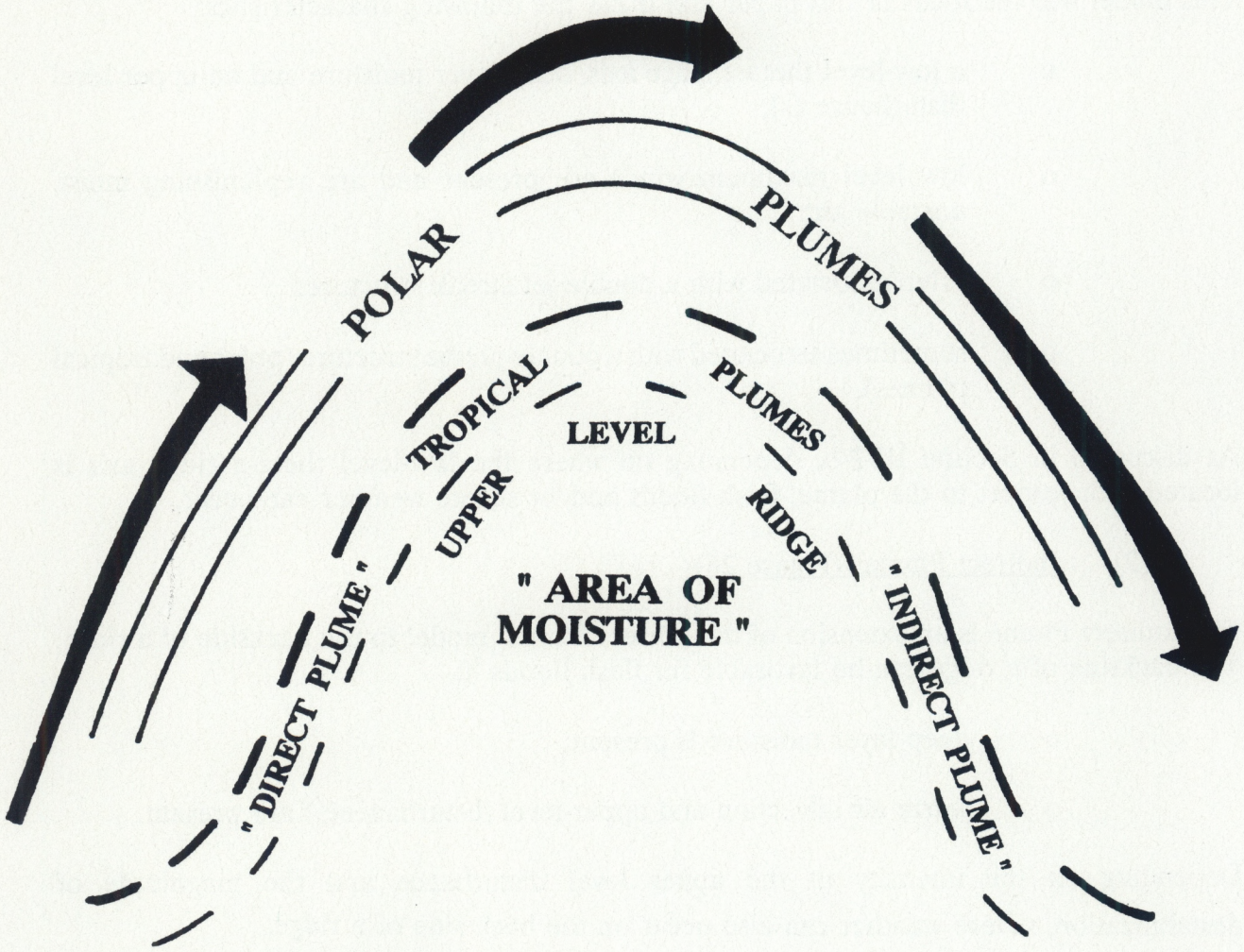

Figure 26. *Conceptual Model of the direct plume, indirect plume and area of moisture under a ridge as seen in the water vapor imagery.*

(4) Cyclonic Circulations (Figure 27a)

This model is readily identified in the WV imagery and is normally associated with a rather strong dynamical system in the westerlies. Not only can the heavy rainfall occur within the area labelled "Summer" but also in areas "A" and "B" where the upper level flow is diffluent. Its characteristics include the presence of:

- o a pronounced cyclonic circulation in the WV imagery, though sometimes better resolved in the 500 mb vorticity analysis;
- o jet streaks;
- o a tropical plume sometimes one or two days before a heavy rain event that serves to pre-condition the environment;
- o MCSs possessing cold tops in the IR;
- o severe weather that often accompanies the flash floods.

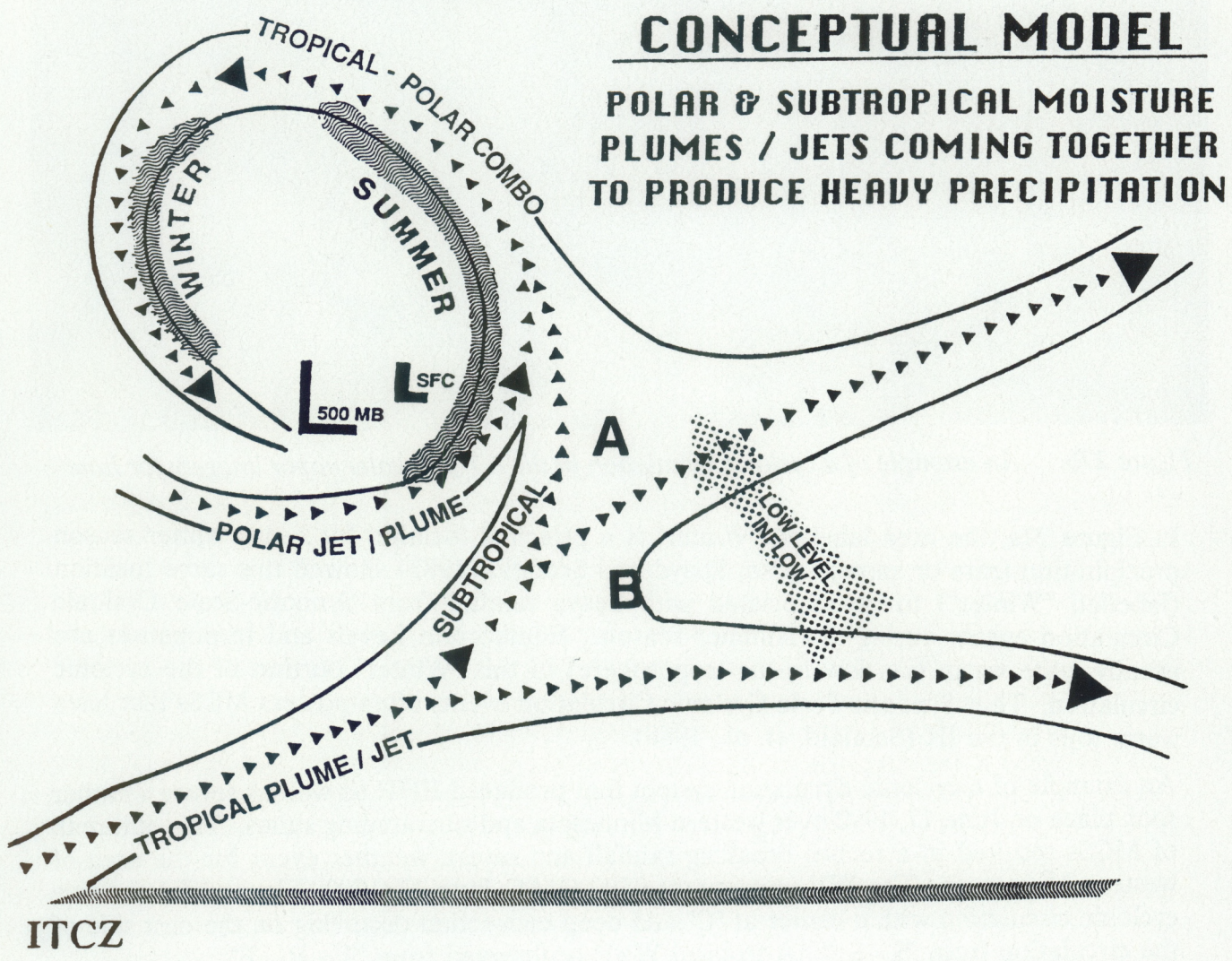

Figure 27a. Conceptual Model of the cyclonic circulation as seen in the water vapor imagery.

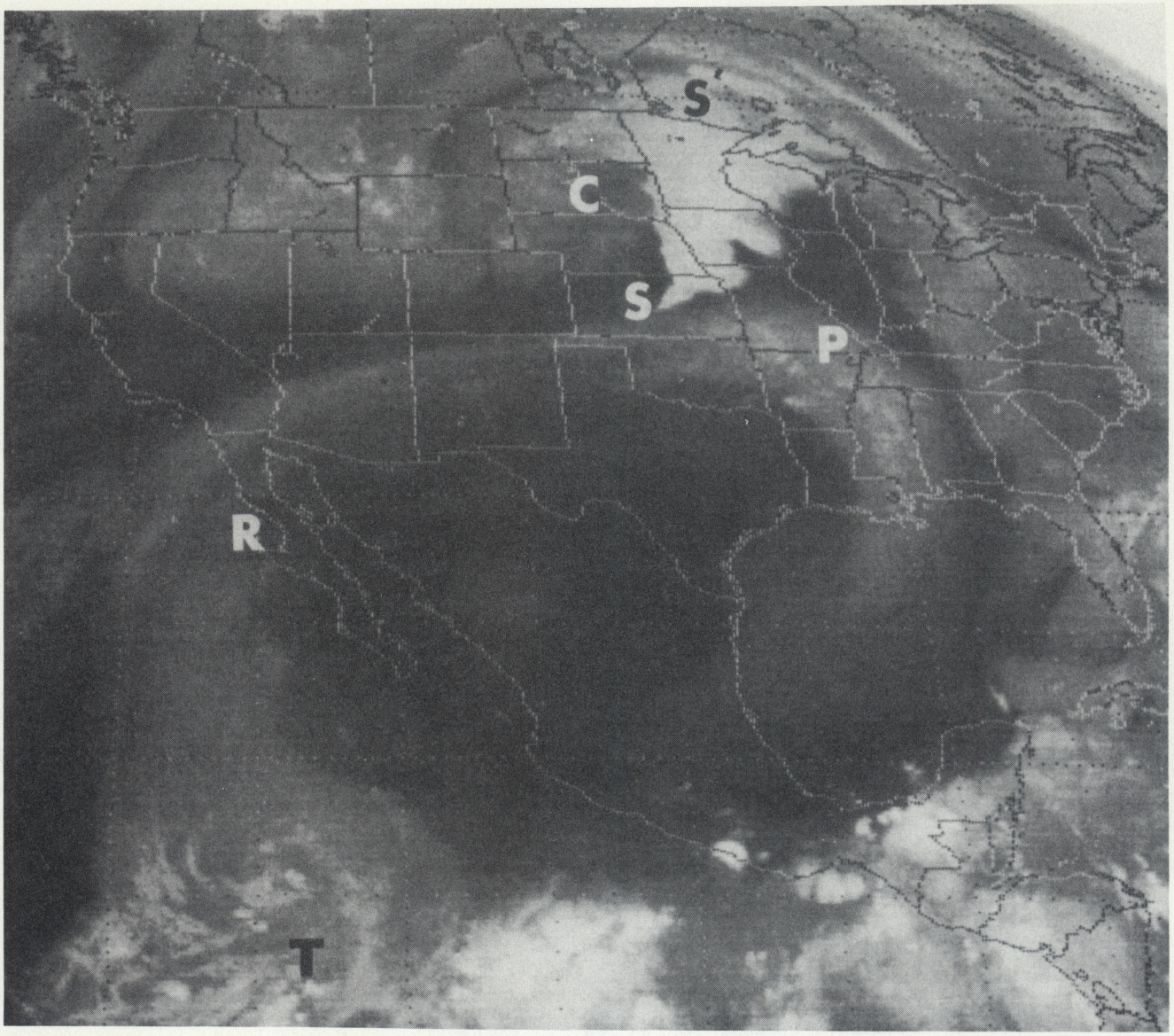

Figure 27b. An example of a cyclonic circulation in the 6.7 μm water vapor imagery for June

In Figure 27a, the area labelled "Winter" is a principal location for heavy winter season precipitation (rain or snow). Also, Spayd and Scofield (1983) showed this same location (labelled "Winter") to be associated with heavy rainfall from Synoptic-Scale Cyclonic Circulation events during the summer season. Equilibrium Levels and tropopauses are usually quite warm (i.e. low in the troposphere) in this "Winter" portion of the cyclonic circulation. Thus Synoptic-Scale Cyclonic Circulation events often possess MCSs that have warm tops in the IR (Scofield, et. al., 1980).

An example of a cyclonic circulation system that produced EHR as well as severe weather took place on June 17, 1992 over western Minnesota and surrounding states. This outbreak of MCSs resulted in a record breaking rainfall and severe weather event for the area of western Minnesota. The WV imagery for 0500 GMT, June 17, 1992 (Figure 27b) shows a cyclonic circulation with a center at "C" and deep convection occurring on the east side of the circulation from "S - S'". A tropical WVP is observed from "T - R - P".

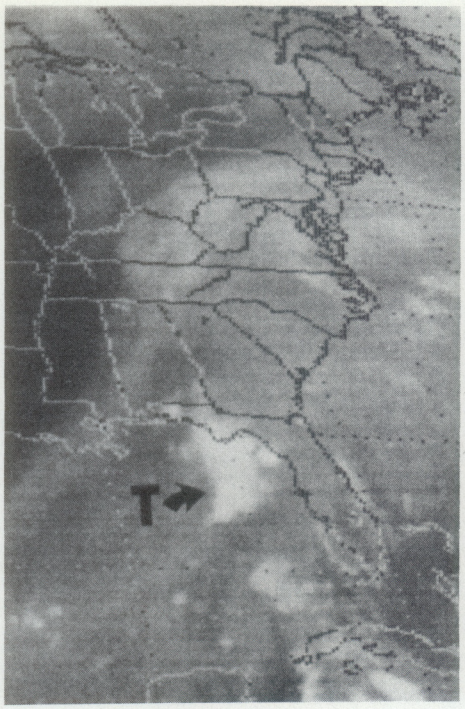

Figure 28a. 6.7 μm water vapor imagery for 5 Sep 92 0900 GMT.

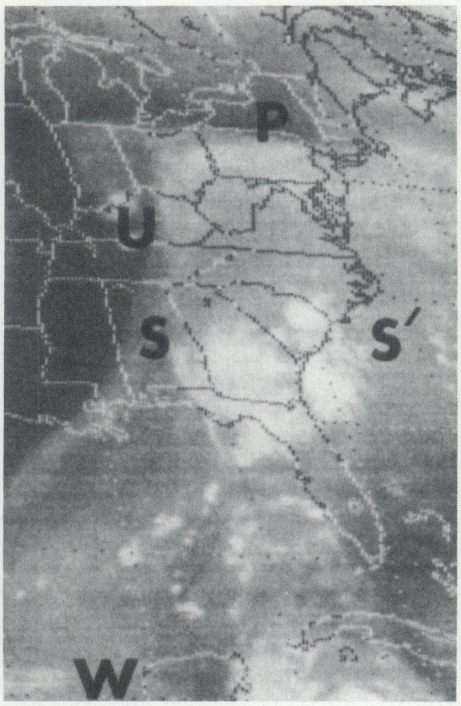

Figure 28b. 6.7 μm water vapor imagery for 5 Sep 92 1500 GMT.

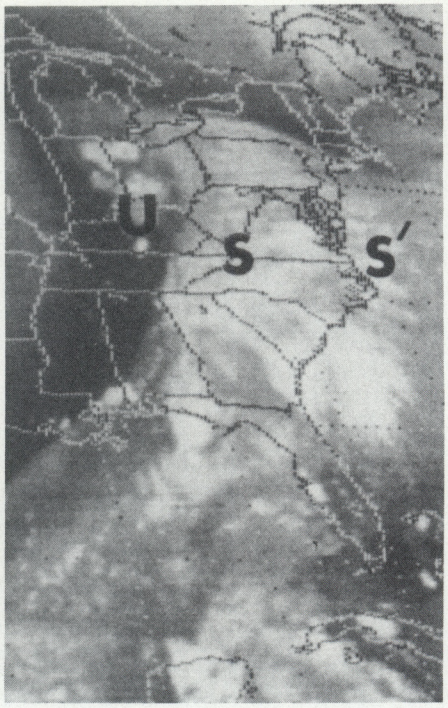

Figure 28c. 6.7 μm water vapor imagery for 5 Sep 92 2100 GMT.

(5) Tropical Systems

It should be obvious that EHR events are associated with most tropical systems. Tropical systems are detectable in the WV imagery as areas of convection (organized and unorganized), tropical waves, or vortices. Sometimes the remnants of previously organized tropical systems can be tracked in the WV imagery as northward surges of moisture from the Pacific, the Baja of California, Gulf of Mexico or the Atlantic Ocean northward into the U.S.. Surges are often embedded within a tropical WVP and show up as enhanced white (gray shade) areas of deeper moisture in the WV imagery. These northward surges of moisture can sometimes be very subtle in the WV imagery and are best detected by using animation. In addition, surges, especially if they interact with systems in the westerlies can produce EHR. An example of a surge of moisture from a tropical system is shown in Figures 28a, b, c. At 0900 GMT, a weak tropical wave is located at "T" in Figure 28a. A surge of moisture (its northern-most edge at "S - S'") moved northward and encompassed southern Virginia and Maryland by 2100 GMT (Figure 28c). Notice that this surge is embedded in a tropical WVP ("W - P" in Figure 28b). As a result of this surge and an upper air disturbance over the Ohio Valley (at "U"), flash floods and extremely heavy rainfall of 5-10 inches were reported over Virginia and southern Maryland.

Even though WV imagery has been emphasized in this investigation, tropical systems, such as tropical cyclones (e.g., hurricanes), are more readily identified, analyzed, and classified (intensity and wind speed) in the visible (VIS) and IR imagery.

(6) Non-Plume/Non-Cyclonic Circulation Events

These are flash flood events in which the MCSs are not associated with plumes or cyclonic circulations. These non-plume/non-cyclonic circulation events are divided into two categories: category A - when moisture is present in the WV imagery as a result of:

- o residual moisture from a previous system or WVP;
- o moisture advected into the area.

catgegory B - when moisture is not initially present in the WV imagery.

In this situation, there must be back building or quasi-stationary MCSs or regenerative MCSs passing over the same area to saturate the environment and deepen the moist layer in the local area of the MCS. Flash floods can occur because of the resulting deeper layer of moisture and slow movement of the thunderstorms. An example of MCSs (at "M") that developed in a dry WV environment, are illustrated in Figure 28d. The WV image in Figure 28d shows a MCS located over Texas ("TX"). Notice how this MCS is surrounded by dry air. Radar-derived rainfall estimates for this storm ranged from 1 to 3 inches of rain.

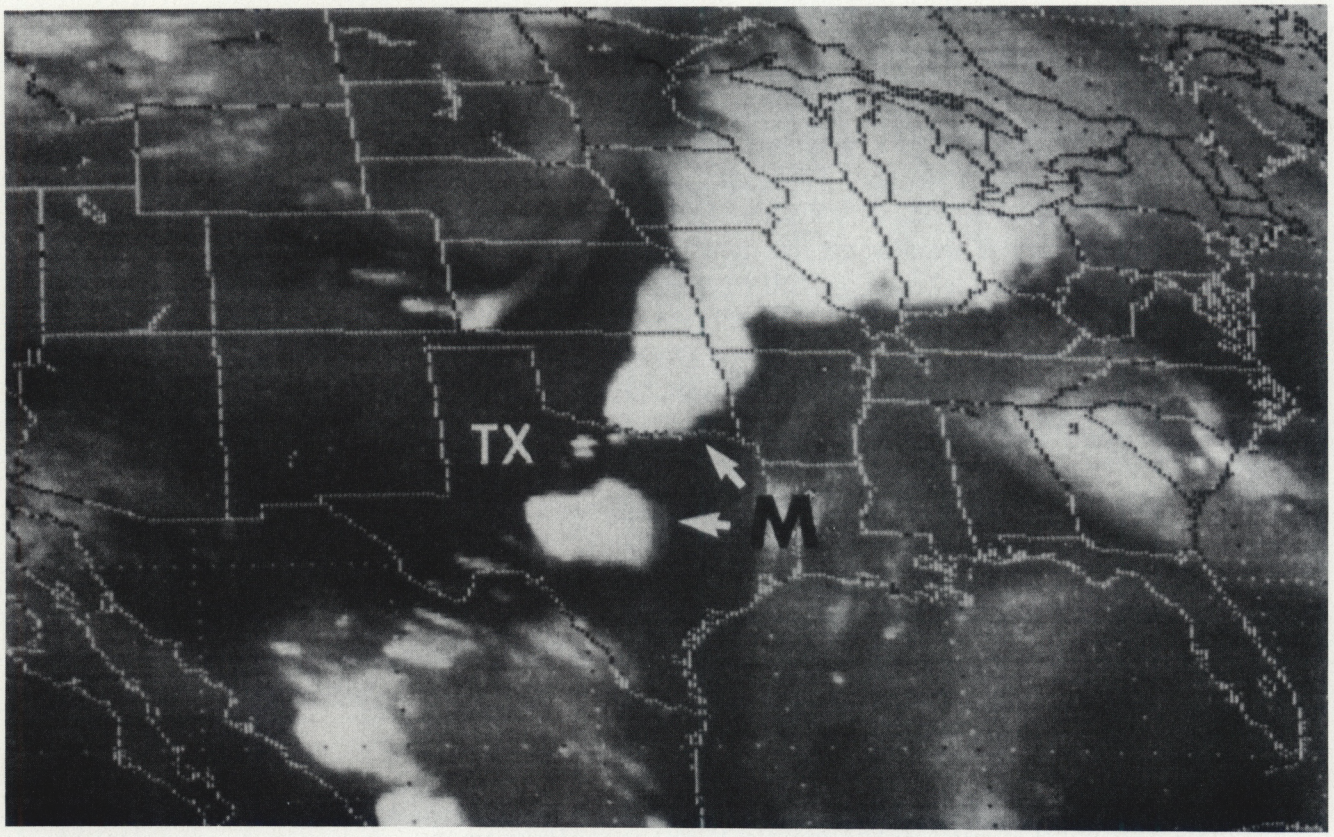

Figure 28d. 6.7 μm water vapor imagery for July 3, 0200 GMT, 1992.

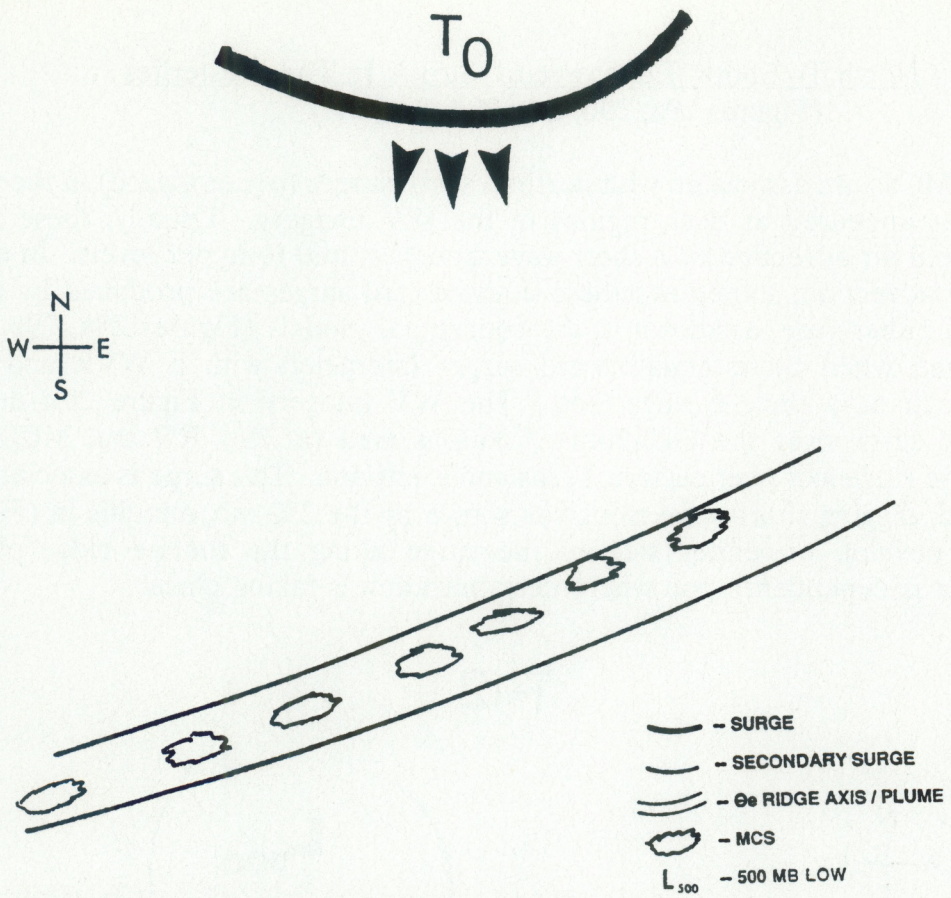

Figure 29a. Conceptual Model of an Equatorward Surge.

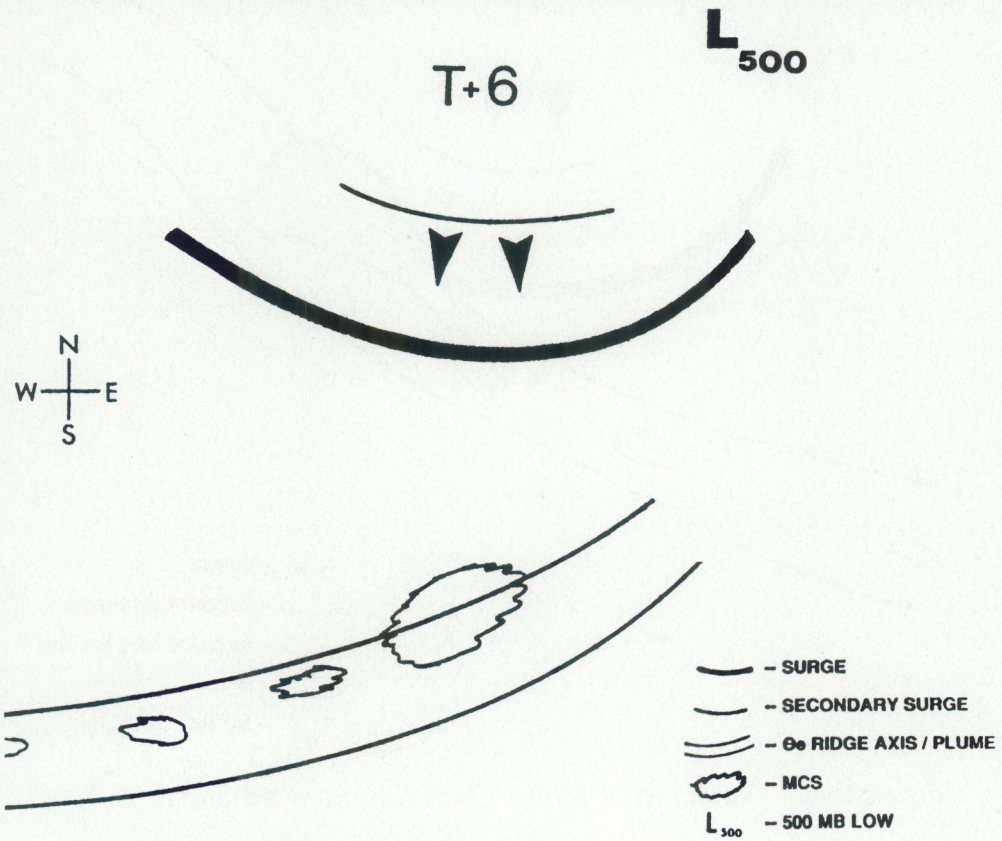

Figure 29b. Conceptual Model of an Equatorward Surge.

North To South "Equatorward" Surges In The Westerlies
(Figures 29a, 29b, 29c, 29d, 29e, 29f)

Sometimes MCSs are associated with north to south surges (equatorward) in the westerlies. These surges appeared as dark regions in the WV imagery. Usually, these surges are related to cold air advection or a short wave trough at mid to upper levels. In addition to the cold air advection, sometimes these equatorward surges are produced by digging jet streams. In either case, as shown in the conceptual models (Figures 29a, 29b, and 29c), MCSs formed when these equatorward surges interacted with a WVP and low level boundary such as a theta-e ridge axis. The WV imagery in Figure 29d depicted an equatorward surge over the Oklahoma/Arkansas area (at "S - R") and MCSs within a WVP/theta-e ridge axis over eastern Texas and Louisiana. This surge is associated with an equatorward, digging short wave trough as shown by the 250 mb, analysis in (Figure 29e). MCSs can develop on either side of the surge along the theta-e ridge/plume axis; development is dependent upon where destabilization is taking place.

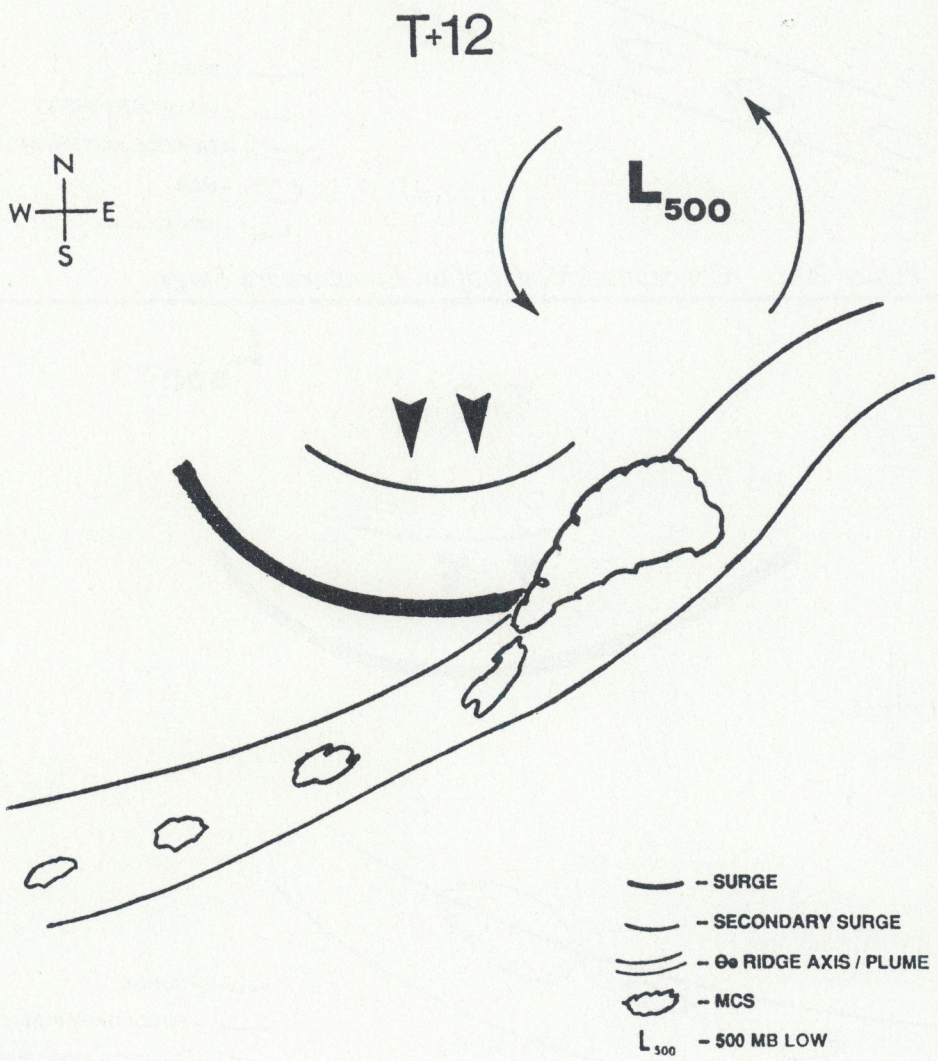

Figure 29c. Conceptual Model of an Equatorward Surge.

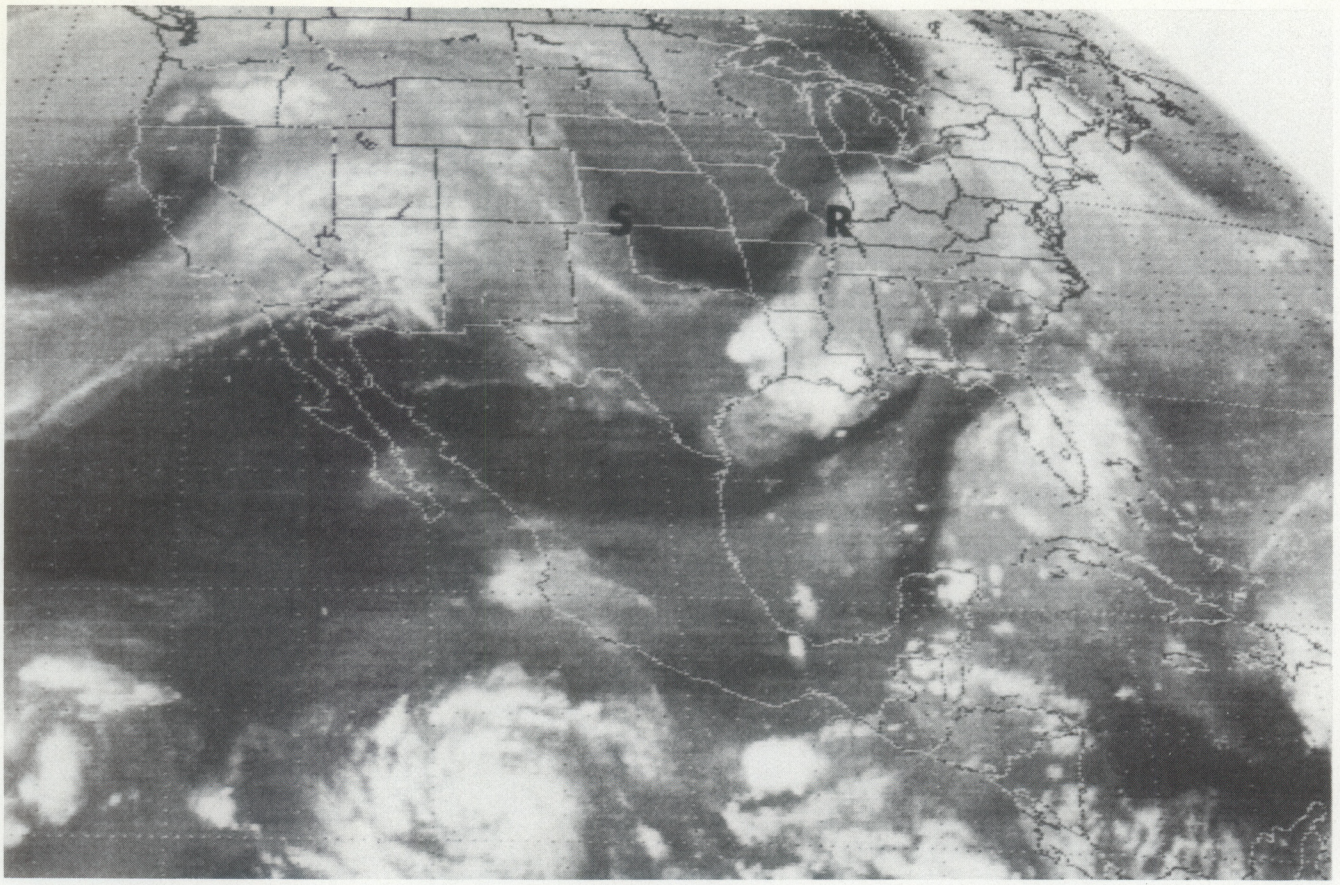

Figure 29d. 6.7 μm water vapor imagery for September 3, 1801 GMT, 1992.

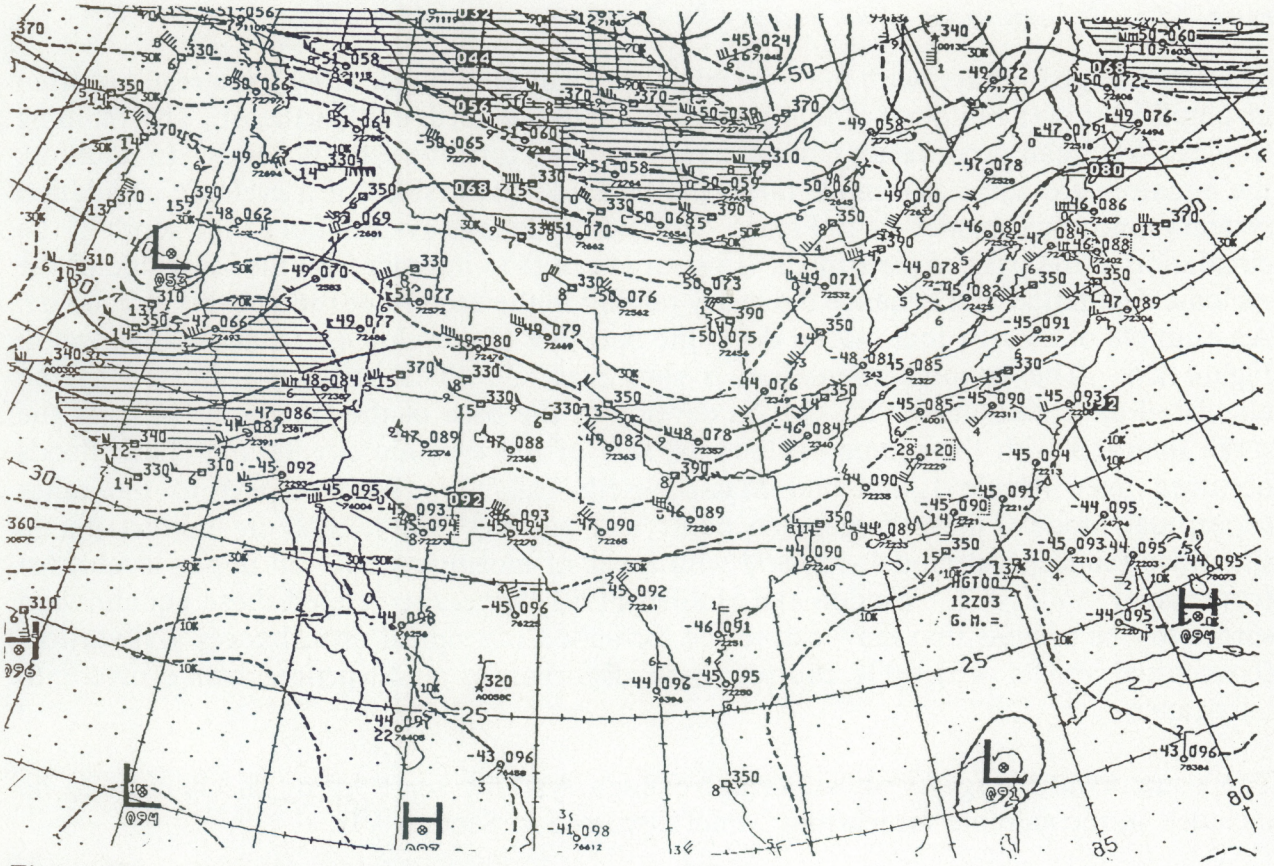

Figure 29e. 250 mb analysis for September 3, 1200 GMT, 1992.

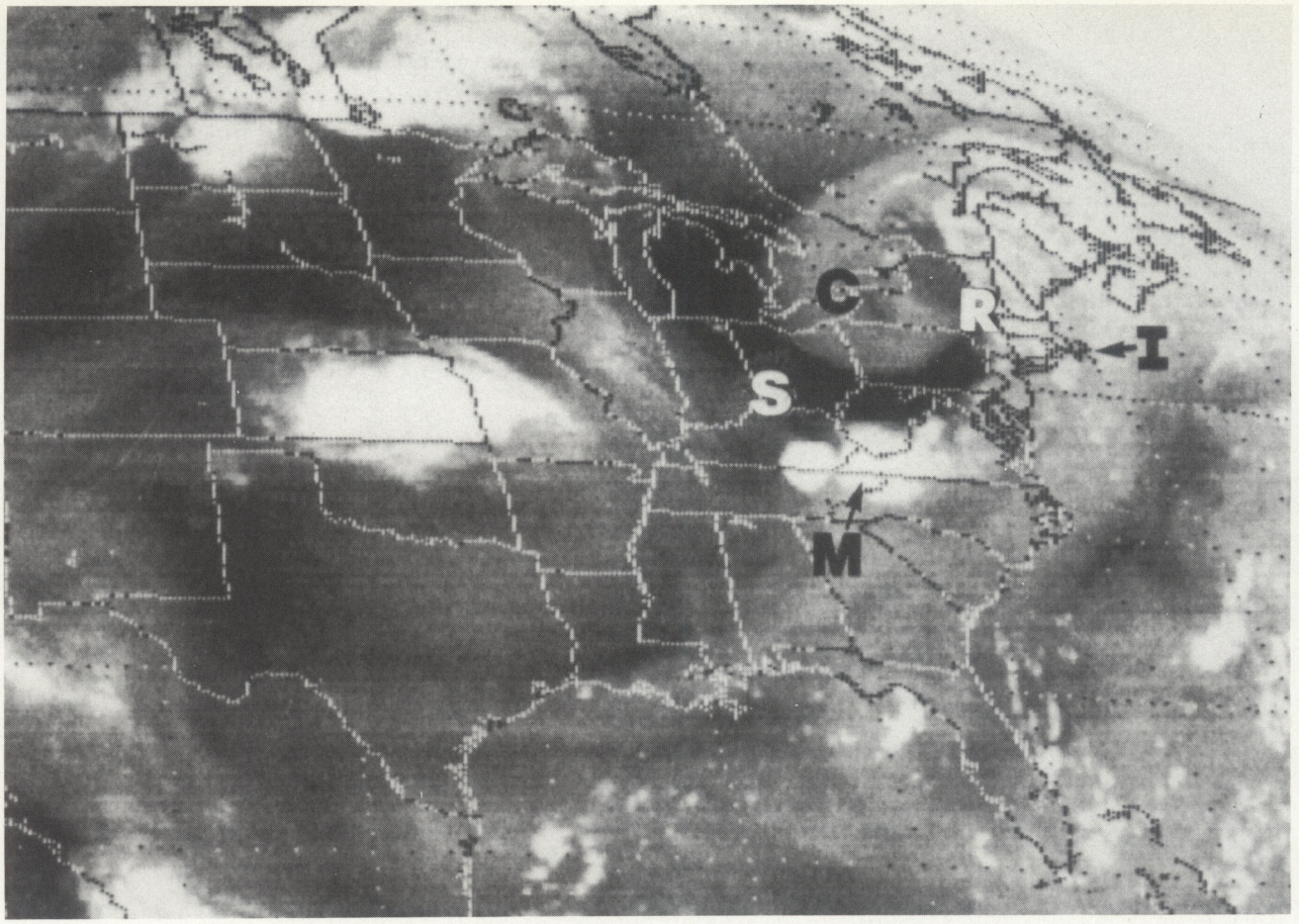

Figure 29f. 6.7 μm water vapor imagery for August 9, 1101 GMT, 1992.

When the surge interacts with the tropical plume (conceptual model #1), the result is often an amplification (a building) of this tropical WVP to the north and northeast. This building tropical WVP can produce an environment favorable for future flash floods. In addition, the equatorward surge can move down the backside (west side) of a cyclonic circulation system (conceptual model #4 in Figure 27a) and produce heavy rainfall to the south of the circulation at the base of the trough. This surge can than interact with the east side of the cyclonic circulation and enhance the heavy rainfall in the eastern portion of this circulation. An example of a surge that moved down the backside of a cyclonic circulation is shown in Figure 29f. The cyclonic circulation is shown at "C". The surge is indicated by the elongated dark area at "S - R". MCSs develop at the base of the trough at "M". As the surge interacts with the plume on the east side of the cyclonic circulation, flash floods occurred over Rhode Island and Massachusetts (at "I"). With respect to the other conceptual models, these surges can occur and enhance the rainfall in indirect plume situations (conceptual model #2) and with areas of moisture under an upper level ridge (conceptual model #3). Weldon and Holmes (1991) have also related these equatorward surges to one process that may lead to the formation of tropical disturbances and vortices (conceptual model #5). Of course, these disturbances and vortices can evolve into hurricanes.

The equatorward surge is an important enough synoptic scale lifting mechanism to be included in the satellite forecasting funnel discussed in Section VII.

A 12-24 Hour Prediction Of Heavy Rainfall

The ultimate objective in satellite imagery interpretation is to quantify features or patterns analyzed in the pictures. This quantification has already been successfully achieved for estimating rainfall from flash flood producing MCSs (Scofield, 1987). Therefore, a logical next step is to quantify how much rainfall could be expected from each of the six conceptual models presented. A preliminary 12 to 24 hour prediction technique of heavy rainfall amounts is presented in the Appendix. A word of caution is neccesary in using this preliminary technique:

(1) the satellite forecasting funnel must be used to diagnose if conditions are favorable from the global - synoptic - mesoscale - storm scale for producing heavy rainfall! (This satellite forecasting funnel is discussed in the next section.); and

(2) tropical moisture must also be present and can be determined from the 1000 - 500 mb Precipitable Water (PW) and Relative Humidity (RH) information:

PW (inches)	RH
good > 1.0 and > 130 % of normal	good > 60 %
better > 1.5 and > 140 % of normal	better > 70 %
best > 1.5 and > 150 % of normal	best > 80 %.

VII. Scales of precipitation and the satellite forecasting funnel

The WVP has to be used in conjunction with the satellite forecasting funnel when predicting flash flood events. This forecasting funnel is similar to the conceptual model developed by Leonard Snellman, for weather forecasting in general. However, the funnel in this section emphasizes satellite imagery, i.e., WV, IR, and VIS. Conceptual models illustrating the scales of precipitation (Figure 30a) and the satellite forecasting funnel (Figures 30b) represent a concatenation of meteorological scales and processes from the global scale to the synoptic scale, to the mesoscale, and finally to the storm scale. MCSs that produce heavy precipitation are a multiscale and concatenating event. A key ingredient of the satellite forecasting funnel is the WVP which is a global scale connection between the tropics and middle latitudes. Other ingredients on the global and synoptic scales (such as cyclonic circulations) are summarized in Section VI, Conceptual Models of Heavy Precipitation in the Water Vapor Imagery.

As mentioned previously, the tropical WVP is often associated with a northward transfer of mid to upper level moisture from the tropics and subtropics. On the synoptic scale and mesoscale, the tropical WVP can align itself with high theta-e air. This high theta-e air is a source of potential energy and moisture, that, if acted upon by an Instability Burst (IB) (Scofield, 1990a, Juying and Scofield, 1989, and Jiang and Scofield, 1987) can produce

SATELLITE FORECASTING FUNNEL

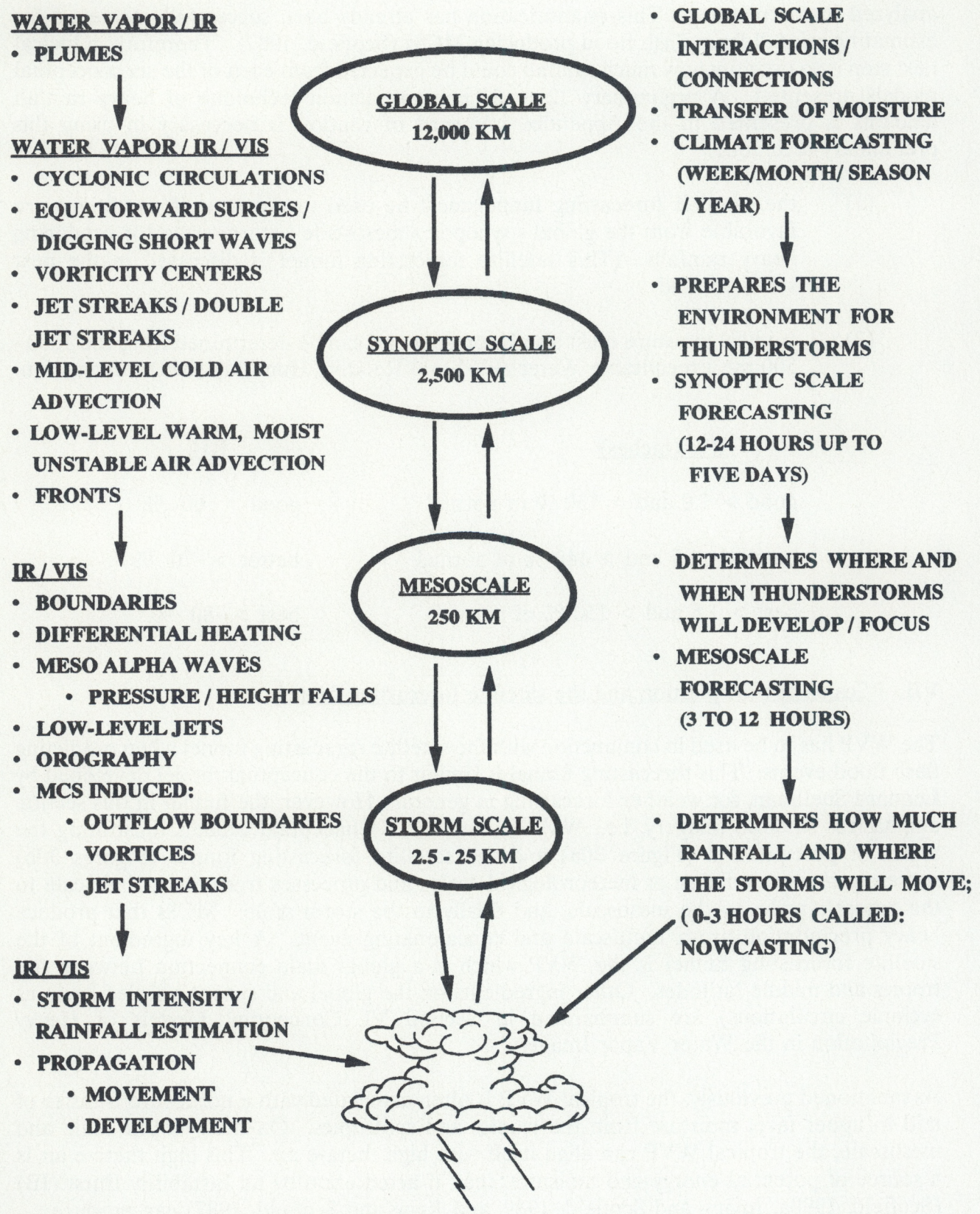

Figure 30b. The satellite forecasting funnel.

convection. IBs are forcing mechanisms that can quickly destabilize an air mass and can remove capping inversions. These mechanisms include:

(1) Low level advection of warm, moist, unstable air (most often at night);

(2) The "lifting" of unstable air due to upper level short waves and jet streaks within subtropical and polar jet streams;

(3) Differential temperature advection (most often during the day);

(4) Heating by solar insolation (day).

Therefore, on the synoptic scale, WV, IR, and VIS imagery can detect moist environments favorable for upward vertical motion; these conditions prepare the atmosphere for convection.

SCALES OF PRECIPITATION

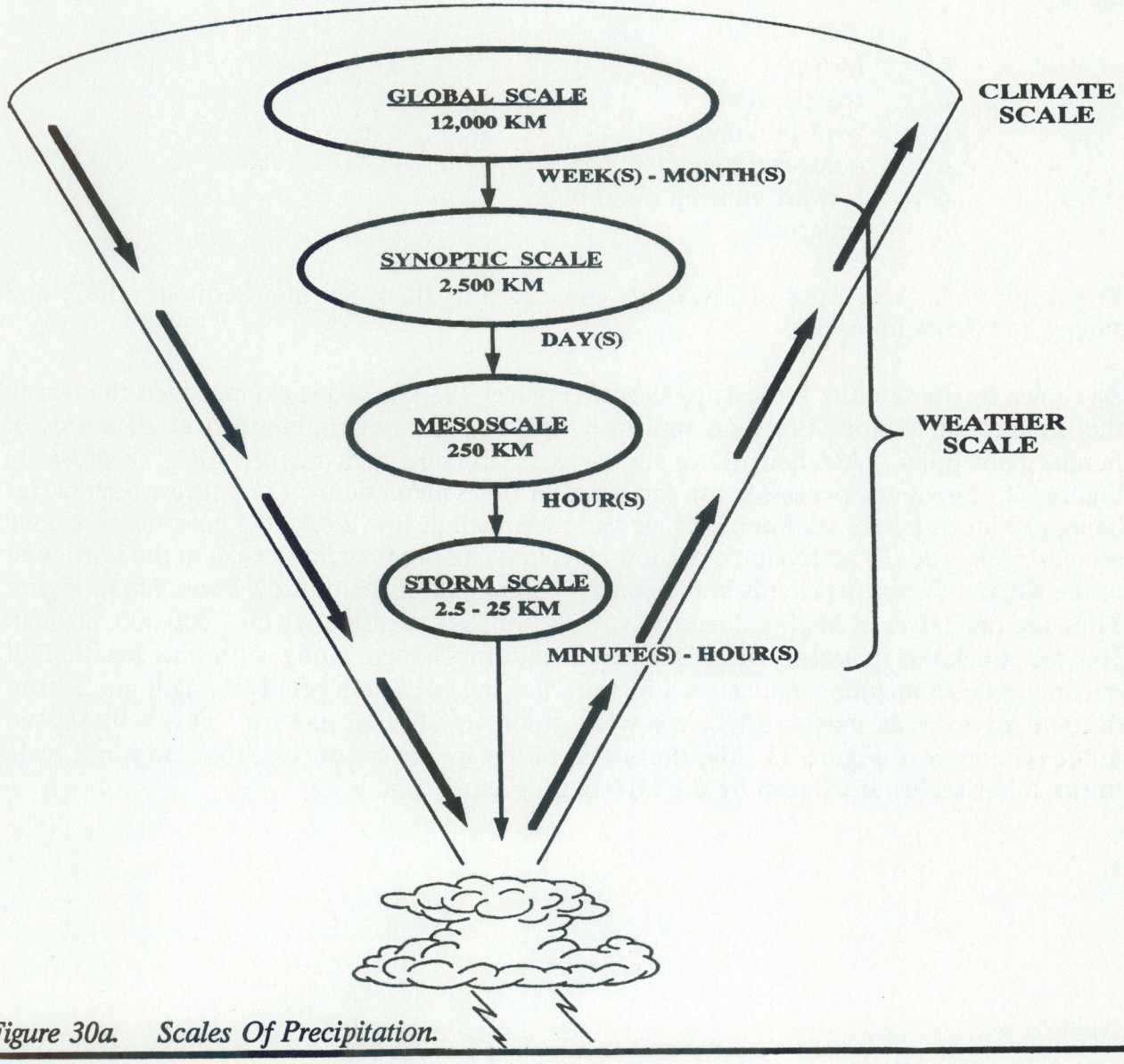

Figure 30a. Scales Of Precipitation.

On the mesoscale, IR, VIS, and WV imagery are used to locate outflow boundaries and short waves that may initiate, focus and maintain the convection along or near the theta-e (potential energy) ridge axis. A conceptual model of an outflow boundary and its convective scale interaction with unstable air and a stationary front is shown in Figure 31a. Another conceptual model of an outflow boundary and its convective scale interaction with unstable air and area of maximum warm air advection is illustrated in Figure 31b. MCSs develop at the intersection of the outflow boundary with: a frontal boundary, hot/unstable air, and an area of warm air advection. Thunderstorms do not develop where the outflow boundary intersects small cumulus clouds that are capped. Purdom and Sinclair (1988) have discussed in detail the life cycle of outflow boundaries; these outflow boundaries are called arc cloud lines by Purdom (1973).

On the storm scale, the intensity, movement, and propagation of the thunderstorms is used to determine how much, when, and where the heavy rain is going to move during the next 0 to 3 hours. High resolution IR and VIS are the principal tools used in this diagnosis. Rainfall intensity (how much ?) is computed through the use of satellite-derived rainfall algorithms (Scofield, 1987). "When" and "Where" the MCS is going to move is determined through the use of MCS propagation models (Chappell, 1985 and 1986). These models include:

- o forward;
- o regenerative
- o back building
- o quasi-stationary
- o forward moving meso beta;
- o supercell.

Propagation characteristics of MCSs are presented in Jiang Shi and Scofield (1987) and Juying and Scofield (1989).

As shown by the satellite forecasting funnel (Figures 30a, b), MCSs can produce changes in the circulation, temperature and moisture fields of the environment, over distances of hundreds of miles. A schematic of the vertical structure of a mature MCC is shown in Figure 32. Feedback processes are indicated in this schematic by: (1) outflow boundaries being produced by the cold dome of air and mesohigh at low levels, (2) a vortex produced at mid-levels, and (3) anticyclonic outflow aloft that can produce jet streaks to the northwest of the MCC. The cirrus clouds in the conceptual models of the outflow boundary in Figure 31a,b are indicative of MCS-induced jet streaks. MCSs can also alter the 1000-500 mb/850-300 mb thickness pattern. This thickness pattern change along with the location of maximum destabilization can cause a forward moving MCS in a relatively tight gradient to become a backward moving MCS in a weak gradient/diffluent pattern. This is illustrated in the schematic in Figure 33. Manifestations of this feedback process from the storm scale to the other scales are shown by the arrows in Figures 30a, b.

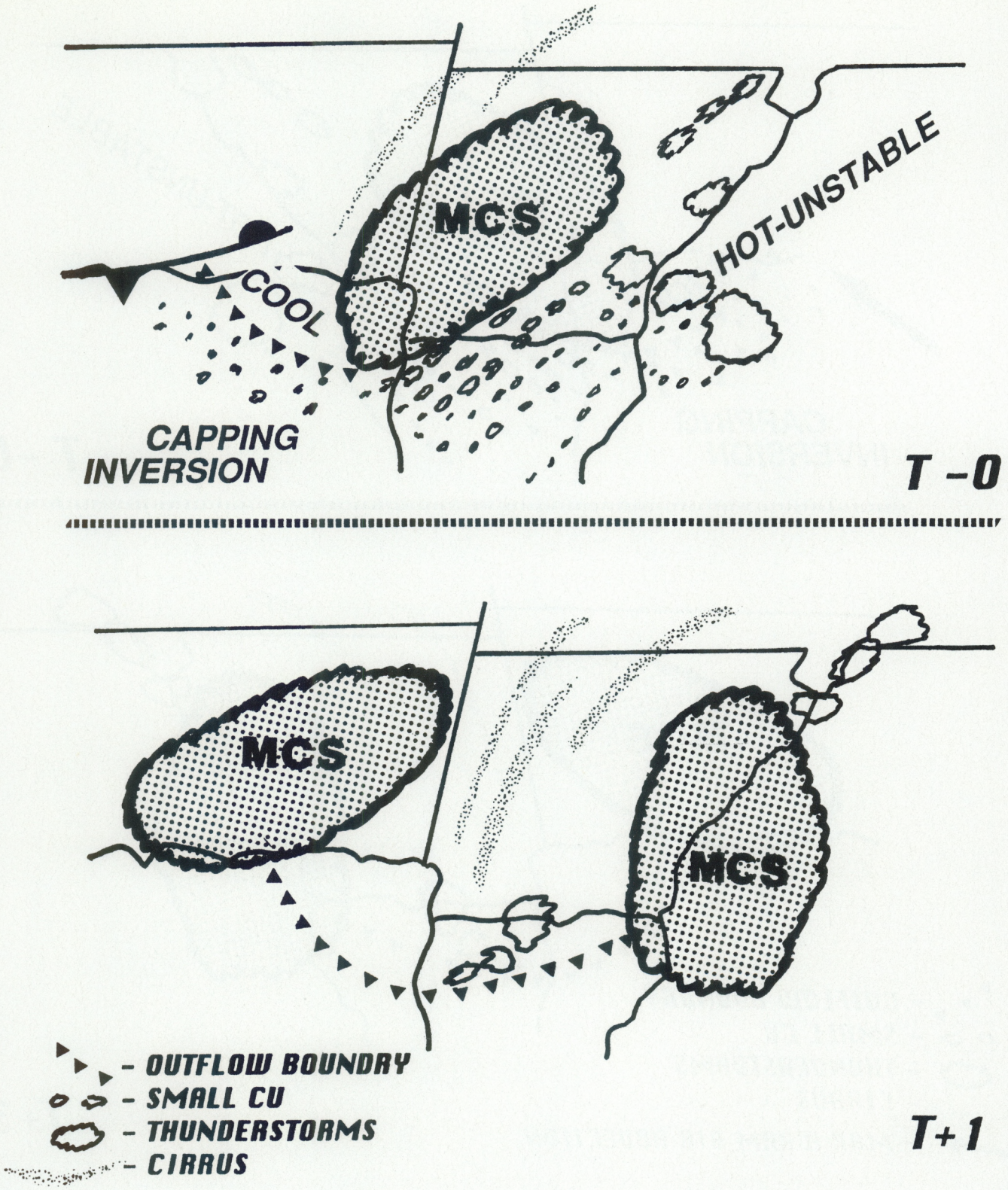

Figure 31a. Conceptual Model of an outflow boundary, convective scale interaction, and MCS initiation.

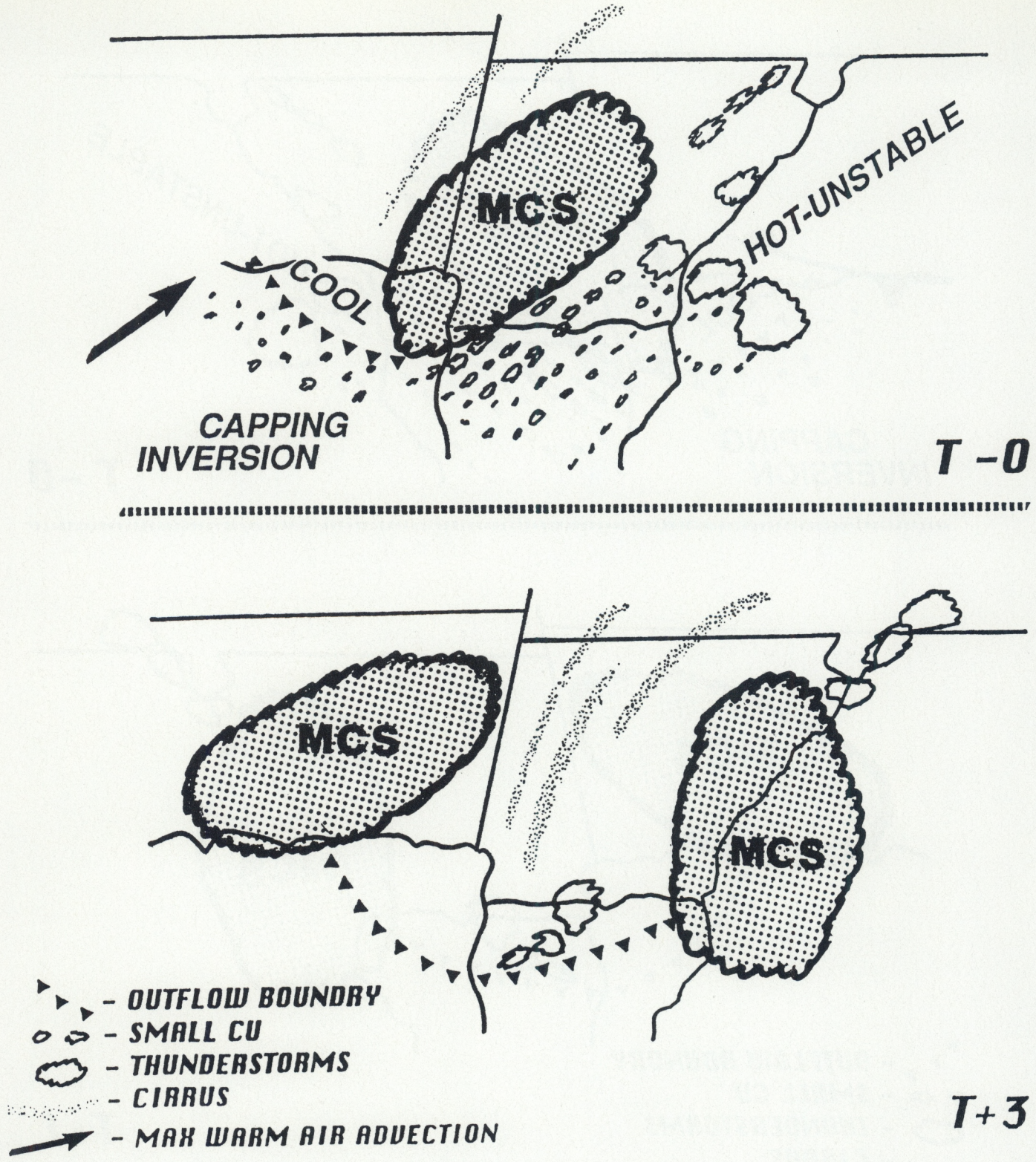

Figure 31b. Conceptual model of an outflow boundary, convective scale interaction, and MCS initiation.

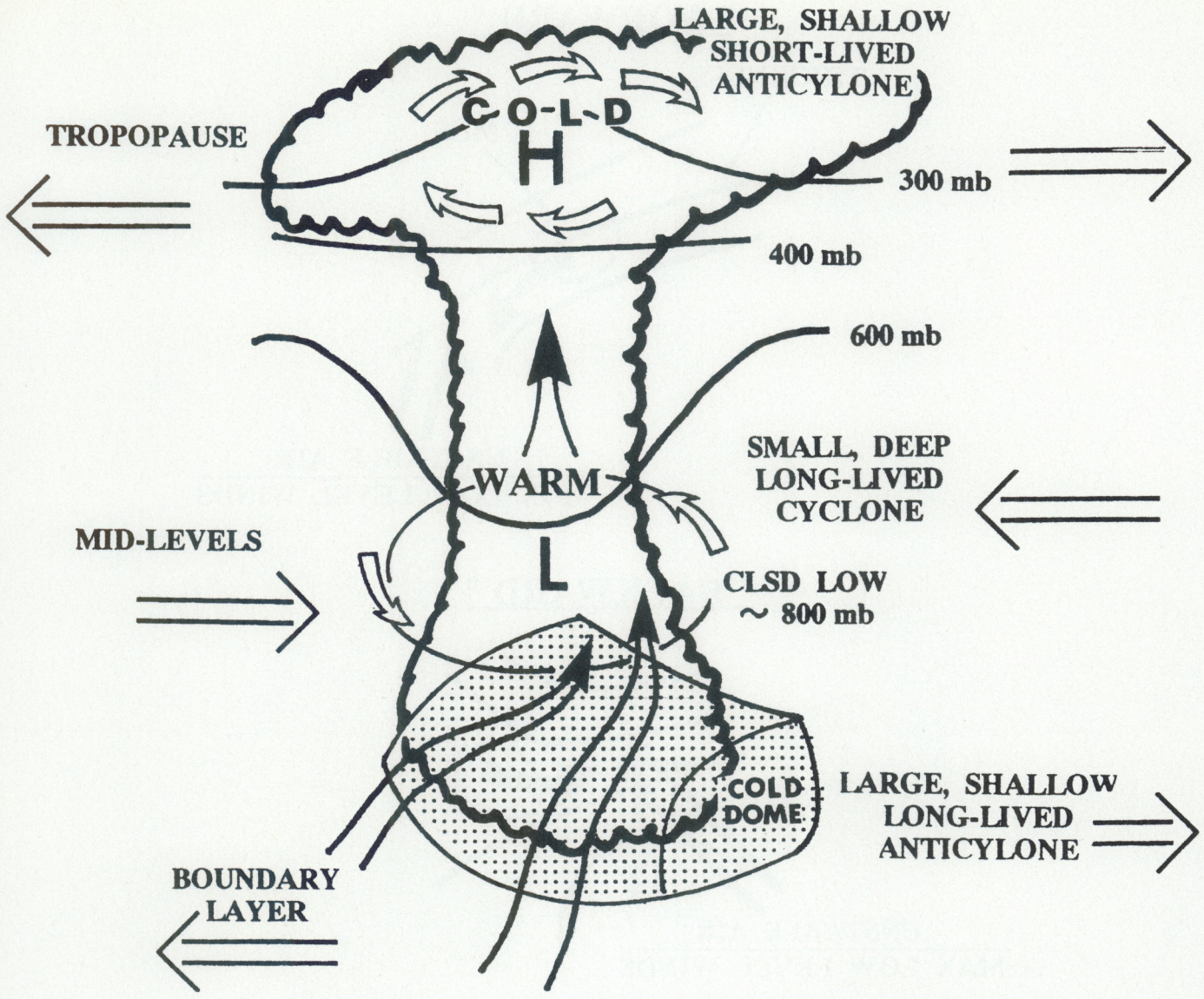

Figure 32. Conceptual model of the vertical structure of a mature MCC.

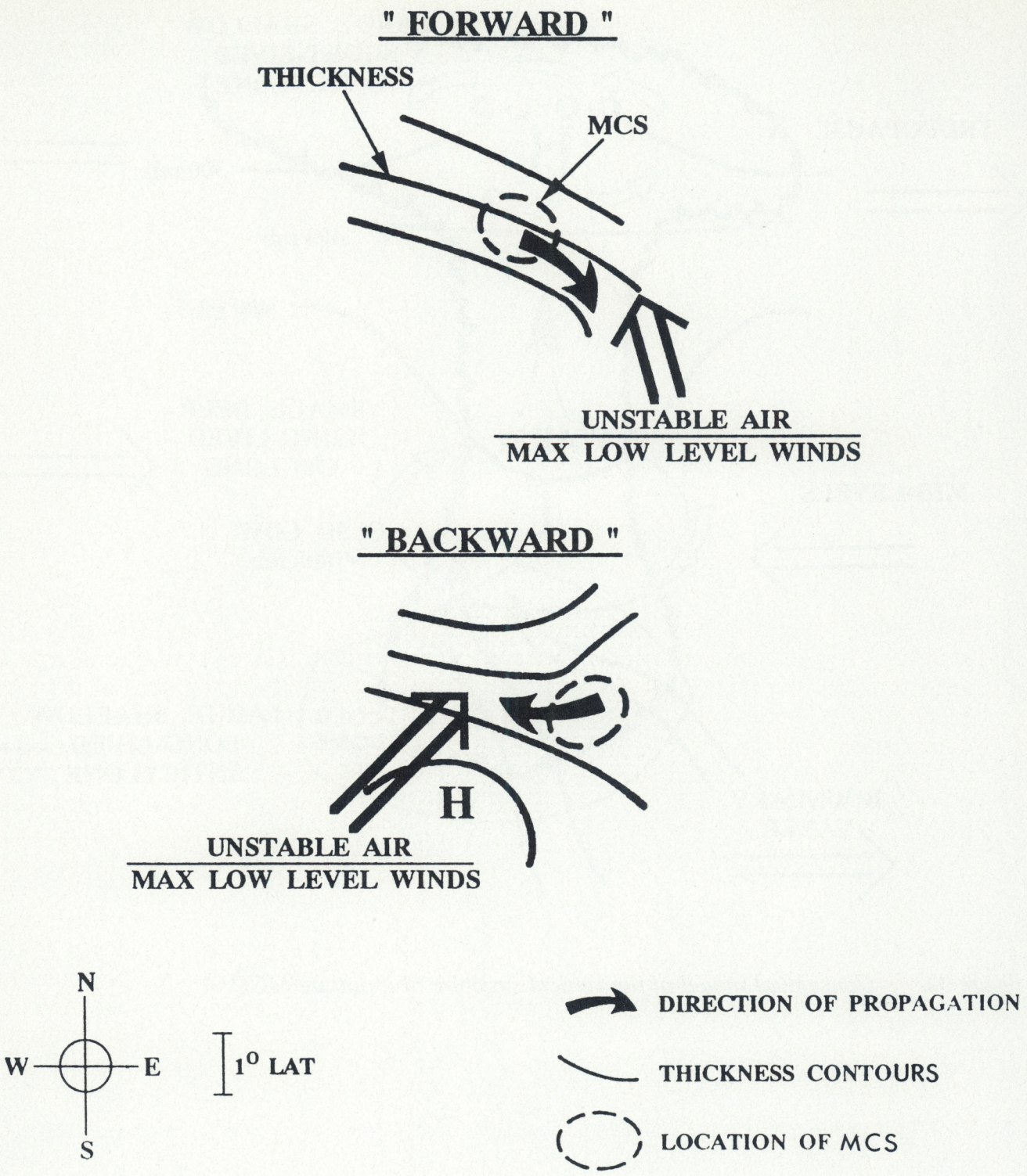

Figure 33. The relationship of thickness patterns and destabilization to MCS propagation.

Finally, the satellite forecasting funnel must be quantified in order to objectively determine whether or not conditions are favorable for flash floods. It is also a necessity that the satellite forecasting funnel incorporates surface and upper air data, moisture criteria such as that presented at the end of section VI, radar data, numerical model guidance, Q-Vectors and other synoptic scale/mesoscale analysis programs in order to forecast mesoscale events such as flash floods. An excellent summary of forecasting flash floods and heavy precipitation is presented in Module 3, produced by COMET (Cooperative Program for Operational Meteorology, Education and Training). Module 3 addresses the need for weather forecasters to anticipate when imminent severe weather conditions will result in heavy precipitation sufficient to cause flash flooding. Though severe weather conditions develop over time and their evolution can be traced from the global/synoptic scale level down through the mesoscale/storm scale levels of analysis and prediction, the issuance of flash flood watches or warnings occurs in the time frame of those few hours prior to the actual occurrence of heavy precipitation. Thus, the emphasis of Module 3 is on the following: "What is the data telling you about the storm condition, and what questions should you be asking next" ?

VIII. Summary and conclusions

The WVP characteristics associated with EHR over the U.S. during a three year summer season were presented in this paper. The WVP appeared to be an important component for intense convection and the development of MCSs that produced EHR; 114 of the 129 event days (88%) were associated with a well defined WVP. Two different configurations were depicted: the single WVP structure was found most frequently on 84% of the total event days while the double WVP structure represented only 4% of the cases. The WVPs documented 99 of the 119 (83 %), originated mainly from the tropics and were referred to as tropical plumes. WVPs were usually tropical plumes but 20 of the 119 (17%) were subtropical or polar plumes. The tropical plumes originated mainly from the Pacific Ocean (76%) while 22% and 2% of the cases originated from the Gulf of Mexico and the Caribbean Sea, respectively.

Over the ocean areas, we are just beginning to use Special Sensor Microwave/Imager (SSM/I)-derived Total Precipitable Water (TPW) fields for analyzing the depth of the moisture under the WVP. In addition, SSM/I-derived sea surface winds in conjunction with the above TPW fields are being used to compute moisture advection --- a key ingredient for heavy precipitation. SSM/I data is received from the Defense Military Satellite Program (DMSP). The use of sea surface temperatures for representing low-level theta-e will also be explored. Such a possibility may be an effective way of quantifying the energized return flow from the warm waters of the Gulf of Mexico.

An examination of analyses of theta-e at 850 to 700 mb revealed that for 84% of the event days, the WVP was closely aligned with the theta-e ridge axis. Additionally, the 850 mb wind analyses documented in the two examples, June 16, 1989 and August 29, 1989, possessed wind maxima from a southerly direction. Such a wind direction was associated with a transport of warm, moist, unstable air from the subtropics. The 300 mb jet maxima played a major role in initiating storms that produced heavy precipitation. Seventy seven percent of the cases were associated with a double jet streak structure configuration that if coupled with lower-tropospheric jet maxima was shown (Junker et al., 1990 and Corfidi et

al., 1990) to destabilize the atmosphere; this also contributed to low-level heat and moisture transports that acted to initiate heavy precipitation producing MCSs. Some of these double jet streak structures were the result of the MCS modifying the environment to produce a mesoscale induced jet streak to the north of the MCS (see Section VII/Figure 32).

Four categories of WVPs were formulated: the single WVP associated with: 1) a double jet streak structure; 2) a single jet streak structure; 3) no jet; and 4) the double WVP structure that is often associated with a double jet stream configuration.

On many occasions, the WVP moved northeastward on the backside of a 300 mb anticyclone or on the forward side of a trough. MCSs usually developed within the moist, unstable (theta-e ridge axis) air on the eastern side of the WVP. In addition to this orientation in the eastern portion, the northern part of the tropical plume was often where the low-level forcing (theta-e ridge axes and warm air advection) became coupled with upper level forcing mechanisms (jet streaks) creating favorable conditions for development of MCSs. The southerly upper level flow seemed to maintain the northward transport of the WVPs.

Although the WVPs and the upper tropospheric jet streaks appeared to be related to the EHR events documented in this study, 12% of the event days did not present a well defined WVP. As a result, conceptual models of several types of heavy precipitation situations were presented in Section VI; some of these models do not have plumes associated with them. On a few occasions, there was not an obvious jet stream detected at 300 mb at the time of the EHR event. Thus, differential temperature advection and/or low-level advection of warm, moist, unstable air were additional contributing factors for destabilizing the atmosphere and creating conditions favorable for the development of MCSs that produce EHR.

In closing, flash flood producing MCSs are a multiscale and concatenating event. Therefore, in the future as we merge the WSR-88D radar data with the various GOES multi-spectral images, GOES-derived sounding data, and SSM/I data, a better understanding of the multiscale nature of heavy precipitation will be attainable. As a result, this better understanding will allow us to modify and refine the conceptual models and the satellite forecasting funnel for predicting heavy precipitation.

IX. Acknowledgements

The authors thank Frances Holt and Donald Miller of the Satellite Applications Laboratory of NESDIS and LeRoy Spayd, Jr., Training Program Leader for the NWS, for their constructive criticism in the preparation of this manuscript. Special thanks goes to Roger Weldon for his help on our case studies and to Sheldon Kusselson of the Synoptic Analysis Branch of NESDIS for his enlightening discussions and formulation of the "Cyclonic Circulation" Conceptual Model for heavy precipitation. Finally, we thank Lori Paschal and John Shadid for the layout and Paige Bridges, Phil Golden, John Shadid, and Dick Pritchard, for the preparation of the illustrations.

X. References

Adang, T. C. and R. L Gall, 1989: Structure and dynamics of the Arizona monsoon boundary. Mon. Wea. Rev., 117, 1423-1437.

Chappell, C.F., 1985: Requisite conditions for the generation of stationary thunderstorm systems having attendant excessive rains. Proceedings of the sixth Conference on Hydrometeorology, Indianapolis, IN, 221-225.

Chappell, C.F., 1986: Quasi-stationary convective events. Chapter 13 (pp. 289-305) of Mesoscale Meteorology and Forecasting, editor Peter Ray, Amer. Meteor. Soc., Boston, 793 pp.

Corfidi, S.F., N.W. Junker and F.H. Glass, 1990: The Louisiana/MS flash flood and severe weather outbreak of 15-16 November 1987. Proceedings of the 16th Conference on Severe Local Storms, Kanaskis Park, ALTA, CAN, 627-633.

Ellrod, G., 1990: A Water Vapor image feature related to severe thunderstorms. Nat. Wea. Dig., 15, 21-29.

Funk, T. W., 1990: The use of Water Vapor imagery in the analysis of the November 1985 middle Atlantic states record flood event. Nat. Wea. Dig., 11, 12-19.

Funk, T.W. 1989: Evaluation of satellite-derived precipitation estimates and short range forecasting tools during a Texas excessive convective rainfall and flash flood event. Proceedings of the twelfth Conference on Weather Analysis and Forecasting, October 2-6, 1989, Monterey, CA, 459-466.

Funk, T.W., 1991: Forecasting techniques utilized by the forecast branch of the National Meteorological Center during a major convective rainfall event. Wea. and Forecast., 6 (4), 548 - 564.

Jiang, Shi and R. A. Scofield, 1987: Satellite observed convective system (MCS) propagation characteristics and a 3-12 hour heavy precipitation forecast index. NOAA Technical Memorandum NESDIS 20, December 1987, Washington, DC, 43pp.

Junker, N.W., R.E. Bell and R.H. Grumm, 1990: The development, maintenance and strengthening of a cyclonic circulation system by coupled jets. Proceedings of the 16th Conference on Severe Local Storms, Kanaskis Park ALTA, CAN, 627 - 633.

Juying, Xie and R.A. Scofield, 1989: Satellite-derived rainfall estimates and propagation characteristics associated with Mesoscale Convective Systems (MCSs). NOAA Technical Memorandum NESDIS 25, May 1989, Washington, DC, 49 pp.

Kocin, P.J., L.W. Uccellini and R.A. Peterson, 1986: Rapid evolution of a jet streak circulation in a pre-convective environment. Meteorol. Atmos. Phys., 35, 103-138.

Maddox, R.A., 1980: Mesoscale Convective Complexes. Bull. Amer. Meteor. Soc., 61, 1374-1387.

McGuirk, J.P. and D.J. Ulsh, 1990: Evolution of tropical plumes in VAS water vapor imagery. Mon. Wea. Rev., 118, 1758 - 1766.

Purdom, J.F.W. and P.C. Sinclair, 1988: Dynamics of convective scale interaction. Proceedings of the 15th Conference on Severe Local Storms, Feb. 22-26, 1988, Baltimore, MD, 354-359.

Purdom, J.F.W., 1973: Meso-highs and satellite imagery. Mon. Wea. Rev., 101, 180-181.

Scofield, R. A. and J. Robinson, 1992: The "Water Vapor plume/potential energy axis connection" with heavy convective rainfall. Proceedings of the Symposium on Weather Forecasting and the Sixth Conference On Satellite Meteorology and Oceanography, January 5-10, 1992, Atlanta, GA, J 36 - J43.

Scofield, R.A., 1991: Satellite discussion of the Shadyside, Ohio flash flood event of June 14, 1990. Appendix D of the Natural Disaster Survey Report Shadyside, Ohio, Flash Floods, June 14, 1990. NOAA/NWS Report, U.S. Department of Commerce, Silver Spring, MD, pages D-1 to D-18.

Scofield, R.A. and J. Robinson, 1990: The "Water Vapor imagery/theta-e connection" with heavy convective rainfall. Satellite Applications Information Note, 90/7, 7pp.

Scofield, R. A., 1990a: Instability Bursts Associated With Extratropical Cyclone Systems (ECSs) And A Forecast Index Of 3-12 Hour Heavy Precipitation. NOAA Technical Memorandum NESDIS 30, July 1990, Washington, DC, 77 pp.

Scofield, R.A., 1990b: The "water vapor imagery/theta-e connection" with heavy convective rainfall. Proceedings of the EUMETSAT workshop on NOWCASTING and very short range forecasting, July 16 - 20, 1990, Shinfield Park, England, 173 - 178.

Scofield, R.A., 1987: The NESDIS operational convective precipitation estimation technique. Mon. Wea. Rev., 115 (8), 1773-1792.

Scofield, R.A. and T. Funk, 1986: The use of water vapor imagery (6.7 m) in the analysis and forecasting of heavy precipitation. 1986 NWS Southern Region QPF Workshop. NOAA Technical Memorandum NWS SR - 117, 77 - 82.

Scofield, R.A., 1985: Satellite convective cloud categories associated with heavy rainfall. 1985 NWS Southern Region QPF Workshop. NOAA TM NWS SR-112, 67-74.

Scofield, R.A., V.J. Oliver, and L.E. Spayd, Jr., 1980: Estimating rainfall from thunderstorms with warm tops in the infrared imagery. Proceedings of the Eighth Conference on Weather Forecasting and Analysis, June 10-13, 1980, Denver, CO, AMS, Boston, MA, 85-92.

Spayd, L.E., Jr. and R.A. Scofield, 1983: Operationally detecting flash flood producing thunderstorms which have subtle heavy rainfall signatures in GOES imagery. Proceedings of the Fifth Conference on Hydrometeorology, Tulsa, OK, AMS, 190-197.

Uccellini, L. W. and D. R. Johnson, 1979: The coupling of upper and lower tropospheric jet streaks and implications for the development of severe convective storms. Mon. Wea. Rev., 107, *682-702.*

Weldon, R. and S. Holmes, 1991: Water Vapor imagery interpretation and applications to Weather Analysis and Forecasting. NOAA Technical Report NESDIS 57, *April 1991, Washington, DC, 213 pp.*

Whitney Jr., L. F., 1976: Relationship of the subtropical jet stream to severe local storms. Mon. Wea. Rev., 105, *398-412.*

XI. Appendix A

Conceptual models in the water vapor imagery for 12 to 24 hour prediction of heavy rainfall amounts:

I) conceptual models of heavy precipitation using the water vapor imagery

II) using the satellite forecasting funnel to diagnose if conditions are favorable from the global - synoptic - mesoscale to storm scale for producing heavy rainfall:

- o features to detect within the satellite forecasting funnel that are associated with heavy convective rainfall
- o mesoscale convective system/flash flood forecasting
- o moisture criteria in order to use this technique
- o a conceptual model of a backward building MCS

I

CONCEPTUAL MODELS OF HEAVY PRECIPITATION USING WATER VAPOR IMAGERY

(1) PLUME MODEL - (DIRECT PORTION OF PLUME)

- characterized by a low-level theta-e ridge axis, deep layer moisture and an upper level disturbance (s)
- low level maximum winds are present and are replenishing moist, unstable air
- sometimes identified by double plume structure (polar and tropical plume)

(2) CYCLONIC CIRCULATION MODEL

- a pronounced cyclonic circulation is present; usually observed in the Water Vapor Imagery, though sometimes better resolved in the 500 mb vorticity analysis
- jet streaks are often present
- sometimes a tropical plume is present one or two days before to pre-condition the environment

CONCEPTUAL MODELS OF HEAVY PRECIPITATION USING WATER VAPOR IMAGERY con't

(3) PLUME MODEL - (INDIRECT / RETURN PORTION OF PLUME)

- backside of a ridge with warm air advection and an upper level disturbance

(4) PLUME MODEL - AREA OF MOISTURE UNDER AN UPPER LEVEL RIDGE

- heating is the dominant mechanism and convection will usually dissipate after sunset

(5) TROPICAL DISTURBANCE / VORTEX

(6) NON-PLUME / NON-CYCLONIC CIRCULATION EVENTS

- CASE 1 - either "residual" moisture in the water vapor imagery was present or was advected into the area
- CASE 2 - moisture in the water vapor imagery was not originally present

II

Rainfall amounts assume that all the conditions of the SATELLITE FORECASTING FUNNEL HAVE BEEN SATISFIED ! ! !

SATELLITE FORECASTING FUNNEL

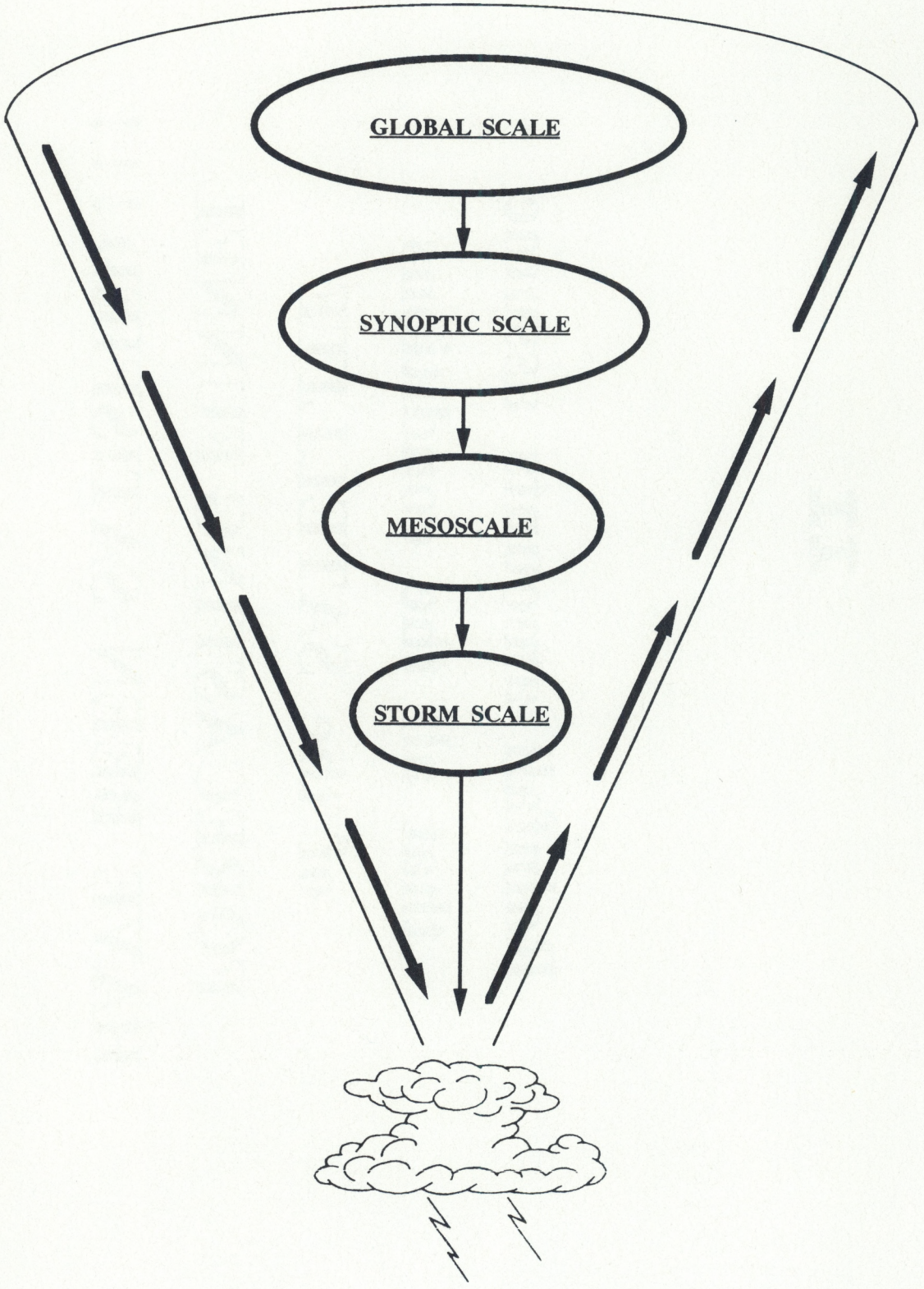

FEATURES TO DETECT WITHIN THE SATELLITE FORECASTING FUNNEL THAT ARE ASSOCIATED WITH HEAVY CONVECTIVE RAINFALL

GLOBAL SCALE

- WATER VAPOR PLUMES

SYNOPTIC SCALE

- CYCLONIC CIRCULATIONS
- THETA - E RIDGE AXES
- THICKNESS RIDGE AXES AND DIFFLUENCE
- FRONTS
- PATTERN OF JET STREAMS (DOUBLE JET STREAKS)
- INSTABILITY OR WARM MOIST AIR / INSTABILITY ADVECTION
- VORTICES
- EQUATORWARD SURGES / " DIGGING " SHORT WAVES

MESOSCALE

- BOUNDARIES
- MESO ALPHA WAVES
- " STRONGEST " LOW LEVEL WINDS
- OUTFLOW BOUNDARIES / VORTICES / JET STREAKS

STORM SCALE

- STORM MOTION AND PROPAGATION

MESOSCALE
CONVECTIVE SYSTEM / FLASH FLOOD FORECASTING

GLOBAL SCALE **AND** **SYNOPTIC SCALE**

WATER VAPOR

- PLUMES
  - TROPICAL
  - POLAR
- CYCLONIC CIRCULATIONS

THETA-E (θe)

- RIDGE AXES
- RELATIVE MAXIMA
- GRADIENTS (NORTH OF RIDGE AXES)

LIFTING AND DESTABLILIZATION MECHANISMS

- HEATING
- ADVECTION OF WARM/MOIST UNSTABLE AIR
- DIFFERENTIAL TEMPERATURE ADVECTION
- UPWARD VERTICAL MOTION/MOISTURE CONVERGENCE

MOISTURE

- PRECIPITABLE WATER
- RELATIVE HUMIDITY

ENVIRONMENTAL CONDITIONS THAT CONTROL STORM MOTION

- THICKNESS
- VERTICAL WIND SHEAR
- LOCATION OF DESTABILIZATION

MESOSCALE

- BOUNDARIES, e.g., OUTFLOW
- VORTICES
- JET STREAKS
- MESO ALPHA WAVES
- LOW LEVEL JETS
- PRESSURE / HEIGHT FALLS
- OROGRAPHIC CIRCULATION

STORM SCALE

RAINFALL INTENSITY AND ACCUMULATION **MOVEMENT** **PROPAGATION**

moisture criteria in order to use this technique

tropical moisture must also be available and can be evaluated from the 1000-500 mb Precipitable Water (PW) and Relative Humidity (RH) information:

PW (inches)	RH
good > 1.0 and > 130 % of normal	good > 60 %
better > 1.5 and > 140 % of normal	better > 70 %
best > 1.5 and > 150 % of normal	best > 80 %.

CONCEPTUAL MODEL OF A BACKWARD-PROPAGATING MCS

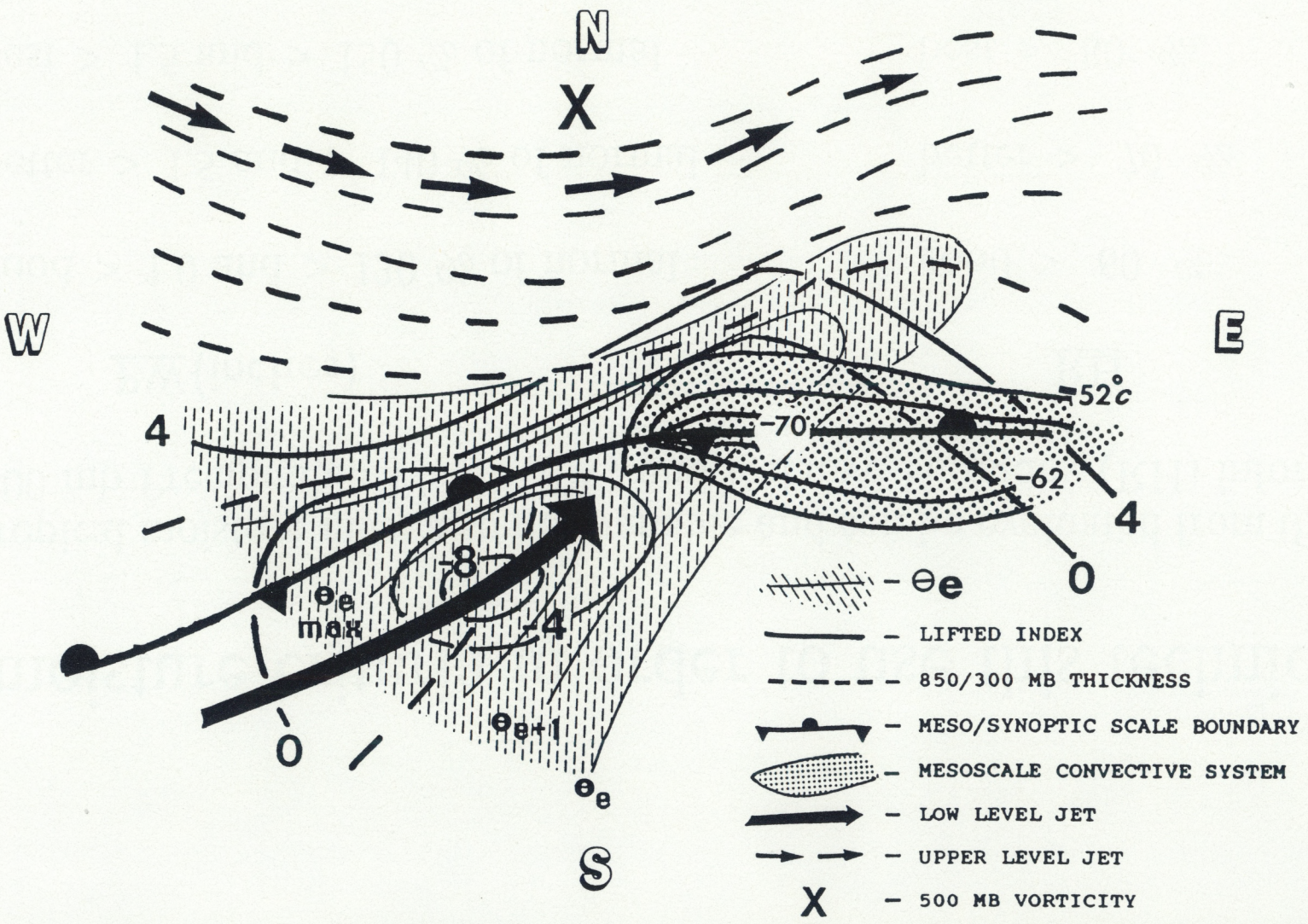

III

CATEGORY - 1
DIRECT PLUME (S)

- **5 - 10 inches or more**
- **Western Region :**
  2 - 5 inches (possibly more)
- **Severe WX if located in Western Portion of Plume**

CATEGORY - 2
CYCLONIC CIRCULATION

- 3 - 7 inches
- If Connected to a Tropical Plume :
    - 5 - 10 inches
- Western Region :
    - 2 - 4 inches
    - if connected to a Tropical Plume
      2 - 5 inches (possibly more)
- Severe WX !

CATEGORY - 3

INDIRECT PLUME

- **2 - 5 inches**
- **Severe WX**

CATEGORY - 4

AREA OF MOISTURE UNDER RIDGE

- **2 - 4 inches**

CATEGORY - 5

TROPICAL DISTURBANCE / VORTEX

- **5 - 10 inches or more**

CATEGORY - 6
NON-PLUME / NON-CYCLONIC CIRCULATION EVENTS

CASE 1 - Moisture PRESENT in the Water Vapor Imagery

- **4 - 8 inches**
- **Western Region: 2 - 4 inches**

CASE 2 - Moisture NOT PRESENT in the Water Vapor Imagery

- **3 - 6 inches**
- **Western Region: 1 - 3 inches**
- **Severe WX**

APPENDIX B

DATE AND LOCATION OF THE EXTREME HEAVY RAINFALL DURING THE SUMMERS OF 1989 - 1991

Year	Case	State	Date	Max. Prcp.(inch)
1989	1	LA	05/5	11.8
	2	AR	05/9	5.8
	3	TX	05/16	8.1
	4	TX	05/17	11.2
	5	TX, LA	05/18	13
	6	MO, TX, LA, MS	05/19	11
	7	MS	05/21	6.1
	8	MO	05/22	7.4
	9	MS	05/24	5.4
	10	MI	05/3	16
	11	LA	06/2	5.8
	12	TX	06/4	5.2
	13	TX, MS	06/5	6.3
	14	TX, MS	06/8	7.9
	15	MS, AL, GA, FL	06/9	15.6
	16	TX, OK, KS	06/11	9.2
	17	MO	06/12	5.2
	18	TX	06/14	5
	19	MS, LA	06/15	5.8
	20	KY, AL	06/16	9.6
	21	AL	06/19	5.5
	22	TN, SC	06/20	5.2
	23	AL	06/21	5.8
	24	IA	06/22	5.4
	25	NE	06/25	6.6
	26	TX, LA	06/27	10.2
	27	LA	06/28	10
	28	LA	06/29	12.9
	29	TX	06/30	6
	30	NE	07/1	6
	31	TN, MS	07/2	7.3
	32	NC, SC	07/4	6.6
	33	MI	07/9	5
	34	TN, KS	07/12	8.2
	35	LA	07/14	7.5
	36	LA	07/15	6.1
	37	VA	07/17	5.4
	38	OK	07/18	5
	39	AR	07/19	5.3
	40	OK	08/17	6.3

Year	Case	State	Date	Max. Prcp (inch)
1989	41	OK	08/20	6.8
	42	MO, IN	08/29	5.8
	43	OK	09/13	6.8
	44	IL,TX,TN	09/14	7.3
	45	PA	09/20	5.4
	46	FL, AL, GA	10/1	7.2
1990	47	TX	05/2	5.4
	48	OK, TX, AR	05/3	8.6
	49	TX	05/4	5.4
	50	LA	05/9	5.2
	51	MS, AL	05/13	10
	52	LA	05/14	6
	53	MO	05/16	8.3
	54	IA	05/19	5.1
	55	AR	05/20	13
	56	MO	05/26	6.5
	57	KS	05/27	5.6
	58	LA, MS, TX	06/1	8.4
	59	SD	06/02	5.4
	60	NE	06/15	5.8
	61	NE, SD	06/16	5.6
	62	IA	06/17	7.5
	63	WI	06/23	6.5
	64	WI	06/29	7.3
	65	KY, VA	07/15	9.7
	66	TX	07/16	7.3
	67	TX	07/19	5.2
	68	NE, IA, KS	07/26	9.6
	69	IA	07/27	5.3
	70	IN	08/18	6.3
	71	IA	08/25	5.2
	72	MN	09/06	8.4
	73	TX	09/17	8.8
	74	TX, KS	09/21	6.5
	75	TX	09/22	5.9
	76	TX	09/23	6
	77	OK, AR	10/8	7.8
	78	AR	10/9	5.8
	79	SC, VA	10/11	10
	80	GA	10/12	11.3
	81	NC, SC	10/13	7.9
	82	NC, SC	10/23	5.3
1991	83	TX	05/3	6.5
	84	LA, MS	05/4	5.9
	85	TX	05/8	6

Year	Case	State	Date	Max. Prcp (inch)
1991	86	LA	05/9	7.9
	87	LA	05/10	5.3
	88	TX	05/15	5
	89	NE	05/17	5.2
	90	FL	05/21	6.7
	91	FL	05/24	6.1
	92	MS	05/26	6
	93	OK	06/8	5.1
	94	TX	06/9	5.5
	95	TX	06/10	6.5
	96	TX, LA	06/11	6.9
	97	TN	06/13	5.6
	98	IA	06/14	6
	99	SC	06/18	5.2
	100	KY, TN	06/22	5.8
	101	AL, FL	06/26	7.8
	102	LA	07/4	5.3
	103	KY	07/9	6
	104	MO	07/10	7.5
	105	MN	07/22	5.9
	106	AR, KS, TX	07/28	6.7
	107	SC	08/2	5.8
	108	MN, IA, NE	08/8	7.3
	109	PA	08/10	5.1
	110	SC	08/12	6
	111	TX	08/15	6.8
	112	NC	08/19	5.3
	113	CT, NH	08/20	7.3
	114	GA	08/26	5.7
	115	MS	08/28	5.1
	116	TX	09/1	6.8
	117	OK, MO	09/4	5.1
	118	MD, TX	09/19	7.1
	119	MS	09/25	5.8
	120	FL	09/30	5
	121	FL	10/2	6.8
	122	FL	10/8	8.3
	123	FL	10/9	7.2
	124	MS	10/23	6.4
	125	OK, IA	10/25	9
	126	OK	10/26	6.5
	127	TX	10/27	7.3
	128	LA, TX	10/28	5.9
	129	MO, LA	10/29	8.8

(continued from inside cover)

NESDIS 31 Data Processing Alogorithms for Inferring Stratospheric Gas Concentrations from Balloon-Based Solar Occultation Data. I-Lok Chang (American University) and Michael P. Weinreb, April 1987. (PB87 196424)

NESDIS 32 Precipitation Detection with Satellite Microwave Data. Yang Chenggang and Andrew Timchalk, June 1988. (PB88 240239)

NESDIS 33 An Introduction to the GOES I-M Imager and Sounder Instruments and the GVAR Retransmission Format. Raymond J. Komajda (Mitre Corp) and Keith McKenzie, October 1987. (PB88 132709)

NESDIS 34 Balloon-Based Infrared Solar Occultation Measurements of Stratospheric 03, H20, HNo3, and CF2C12. Michael P. Weinreb and I-Lok Chang (American University), September 1987. (PB88 132725)

NESDIS 35 Passive Microwave Observing From Environmental Satellites, A Status Report Based on NOAA's June 1-4, 1987, Conference in Williamsburg, VA. James C. Fisher, November 1987. (PB88 208236)

NESDIS 36 Pre-Launch Calibration of Channels 1 and 2 of the Advanced Very High Resolution Radiometer. C. R. Nagaraja Rao, October 1987. (PB88 157169/AS)

NESDIS 39 General Determination of Earth Surface Type and Cloud Amount Using Multispectral AVHRR Data. Irwin Ruff and Arnold Gruber, February 1988. (PB88 199195/AS)

NESDIS 40 The GOES I-M System Functional Description. Carolyn Bradley (Mitre Corp), November 1988.

NESDIS 41 Report of the Earth Radiation Budget Requirements Review - 1987, Rosslyn, VA, 30 March-3 April 1987. Larry L. Stowe (Editor), June 1988.

NESDIS 42 Simulation Studies of Improved Sounding Systems. H. Yates, D. Wark, H. Aumann, N. Evans, N. Phillips, J. Sussking, L. McMillin, A. Goldman, M. Chahine and L. Crone, February 1989.

NESDIS 43 Adjustment of Microwave Spectral Radiances of the Earth to a Fixed Angle of Progagation. D. Q. Wark, December 1988. (PB89 162556/AS)

NESDIS 44 Educator's Guide for Building and Operating Environmental Satellite Receiving Stations. R. Joe Summers, Chambersburg Senior High, February 1989.

NESDIS 45 Final Report on the Modulation and EMC Consideration for the HRPT Transmission System in the Post NOAA-M Polar Orbiting Satellite ERA. James C. Fisher (Editor), June 1989. (PB89 223812/AS)

NESDIS 46 MECCA Program Documentation. Kurt W. Hess, September 1989.

NESDIS 47 A General Method of Using Prior Information in a Simultaneous Equation System. Lawrence J. Crone, David S. Crosby and Larry M. McMillin, October 1989.

NESDIS 49 Implementation of Reflectance Models in Operatioal AVHRR Radiation Budget Processing. V. Ray Taylor, February 1990.

NESDIS 50 A Comparison of ERBE and AVHRR Longwave Flux Estimates. A. Gruber, R. Ellingson, P. Ardanuy, M. Weiss, S. K. Yang, (Contributor: S.N. Oh).

NESDIS 51 The Impact of NOAA Satellite Soundings on the Numerical Analysis and Forecast System of the People's Republic of China. A. Gruber and W. Zonghao, May 1990.

NESDIS 52 Baseline Upper Air Network (BUAN) Final Report. A. L. Reale, H. E. Fleming, D. Q. Wark, C. S. Novak, F. S. Zbar, J. R. Neilon, M. E. Gelman and H. J. Bloom, October 1990.

NESDIS 53 NOAA-9 Solar Backscatter Ultraviolet (SBUV/2) Instrument and Derived Ozone Data: A Status Report Based on a Review on January 29, 1990. Walter G. Planet, June 1990.

NESDIS 54 Evaluation of Data Reduction and Compositing of the NOAA Global Vegetation Index Product: A Case Study. K. P. Gallo and J. F. Brown, July 1990.

NESDIS 55 Report of the Workshop on Radiometric Calibration of Satellite Sensors of Reflected Solar Radiation, March 27-28, 1990, Camp Springs, MD. Peter Abel (Editor), July 1990.

NESDIS 56 A Noise Level Analysis of Special 10-Spin-Per-Channel VAS Data. Donald W. Hillger, James F. W. Purdom and Debra A. Lubich, February 1991.

NESDIS 57 Water Vapor Imagery Interpretation and Applictions to Weather Analyis and Forecasting. Roger B. Weldon and Susan J. Holmes, April 1991.

NESDIS 58 Evaluating the Design of Satellite Scanning Radiometers for Earth Radiation Budget Measurements with System, Simulations. Part 1: Instantaneous Estimates. Larry Stowe, Philip Ardanuy, Richard Hucek, Peter Abel and Herberet Jacobowitz, October 1991.

NESDIS 59 Interactive Digital Image Display and Analysis System (IDIDAS) User's Guide. Peter J. Celone and William Y. Tseng, October 1991.

NESDIS 60 International Dobson Data Workshop Summary Report. Robert D. Hudson (University of Maryland) and Walter G. Planet, February 1992.

NESDIS 61 Tropical Cyclogenesis in the Western North Pacific. Raymond M. Zehr, July 1992.

NESDIS 62 NOAA Workshop on Climate Scale Operational Precipitation and Water Vapor Products. Ralph Ferraro (Editor), October 1992.

NESDIS 63 A Systematic Satellite Approach for Estimating Central Pressures of Mid-Latitude Oceanic Storms. Frank J. Smigielski and H. Michael Mogil, December 1992.

NOAA SCIENTIFIC AND TECHNICAL PUBLICATIONS

The National Oceanic and Atmospheric Administration was established as part of the Department of Commerce on October 3, 1970. The mission responsibilities of NOAA are to assess the socioeconomic impact of natural and technological changes in the environment and to monitor and predict the state of the solid Earth, the oceans and their living resources, the atmosphere, and the space environment of the Earth.

The major components of NOAA regularly produce various types of scientific and technical information in the following kinds of publications:

PROFESSIONAL PAPERS - Important definitive research results, major techniques, and special investigations.

CONTRACT AND GRANT REPORTS - Reports prepared by contractors or grantees under NOAA sponsorship.

ATLAS - Presentation of analyzed data generally in the form of maps showing distribution of rainfall, chemical and physical conditions of oceans and atmosphere, distribution of fishes and marine mammals, ionospheric conditions, etc.

TECHNICAL SERVICE PUBLICATIONS - Reports containing data, observations, instructions, etc. A partial listing includes data serials; prediction and outlook periodicals; technical manuals, training papers, planning reports, and information serials; and miscellaneous technical publications.

TECHNICAL REPORTS - Journal quality with extensive details, mathematical developments, or data listings.

TECHNICAL MEMORANDUMS - Reports of preliminary, partial, or negative research or technology results, interim instructions, and the like.

U.S. DEPARTMENT OF COMMERCE
National Oceanic and Atmospheric Administration
National Environmental Satellite, Data, and Information Service
Washington, D.C. 20233